Synthesis and Characterization of Ruthenium Oxyl Radical Complexes

Katsuaki Kobayashi

Department of Structural Molecular Science
School of Mathematical and Physical Science
The Graduate University for Advanced Studies

Contents

Contents p.ii

Chapter 1

General Introduction

1, General Introduction

1-1 Metal-oxo Complexes in Biological Systems

Reactivity of high-valent metal-oxo complexes attracts much attention from the viewpoint of enzymatic activation of dioxygen on metals via O_2-binding,[1,2,3,4] O_2-reduction, and oxidation or oxygenation of organics by such as P-450 enzymes,[2,3] MMO(methane monooxygenase),[4] and so on. Reductive cleavage of the O-O bond on metal ions has been considered as a key process in enzymatic activation of dioxygen. Among various oxygenases, dioxygen activation by Cytochrome P450 has been most extensively examined,[2,3] and the proposal catalytic cycle by P-450 is shown in Scheme 1. An electrophilic attack of O_2 on (Por)Fe(II) forms the (Por)Fe(II)-O_2^- adduct. One electron reduction of the Fe(III) peroxo species followed by successive protonation on the terminal oxygen produces ($Por^{\bullet+}$)Fe(IV)=O (Compound I) with liberating H_2O. Compound I is considered as the active form of Cytochrome P-450 and catalyzes oxidation and hydroxylation of organic substrates. The catalytic cycle of Scheme 1, however, has not been constructed so far in artificial systems, because of the difficulty of not only the selective reduction of the terminal oxygen of the Fe-O_2 moiety but also participation of various oxidation states of iron such as Fe(II), Fe(III) and Fe(IV) or Fe(V) in the catalytic cycle.

1-2 High-valent Metal-oxo Complexes in Artificial Systems

There are two synthetic strategies for the preparation of high-valent metal-oxo complexes, one is reductive activation of a dioxygen (O_2) via metal-O_2 complex and the other is oxidative activation of a water molecule (OH_2) via metal-OH_2 one. As

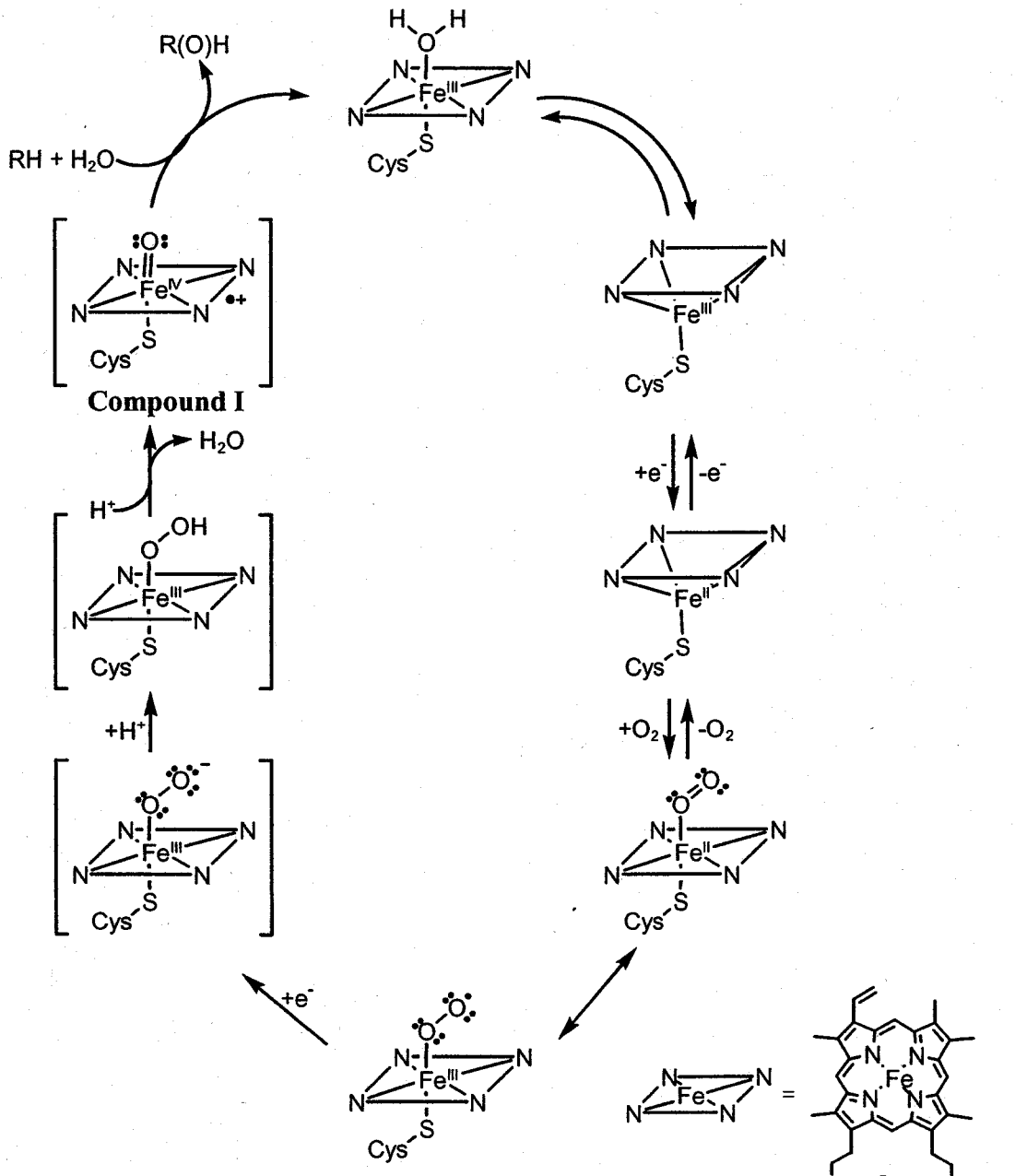

Scheme 1

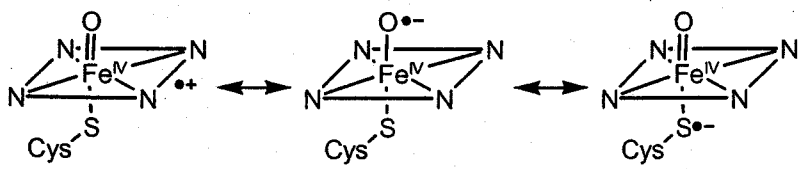

Scheme 2

mentioned above, selective cleavage of a O-O bond of the metal-O2 adducts under reductive conditions has not been succeeded yet. Alternatively, double deprotonation of metal-aqua complexes would give metal-oxo ones if μ-oxo dimmer (or oligomers) formation through the nucleophilic attack of the resultant strong basic metal-oxo to

$$[Ru^{II}\text{-}OH_2]^{2+} \xrightarrow{-2H^+} [Ru^{II}\text{-}O]^0 \xrightarrow{[Ru^{II}\text{-}OH_2]^{2+}} [Ru^{II}\text{-}O\text{-}Ru^{II}]^{2+} \quad (1)$$

metal-aqua complexes (eq 1) can be depressed under basic conditions. Indeed, oxidation of aqua-ruthenium complexes is accompanied with dissociation of proton to give the corresponding higher oxidation states of Ru-OH and Ru=O ones (eq 2)

$$[Ru^{II}\text{-}OH_2]^{2+} \underset{}{\overset{-e^-,\,-H^+}{\rightleftharpoons}} [Ru^{III}\text{-}OH]^{2+} \underset{}{\overset{-e^-,\,-H^+}{\rightleftharpoons}} [Ru^{VI}\text{-}O]^{2+} \quad (2)$$

Meyer et al. synthesized a variety of high-valent oxo-ruthenium (Ru=O) complexes by the sequential proton and electron loss of aqua-ruthenium complexes (eq 2).[5] In fact, a variety of high-valent Ru=O complexes have been prepared by treatment of Ru-OH_2 complexes with Ce(IV),[6] and some of them have been proven to work as oxidants for hydrocarbons,[7] alcohols,[8] olefins,[9] phenols,[10] phosphines,[11] and so on. The view that the strong electron donor ability of O^{2-} formed in eq 2 stabilizes the higher oxidation states of Ru^{IV}=O species is based on the assumption that the charge of oxygen atom of 2– is always maintained irrespective of oxidation stats of metals. On the other hand, oxyl radical species has been proposed in cytchrome P-450 in theoretical studies (Scheme 2), and the actual electronic state of the Fe-O framework has not been fully elucidated so far.

1-3 Aqua-ruthenium Complexes Containing a dioxolene Ligand

Dioxolene is an electrochemically non-innocent ligand and undergoes the stepwise

reduction to yield semiquinone (SQ) and catecholate (Cat) from Quinone (Q) (eq3).

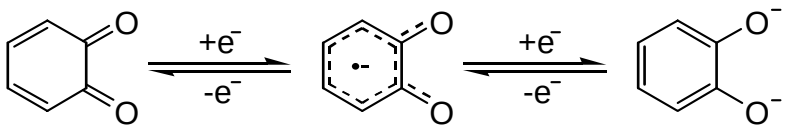

(3)

Therefore, dioxolene has a function of two-electron reservoir in redox reactions of metal-dioxolene complexes. Pierpont et al. have synthesized a variety of ruthenium-dioxolene complexes, which substantially serve the understanding of the structure and physicochemical properties of the complexes.[12,13,14,15,16] The noticeable feature of ruthenium-dioxolene complexes is the charge distribution between central metal ions and the ligands on account of accessible reduction states of quinone (eq 4). The charge distribution is caused by the mixing of dπ (Ru) and π* (dioxolene), both of

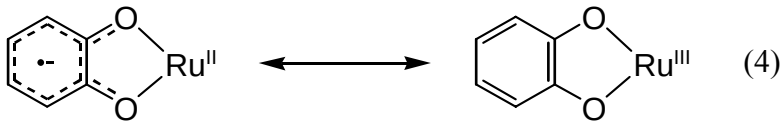

(4)

Ru^{II}-semiquinone Ru^{III}-catecholate

which are in the close orbital energy level. Therefore, the redox potential of a Ru-dioxolene complex is relatively subject to that of the dioxolene ligand.

Higher oxidation states of Ru=O complexes have been obtained by oxidation of central metals coupled with deprotonation of Ru-OH_2 ones. Introduction of a dioxolene ligand as an electron acceptor into the Ru-OH_2 framework, therefore, also would induce deprotonation of the aqua ligand instead of the oxidation of the central Ru ion. Such redox reactions of dioxolene driven by deprotonation of aqua-Ru-dioxolene complexes would serve not only smooth conversion from aqua- to oxo-group without changing the oxidation states of Ru but also the control of redox potentials of oxo-Ru complexes, which contributes to development of a new type of electrocatalysis.

Tsuge and Tanaka et al. briefly reported spectral change and electrochemical

behavior of the aqua-Ru-dioxolene complex, $[Ru^{III}(trpy)(Bu_2SQ)(OH_2)](ClO_4)_2$ (trpy = 2,2':6',2"-terpyridine, Bu_2SQ = 3,5-di-*tert*-butyl-1,2-benzosemiquinone) in acetone, but the details of those have remained unclear.[17,18,19]

This paper consists of five chapters. The chapter 2 shows the synthetic procedure of the series of Ru-dioxolene complexes, $[Ru^{II}(trpy)(Bu_2SQ)(OAc)]$ (**1**) (Bu_2SQ = 3,5-di-*tert*-butyl-1,2-benzosemiquinone), $[Ru^{II}(trpy)(4ClSQ)(OAc)]$ (**2**) (4ClSQ = 4-chloro-1,2-benzosemiquinone), $[Ru^{III}(trpy)(Bu_2SQ)(OH_2)](ClO_4)_2$ (**3**), $[Ru^{III}(trpy)(4ClSQ)(OH_2)](ClO_4)_2$ (**4**), and $[Ru^{II}(trpy)(Bu_2SQ)(O^{\bullet-})]$ (**5**), and elucidates crystal structures of **1**, **3**, and **5** by X-ray analysis. The chapter 3 describes the redox behavior of aqua-Ru^{III}-semiquinone complexes **3** and **4** coupled with acid-base equilibrium of the aqua ligand. The chapter 4 describes the characterization of oxyl radical complex by the spin trapping technique and ESR spectra. Finally, general conclusion of this study is included in chapter 5.

2, References

(1) Feig, A. L.; Lippard, S. J. *Chem. Rev.* **1994**, *94*, 759.

(2) Sano, M.; Roach, M. P.; Coulter, E. D.; Dawson, J. H. *Chem. Rev.* **1996**, *96*, 2841.

(3) Watanabe, Y. J. Biol. *Inorg. Chem.* **2001**, *6*, 846.

(4) Wallar, B. J.; Lipscomb, J. D. *Chem. Rev.* **1996**, *96*, 2625.

(5) (a) Moyer, B. A.; Meyer, T. J. *Inorg. Chem.* **1981**, *20*, 436. (b) Takeuchi, K. J.; Thompson, M. S.; Pipes, D. W.; Meyer, T. J. *Inorg. Chem.* **1984**, *23*, 1845.

(6) (a) Szczepura, L. F.; Maricich, S. M.; See, R. F.; Churchill, M. R.; Takeuchi, K. J. *Inorg. Chem.* **1995**, *34*, 4198. (b) Che, C.-M.; Tang, W.-T.; Wong, W.-T.; Lai, T.-F. *J. Am. Chem. Soc.* **1989**, *111*, 9048. (c) Geselowiz, D.; Meyer, T. J. *Inorg. Chem.* **1990**, *29*, 3894.

(7) (a) Murahashi, S.; Oda, Y.; Naota, T.; Kuwabara, T. *Tetrahedron lett.* **1993**, *34*, 1299. (b) Moyer, B. A.; Tompson, M. S.; Meyer, T. J. *J. Am. Chem. Soc.* **1980**, *102*, 2310.

(8) (a) Marmion, M. E.; Takeuchi, K. J. *J. Chem. Soc., Dalton Trans.* **1988**, 2385 (b) Wong, K.–Y.; Yam, V. W.-W.; Lee, W. W.-S. *Electrochim. Acta.* **1992**, *37*, 2645 (c) Che, C.-M.; Lee, W.-O. *J. Chem. Soc., Chem. Commun.*, **1988**, 881 (d) Muller, J. G.; Acquaye, J. H.; Takeuchi, K. J. *Inorg. Chem.* **1992**, *31*, 4552 (e) Wong, K.-Y.; Che, C,-M.; Anson, F. C. Inorg. Chem. **1987**, *26*, 737 (f) Goldstein, A. S.; Beer, R. H.; Drago, R. S. *J. Am. Chem. Soc.* **1994**, *116*, 2424 (g) Aquaye, J. H.; Muller, J. G.; Takeuchi, K. J. *Inorg. Chem.* **1993**, *32*, 160 (h) Gerli, A. Reedijk, J. Lakin, M. T. Spek, A. L. *Inorg. Chem.* **1995**, *34*, 1836 (i) Groves, J. T.; Quinn, R. *J. Am. Chem. Soc.* **1985**, *107*, 5790 (j) Roecker, L.; Meyer, T. J. *J. Am. Chem. Soc.* **1987**,

109, 746.

(9) (a) Dobson, J. C.; Seok, W. K.; Meyer, T. J. *Inorg. Chem.* **1986**, *25*, 1514 (b) Che, C.-M.; Ho, C.; Lau, T.-C. *J. Chem. Soc., Dalton Trans.* **1991**, 1901 (c) Stultz, L. K.; Binstead, R. A.; Reynolds, M. S.; Meyer, T. J. *J. Am. Chem. Soc.* **1995**, *117*, 2520.

(10) Soek, W. K.; Meyer, T. J. *J. Am. Chem. Soc.* **1988**, *110*, 7358.

(11) Dovletoglou, A.; Meyer, T. J. *J. Am. Chem. Soc.* **1994**, *116*, 215.

(12) (a) Pierpont, C. G.; Buchanan, R. M. *Coord. Chem. Rev.* **1981**, *38*, 45. (b) Pierpont, C. G.; Lange, C. W. *Prog. Inorg. Chem.* **1994**, *41*, 331.

(13) (a) Haga, M.; Dodsworth, E. S.; Lever, A. P. B.; Boone, S. R.; Pierpont, C. G. *J. Am. Chem. Soc.* **1986**, *108*, 7413. (b) Boone, S. R.; Pierpont, C. G. *Inorg. Chem.* **1987**, *26*, 1769. (c) Bhattacharya, S.; Pierpont, C. G. *Inorg. Chem.* **1991**, *30*, 1511. (d) Bhattacharya, S.; Pierpont, C. G. *Inorg. Chem.* **1992**, *31*, 35. (e) Bhattacharya, S.; Pierpont, C. G. *Inorg. Chem.* **1994**, *33*, 6038. (f) Sugimoto, H.; Tanaka, K. *J. Organomet. Chem.* **2001**, *622*, 280.

(14) (a) Haga, M.; Dodsworth, E. S.; Lever, A. P. B. *Inorg. Chem.* **1986**, 25, 447. (b) Ebadi, M.; Lever, A. P. B. *Inorg. Chem.* **1999**, *38*, 467.

(15) (a) Lever, A. P. B.; Auburn, P. R.; Dodsworth, E. S.; Haga, M.; Liu, W.; Melnik, M.; Nevin, W. A. *J. Am. Chem. Soc.* **1988**, *110*, 8076. (b) Auburn, P. R.; Dodsworth, E. S.; Haga, M.; Liu, W.; Nevin, W. A.; Lever, A. P. B. *Inorg. Chem.* **1991**, *30*, 3502 (c) Bag, N.; Pramanik, A.; Lahiri, G. K.; Chakravorty, A. *Inorg. Chem.* **1992**, *31*, 40 (d) Masui, H.; Lever, A. B. P.; Auburn, P. R. *Inorg. Chem.* **1991**, *30*, 2402.

(16) Kurihara, M.; Daniele, S.; Tsuge, K.; Sugimoto, H.; Tanaka, K. *Bull. Chem. Soc.*

Jpn. **1998**, *71*, 867.

(17) K. Tsuge, K. Tanaka, *Chem. Lett.* **1998**, 1069; K. Tsuge, M. Kurihara, K. Tanaka, *Bull. Chem. So. Jpn.* **2000**, *73*, 607.

(18) Wada, T.; Tsuge, K.; Tanaka, K. *Chem. Lett.* **2000**, 910.

(19) (a) Wada, T.; Tsuge, K.; Tanaka, K. *Angew. Chem., Int. Ed.* **2000**, *39*, 1479. (b) Wada, T.; Tsuge, K.; Tanaka, K. *Inorg. Chem.* **2001**, *40*, 329.

Chapter 2

Syntheses and Electronic Structure of Ruthenium Dioxolene Complexes

(Katsuaki Kobayashi, Hideki Ohtsu, Tohru Wada, and Koji Tanaka, *Chem. Lett.* 2002, 868.)

1, Introduction

There have been great interest in the metal complexes containing noninnocent ligands such as dioxolenes, ditiolenes, benzoquinonediimines. Especially, ruthenium dioxolene complexes have been synthesized and investigated physicochemical and electrochemical properties.[1,2] Dioxolene takes three different electronic states classified as quinone (Q), semiquinone (SQ), and catecholate (Cat). The noticeable feature of Ru-dioxolene complexes is the charge distribution between a central ruthenium ion and dioxolene ligands on account of accessible reduction states of a ruthenium ion and dioxolene ligands. As for total six oxidation states of Ru^{II}- and Ru^{III}-dioxolene complexes, the actual structures of $[Ru^{II}(Q)]$ and $[Ru^{III}(SQ)]$ complexes, and those of $[Ru^{II}(SQ)]$ and $[Ru^{III}(Cat)]$ ones are expressed as resonance hybrids

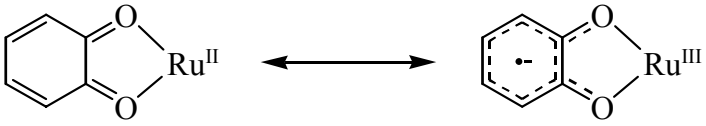

$[Ru^{II}(Q)]$ $[Ru^{III}(SQ)]$ (1)

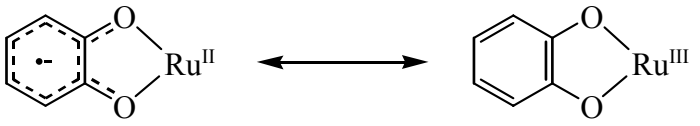

$[Ru^{II}(SQ)]$ $[Ru^{III}(Cat)]$ (2)

between two complexes (eq 1 and 2). The C-O bond lengths of dioxolene ligands and XPS of Ru atoms have been used as criteria for determining whether the resonance of eq 1 and 2 lies to the two extremes. As for the resonance of eq 2, a number of $[Ru^{II}(SQ)]$ and $[Ru^{III}(Cat)]$ complexes have been documented so far. On the other hand, there has been reported only one example of a $[Ru^{III}(SQ)]$ complex with regard to the resonance of eq 1.[3] Thus, dioxolene ligands act as the redox center of the complex as well as a ruthenium ion. This fact indicates that the redox potential of the complex

can be controlled by the substituent of dioxolene ligands.

Tanaka et al. have synthesized the aqua-ruthenium complex with a dioxolene ligand, $[Ru^{III}(trpy)(Bu_2SQ)(OH_2)](ClO_4)_2$ aimed at a new electrocatalyst based on the oxo-ruthenium reactivity.[4] The aqua-Ru-dioxolene complex works as an oxidant for the dehydrogenation of hydrocarbons such as 9,10-dihydroanthoracene in the presence of a base and Ag^+ in acetone (Scheme 1),[5] and as water oxidation catalyst.[6] The active species of this reaction is considered as hydroxyl radical or oxyl radical generated by intramolecular electron transfer from OH^-/O^{2-} to a Ru-dioxolene moiety, though details remain unclear.

In this chapter, the author describes modification of the synthetic procedure of the aqua-Ru-quinone complex and preparation of a series of Ru-dioxolene complexes, $[Ru^{II}(trpy)(Bu_2SQ)(OAc)]$ (**1**) (trpy = 2,2':6',2''-terpyridine, Bu_2SQ = 3,5-di-*tert*-butyl-1,2-benzosemiquinone), $[Ru^{II}(trpy)(4ClSQ)(OAc)]$ (**2**) (4ClSQ = 4-chloro-1,2-benzosemiquinone), $[Ru^{III}(trpy)(Bu_2SQ)(OH_2)](ClO_4)_2$ (**3**), $[Ru^{III}(trpy)(4ClSQ)(OH_2)](ClO_4)_2$ (**4**), and $[Ru^{II}(trpy)(Bu_2SQ)O^{\bullet-}]$ (**5**). The X-ray crystal structure of **1**, **3**, and **5** are also reported. In addition, electronic structures of Ru-dioxolene moiety of these complexes are discussed based on X-ray crystal analysis and X-ray photoelectron spectroscopy. The complex **5** is the first example of an oxyl radical complex.

Scheme 1.

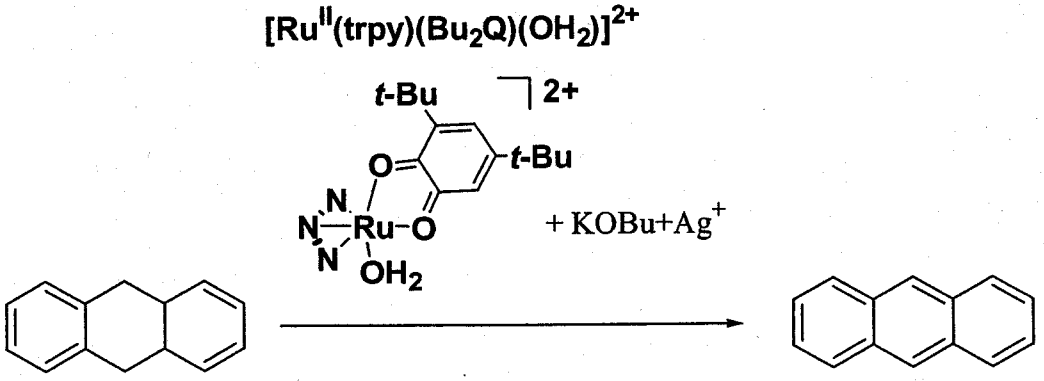

2, Experimental Section

Preparations.

[Ru^{II}(trpy)(Bu_2SQ)(OAc)] (1).[7] A mixture of [Ru^{III}(trpy)Cl_3] (500 mg, 1.14 mmol) and $AgBF_4$ (662 mg, 3.40 mmol) in acetone (50 mL) was refluxed for 2 h.[8] After removal of AgCl by filtration, the filtrate was evaporated under reduced pressure. The residue and 3,5-di-*tert*-butylcatechol (252 mg, 1.14 mmol) was dissolved in deaerated methanol (30 mL) and then potassium acetate (1.11 g, 11.4 mmol) in methanol (20 mL) was added to the solution under N_2. The mixture was stirred for 24 h at room temperature. The resulting purple solution was evaporated under reduced pressure, and the residue was extracted with acetone to remove excess potassium acetate. The acetone solution was loaded on a silica-gel column. After [Ru^{III}(Bu_2SQ)$_3$] was eluted with acetone, [Ru^{II}(trpy)(Bu_2SQ)(OAc)] (**1**) adsorbed on the top of the column was eluted with methanol. Violet plates of **1** crystallized out of the solution and were separated by filtration. Yield 304 mg (43.7%). Anal. Calcd for $C_{31}H_{38}N_3O_6Ru$: C, 57.31; H, 5.91; N, 6.47. Found: C, 57.20; H, 6.53; N, 6.26.

[Ru^{II}(trpy)(4ClSQ)(OAc)] (2). This complex was prepared in a procedure analogous to that described above for **1**. Yield 314 mg (51.6%). Anal. Calcd for $C_{23}H_{19}N_3O_5ClRu$: C, 49.87; H, 3.45; N, 7.58. Found: C, 50.16; H,3.32; N, 7.67.

[Ru^{III}(trpy)(Bu_2SQ)(OH_2)](ClO_4)$_2$ (3).[4] Aqueous $HClO_4$ (70%, 0.25 ml) was added to a methanolic solution (10 mL) of **1** (50 mg, 0.081 mmol). The resultant deep blue solution was stirred overnight at room temperature. After 100 mg of sodium perchlorate and 10 mL of water were added to the solution, the mixture was allowed to stand at room temperature for a week. Deep blue needles of **3** crystallized out of the

solution and were separated by filtration. Yield 38.8 mg (61.7%). Anal. Calcd for $C_{29}H_{35}N_3O_{12}Cl_2Ru$: C, 44.11; H, 4.47; N, 5.32. Found: C, 44.37; H, 4.39; N, 5.31.

$[Ru^{III}(trpy)(4ClSQ)(OH_2)](ClO_4)_2$ (4). Aqueous $HClO_4$ (70%, 0.25 mL) was added to a water/ethylene glycol dimethyl ether solution (1:1 v/v, 6 mL) of **2** (53 mg, 0.080 mmol). The resultant blue purple solution was stirred overnight at room temperature. The volume of the solvent was reduced to about one-forth under N_2 gas flow. Dark purple **4** precipitated out of the solution and was separated by filtration. Yield 32.0 mg (48.9%). Anal. Calcd for $C_{21}H_{20}N_3O_{13}Cl_3Ru$: C, 34.56; H, 2.76; N, 5.76. Found: C, 34.65; H, 2.39; N, 5.79.

$[Ru^{II}(trpy)(Bu_2SQ)O^{\bullet -}]$ (5). A water-methanol solution (1:1 v/v, 40 mL) of **3** (50 mg 0.065 mmol) was dropped to an aqueous NaOH solution (4 M, 20 mL), and the solution was stirred overnight. Then solution was allowed to stand under N_2 flow. Reddish purple needles of **5** crystallized out of the solution, were separated by filtration, and washed with cold water. 16.8 mg (45.6%). Anal. Calcd for $C_{29}H_{33}N_3O_4Ru$: C, 59.17; H, 5.65; N, 7.14. Found: C, 59.02; H, 5.81; N, 7.07.

X-ray Crystallography. Data of **1**, **3**, and **5** were collected on a Rigaku/MSC Mercury CCD diffractometer using graphite monochromated Mo-Kα radiation (λ = 0.71070 Å). In order to determine the cell constants and the orientation matrix, four oscillation photographs were taken with an oscillation angle 0.5˚. The images for intensity data were collected at a temperature of -100 $\pm$ 1 ˚C to a maximum 2θ value of 55.0˚. Each image was taken twice and averaged. Finally, a total of 720 oscillation images were collected. The first sweep of data was done using ω scans from -70.0 to 110.0˚ in 0.5˚ step, at χ= 45.0˚ and ϕ= 0.0˚. The second sweep of data was done using ω scans from -70.0 to 110.0˚ in 0.5˚ step, at χ= 45.0˚ and ϕ= 90.0˚. The detector swing

angle was 20.0˚. The crystal-to-detector distance was 45.0 mm.

The structures were solved by heavy-atom Patterson methods[9] for **1**, direct method SIR92[10] for **3** and **5**, and expanded using Fourier techniques.[11] The non-hydrogen atoms were refined anisotropically. Hydrogen atoms were included at geometrically determined positions (C-H 0.95 Å) but not refined. All calculations were performed using the teXsan[12] crystallographic software package of Molecular Structure Corporation.

X-ray Photoelectron Spectroscopy. X-ray photoelectron spectra (XPS) were recorded on VG Scientific Ltd. ESCA LAB MK II. Mg Kα radiation (1253.6 eV) operated at 14.5 kV and 20 mA was used as an X-ray excitation source. All samples were deposit on gold foil from CH_2C1_2 solutions. The C 1s peak was assigned as the value of 284.6 eV and used the internal reference.

3, Results and Discussion

3-1 Syntheses of Ruthenium Dioxolene Complexes

Preparation of $[Ru^{II}(trpy)(Bu_2SQ)(OAc)]$ (**1**) has been reported elsewhere,[7] but a little modification was carried out to improve the purity of the complex, because the reaction of catechol with $[Ru^{III}(trpy)Cl_3]$ in methanol gave a mixture of $[Ru^{II}(trpy)(R_nSQ)Cl]$ and $[Ru^{II}(trpy)(R_nSQ)(OAc)]$. Treatment of $[Ru^{III}(trpy)Cl_3]$ with $AgBF_4$ in acetone to remove Cl ions produced $[Ru^{II}(trpy)(actone)_3]^{2+}$.[8] Addition of a catechol derivative (R_nCatH_2) and 10 equiv of KOAc to the methanolic solution of $[Ru(trpy)(actone)_3]^{2+}$ gave a mixture of $[Ru^{II}(trpy)(R_nSQ)(OAc)]$ and $[Ru^{III}(R_nSQ)_3]$. Silica Gel column chromatography was applied for the separation of the mixture. The purity of $[Ru^{II}(trpy)(R_nSQ)(OAc)]$ was improved, though the yield slightly decreased compared with the procedure previously reported. In this work, the author synthesized $[Ru^{II}(trpy)(Bu_2SQ)(OAc)]$ (**1**) and $[Ru^{II}(trpy)(4ClSQ)(OAc)]$ (**2**). The former was recrystallized from methanol. ORTEP view of **1** is shown in Figure 1A, crystallographic data, bond lengths, and bond angles are in Appendix section, respectively.

Hydrolysis of **1** under strong acidic conditions produced the blue violet aqua-Ru(III)-semiquinone complex, $[Ru^{III}(trpy)(Bu_2SQ)(OH_2)]^{2+}$ (**3**), which was isolated as single crystals of a perchlorate salt. ORTEP view of complex **3** is shown in Figure 1B. Crystallographic data, bond lengths, and bond angles are summarized in Appendix, respectively.

Preparation of $[Ru^{III}(trpy)(4ClSQ)(OH_2)](ClO_4)_2$ (**4**) was also conducted by hydrolysis of **2** in water/ethylene glycol dimethyl ether solution (1:1 v/v) under strong

acidic conditions as similar to those of **3** in methanol.

The aqua complex **3** is soluble in H_2O and the pK_a value of the aqua ligand of **3** was determined as 5.5 by means of pH titration and changes of the electronic absorption spectra in H_2O at 25 °C. We observed the occurrence of the second deprotonation of **3** at pH higher than 10, but reddish purple solids precipitated out of the aqueous solution in that pH region. The doubly deprotonated form of **3** was not soluble in H_2O, but it was soluble in a CH_3OH/H_2O mixture. We have successfully isolated the doubly deprotonated form of **3** as reddish purple crystals of neutral $[Ru^{II}(trpy)(Bu_2SQ)O^{\bullet-}]$ (**5**) by slow evaporation of CH_3OH from a CH_3OH/H_2O (1:2 v/v) solution of **3** in the strong basic conditions. ORTEP view of **5** is shown in Figure 1C, crystallographic data and bond lengths and bond angles are summarized in Appendix. Treatment of **5** with 2.0 equiv of $HClO_4$ in CH_2Cl_2 regenerated **3** quantitatively. Moreover, the complex **5** has semiquinone and oxyl radical ligands (described in chapter 4), which show the ferromagnetic interaction.

3-2 X-ray Crystal Structures of $[Ru^{II}(trpy)(Bu_2SQ)(OAc)]$ (1), $[Ru^{III}(trpy)(Bu_2SQ)(OH_2)](ClO_4)_2$ (3), and $[Ru^{II}(trpy)(Bu_2SQ)O^{\bullet -}]$ (5)

Figure 1 shows the ORTEP views of complex **1**, **3**, and **5**. Selected bond lengths and angles shown in table 1. There are two possible isomers with respect to the orientation of 3,5-di-*tert*-butyldioxolene ligands of **1**, **3**, and **5**, however, complexes depicted in Figure 1, predominantly crystallized under experimental conditions. These three complexes have a similar configuration; three nitrogen atoms of trpy and one oxygen of dioxolene are bonded to Ru in the equatorial plane, and the remaining one oxygen of dioxolene and another oxygen atom of acetato (**1**), aqua (**3**), or oxyl radical (**5**) ligand are linked to the central metal in the axial position.

Carbon-oxygen bond lengths of dioxolene ligand reflect the charge distribution of metal-dioxolene complexes.[1,2] The two C-O bond distances (C1-O1 and C2-O2) of the dioxolene ligands of **1**, **3** and **5** are (1.328(4) and 1.324(4) Å), (1.293(5)Å and 1.280(5)Å), and (1.35(1) and 1.34(1) Å), respectively. Thus, the C-O bond distances of **1** and **5** are apparently longer than those of **3**. The latter is associated with coordinated semiquinone of $[Ru^{III}(3ClPy)_2(Bu_2SQ)_2]^+$ (3Clpy = 3-chloropyridine, 1.29 Å).[3] On the other hand, C-O bond lengths of $[Ru^{II}(Bu_2SQ)]$ complexes vary in wide ranges; for example, $[Ru^{II}(trpy)(Bu_2SQ)Cl]$ (1.33(2) and 1.30(2) Å, 1.26(2) and 1.33(2) Å; two isomers),[7] and $[Ru^{II}(trpy)(36Bu_2SQ)(CO)]$ ($36Bu_2SQ$ = 3,6-di-*tert*-butyl -1,2-benzosemiquinone, 1.283(9) and 1.301(8) Å).[13] The C1-O1 and C2-O2 bond lengths of **5** (1.35(1) and 1.34(1) Å) are longer than those of **1**, but appear to be somewhat shorter than analogous aqua-metal complexes with Bu_2Cat such as $[Cr(trpy)(Bu_2Cat)(OH_2)](ClO_4)$ (1.361(3) and 1.377(3) Å) and $[Cr(metacn)(Bu_2Cat)(OH_2)](ClO_4)$ (metacn = 1,4,7-trimethyl-1,4,7- triazacyclononane),

1.366(3) and 1.364(3) Å).[14] Although the electronic structures of **1**, **3** and **5** are not clearly defined by the C-O bond lengths, **1** and **5** showed strong CT band at 870 nm, which was observed at 600 nm in the electronic spectrum of **3** (*vide infra*). Based on the fact that CT bands emerged around 600 and 800 nm are associated with the oxidation states of eq 1 and 2, respectively,[1,2] the actual stucture of **3** is close to the $[Ru^{III}(SQ)]$ structure of eq 2, and those of **1** and **5** lie to the $[Ru^{II}(SQ)]$ ones in eq 3.

The Ru-OH_2 bond length (Ru-O3) of **3** (2.099(3) Å) is shorter than that of analogous aqua complexes of $[Ru^{II}(trpy)(bpy)(OH_2)](ClO_4)_2$ (2.136(5) Å)[15] and $[Ru^{II}(dppe)(CO)(OSO_2CF_3)_2(OH_2)]$ (dppe = 1,2-bis(diphenylphosphino)ethylene, 2.198(5) Å)[16] and $[Ru^{II}(Tp^{iPr})(THF)(X)(OH_2)]^{n+}$ (Tp^{iPr} = hydrotris-(3,5-diisopropylpyrazolyl)borate, X = THF, OH_2, py, *t*-BuCN, =C=(H)$SiMe_3$, etc., 2.106(3)-2.189(6) Å).[17] The most striking character of the molecular structure of **5** is the Ru-O bond length of 2.043(7) Å, that is shorter than Ru-OH_2 bond distance of **3** but much longer than that of Ru-OH and Ru=O bond length reported so far; $[Ru^{III}(metacn)(acac)(OH)](PF_6)$ (1.971(9) Å)[18] for Ru-OH, and $[Ru^{IV}(bpy)(DAMP)O](ClO_4)_2$ (DAMP = 2,6-bis((dimethylamino)methyl)pyridine, 1.805(3) Å),[19] $[Ru^{IV}Cl(py)_4O]ClO_4$ (1.862(8) Å),[20] and $[Ru^{IV}X(TMC)O]^+$ (TMC = 1,4,8,11-tetramethyl-1,4,8,11-tetraazacyclotetradecane, X = Cl, N_3 and NCO, 1.765(5) Å)[21] for Ru=O. The Ru-oxyl bond of **5,** therefore, is classified as a single bond rather than a double bond. Thus, the neutral complex **5** is the first example of a terminal metal-O complex with a single bond character.

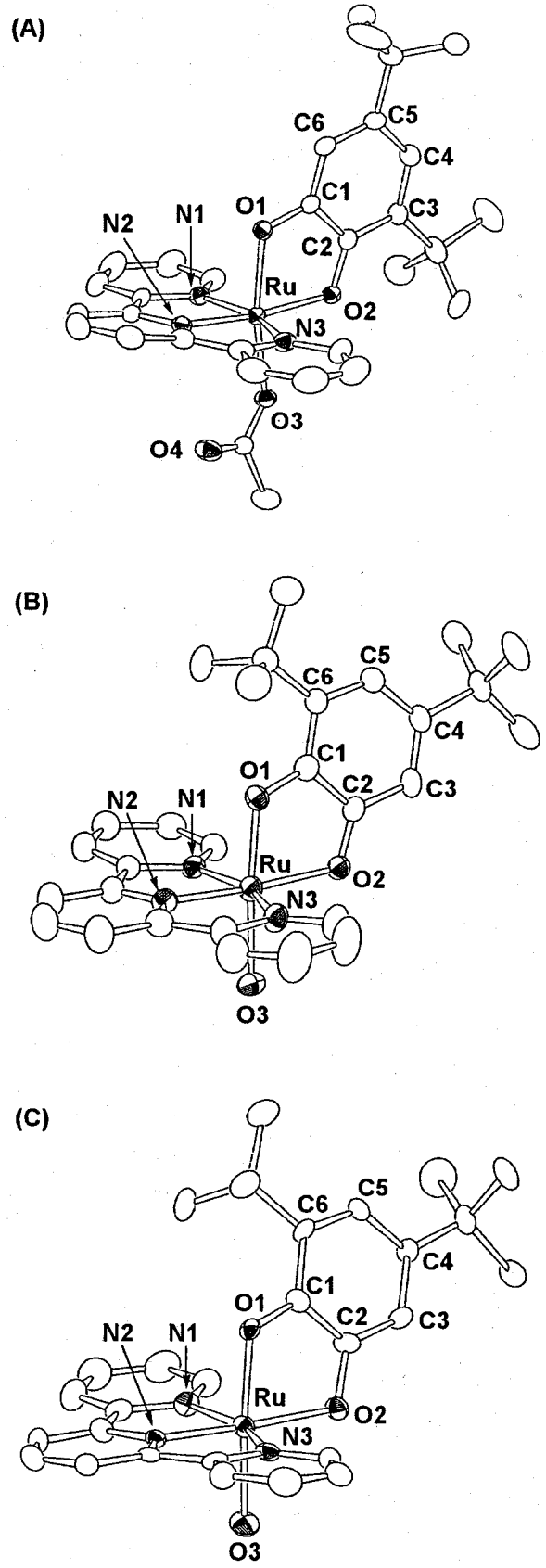

Figure 1. Crystal structures of **1** (A), **3** (B), and **5** (C) with labeling for selected atoms. All hydrogen atoms are omitted for clarity.

Table 1. Selected Bond Lengths (Å) for Complexes **1**, **3** and **5**

	1	**3**	**5**
Ru-O1	2.030(3)	1.968(3)	1.985(6)
Ru-O2	2.019(3)	2.028(3)	2.058(6)
Ru-O3	2.062(3)	2.099(3)	2.043(7)
Ru-N1	2.050(3)	2.063(4)	2.071(8)
Ru-N2	1.952(3)	1.959(4)	1.945(8)
Ru-N3	2.056(3)	2.059(4)	2.050(8)
C1-O1	1.328(4)	1.293(5)	1.35(1)
C2-O2	1.324(4)	1.280(5)	1.34(1)
C1-C2	1.430(5)	1.466(6)	1.43(1)
C2-C3	1.421(5)	1.420(6)	1.39(1)
C3-C4	1.392(5)	1.357(7)	1.38(1)
C4-C5	1.430(5)	1.454(6)	1.39(1)
C5-C6	1.383(5)	1.365(6)	1.39(1)
C6-C1	1.396(5)	1.423(6)	1.44(1)

3-3 X-ray Photoelectron Spectra

The C-O bond distances of coordinated dioxolene of **1**, **3** and **5** did not always define the oxidation states of the ligands. So, the author measured X-ray photoelectron spectra (XPS) in the range 274-296 eV to clarify the oxidation states of Ru of these complexes. Peaks occurred in this region due to ruthenium (Ru $3d_{3/2}$ and Ru $3d_{5/2}$) and carbon (C 1s) electron transition. XPS data of the complex **1**, **3**, and **5** are shown in Figure 2. Binding energy for the Ru $3d_{5/2}$ peaks of the dioxolene complexes **1**, **2**, **3**, and **5** are listed in Table 2. For each complex, the Ru $3d_{3/2}$ peak could not be observed clearly, because the C 1s peak overlapped on the $Ru_{3/2}$ peak. The Ru $3d_{5/2}$ binding energies of **1** and **5** were 280.5 eV and 280.4 eV, respectively, which are good agreement with the values for Ru^{II} $3d_{5/2}$ such as $[Ru^{II}(bpy)_2C1_2]$ (280.1 eV)[22] and $[Ru^{II}(3Clpy)_2(Bu_2SQ)_2]$ (280.4 eV).[23] Thus, **1** and **5** apparently have the Ru^{II} cores. The complex **3** showed the $Ru_{5/2}$ peak at 281.5 eV. This value is significantly larger than those of Ru^{II} complexes and smaller than those of $[Ru^{III}(bpy)_2Cl_2]Cl$ (282.1 eV)[22] and $[Ru^{III}(NH_3)_6]C1_3$ (282.1 eV).[24] On the other hand, not only the C-O_{av} bond distance of the dioxolene ligand (1.29 Å) but also the binding energy of **3** are quite close to those of $[Ru^{III}(3Clpy)_2(Bu_2SQ)_2]ClO_4$ (281.4 eV),[23] indicating that **3** has the $[Ru^{III}(Bu_2SQ)]$ framework. The fact that the binding energy of the $[Ru^{III}(Bu_2SQ)]$ core lies on the boundary between normal Ru^{II} and Ru^{III} complexes may reflect an occurrence of the resonance of eq 2.

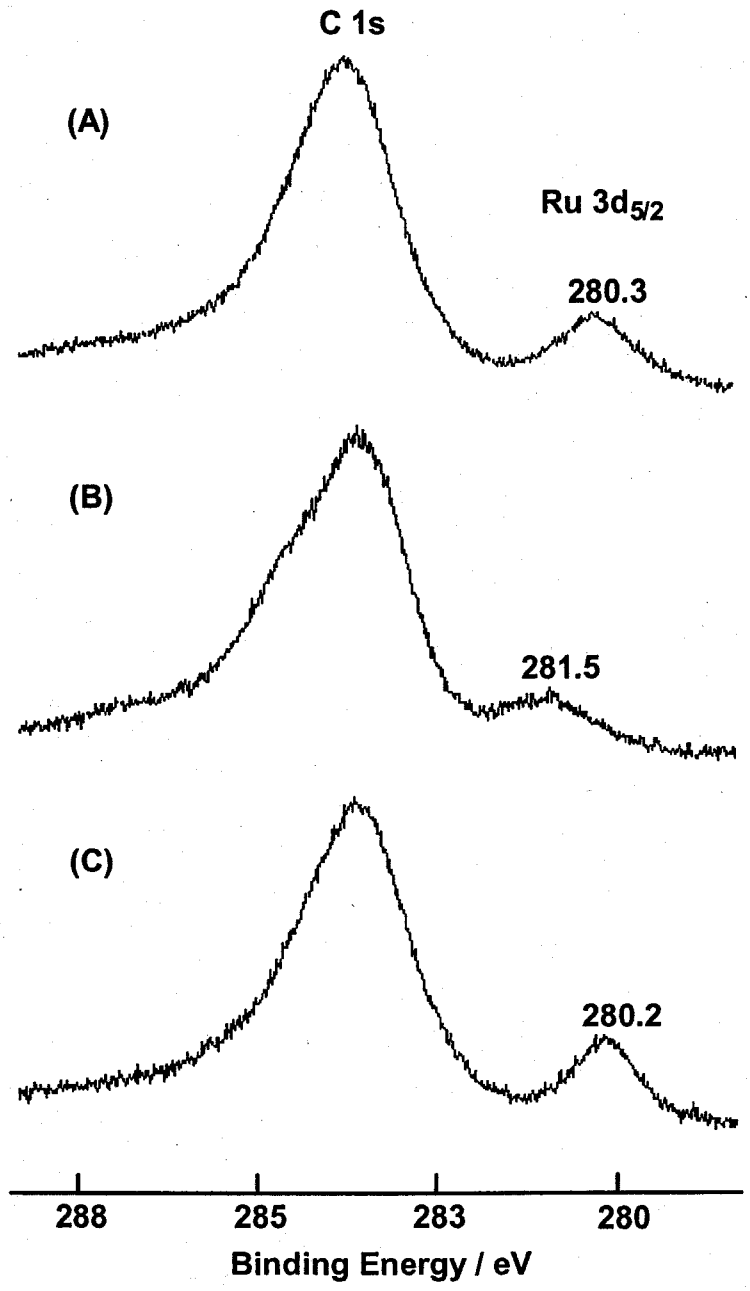

Figure 2. XPS of **1** (A), **3** (B), and **5** (C) showing the binding energies of Ru $3d_{5/2}$ and C 1s. The C 1s reference peak is defined as 284.6 eV in all cases.

Table 2. Ruthenium $3d_{5/2}$ Binging Energies

Complex	Ru $3d_{5/2}$ (eV)	ref.
$[Ru^{II}(trpy)(Bu_2SQ)(OAc)]$	280.5	*a*
$[Ru^{II}(trpy)(4ClSQ)(OAc)]$	280.4	*a*
$[Ru^{III}(trpy)(Bu_2SQ)(OH_2)](ClO_4)_2$	281.5	*a*
$[Ru^{II}(trpy)(Bu_2SQ)O^{\bullet-}]$	280.4	*a*
$[Ru^{II}(bpy)_2Cl_2]$	280.1	22
$[Ru^{II}(3Clpy)_2(Bu_2SQ)_2]$	280.4	23
$[Ru^{III}(bpy)_2Cl_2]Cl$	282.1	22
$[Ru(NH_3)_6]Cl_3$	282.1	24
$[Ru^{III}(3Clpy)_2(Bu_2SQ)_2]ClO_4$	281.4	23

[a] This work

4, References

(1) (a) Pierpont, C. G.; Buchanan, R. M. *Coord. Chem. Rev.* **1981**, *38*, 45. (b) Pierpont, C. G.; Lange, C. W. *Prog. Inorg. Chem.* **1994**, *41*, 331.

(2) (a) Haga, M.; Dodsworth, E. S.; Lever, A. P. B.; Boone, S. R.; Pierpont, C. G. *J. Am. Chem. Soc.* **1986**, *108*, 7413. (b) Boone, S. R.; Pierpont, C. G. *Inorg. Chem.* **1987**, *26*, 1769. (c) Bhattacharya, S.; Pierpont, C. G. *Inorg. Chem.* **1991**, *30*, 1511. (d) Bhattacharya, S.; Pierpont, C. G. *Inorg. Chem.* **1992**, *31*, 35. (e) Bhattacharya, S.; Pierpont, C. G. *Inorg. Chem.* **1994**, *33*, 6038. (f) Sugimoto, H.; Tanaka, K. *J. Organomet. Chem.* **2001**, *622*, 280.

(3) Boone, S. R.; Pierpont, C. G. *Polyhedron* **1990**, *9*, 2267.

(4) K. Tsuge, K. Tanaka, *Chem. Lett.*, **1998**, 1069; K. Tsuge, M. Kurihara, K. Tanaka, *Bull. Chem. So. Jpn.*, **2000**, *73*, 607.

(5) Wada, T.; Tsuge, K.; Tanaka, K. *Chem. Lett.* **2000**, 910.

(6) (a) Wada, T.; Tsuge, K.; Tanaka, K. *Angew. Chem., Int. Ed.* **2000**, *39*, 1479. (b) Wada, T.; Tsuge, K.; Tanaka, K. *Inorg. Chem.* **2001**, *40*, 329.

(7) Kurihara, M.; Daniele, S.; Tsuge, K.; Sugimoto, H.; Tanaka, K. *Bull. Chem. Soc. Jpn.* **1998**, *71*, 867.

(8) Gourdon, A.; Launay, J.-P. *Inorg. Chem.* **1998**, *37*, 5336.

(9) PATTY: Beurskens, P. T.; Admiraal, G.; Beurskens, G.; Bosman, W. P.; de Gelder, R.; Israel, R.; Smits, J. M. M. (1994). The DIRDIF-94 program system, Technical Report of the Crystallography Laboratory, University of Nijmegen, The Netherlands.

(10) SIR92: Altomare, A.; Burla, M. C.; Camalli, M.; Cascarano, M.; Giacovazzo, C.;

Guagliardi, A.; Polidori, G. *J. Appl. Cryst.* **1994**, *27*, 435.

(11) DIRDIF94: Beurskens, P. T.; Admiraal, G.; Beurskens, G.; Bosman, W. P.; de Gelder, R.; Israel, R.; Smits, J. M. M. (1994). The DIRDIF-94 program system, Technical Report of the Crystallography Laboratory, University of Nijmegen, The Netherlands.

(12) teXsan: Crystal Structure Analysis Package, Molecular Structure Corporation (1985 & 1992).

(13) Sugimoto, H.; Tanaka, K. *J. Organomet. Chem.* **2001**, *622*, 280.

(14) Shiren, K.; Tanaka, K. Inorg. Chem. **2002**, *41*, 5912.

(15) Seok, W. K.; Kim, M. Y.; Yokomori, Y.; Hodgson, D. J.; Meyer, T. J. *Bull. Korean Chem. Soc.* **1995**, *16*, 619.

(16) Mahon, M. F.; Whittlesey, M. K.; Wood, P. T. *Organometallics* **1999**, *18*, 4068.

(17) Takahashi, Y.; Akita, M.; Hikichi, S.; Moro-oka, Y. *Inorg. Chem.* **1998**, *37*, 3186.

(18) Schneider, R.; Weyhermüller, T.; Wieghardt, K. *Inorg. Chem.* **1993**, *32*, 4925.

(19) Welch, T. W.; Ciftan, S. A.; White, P. S.; Thorp, H. H. *Inorg. Chem.* **1997**, *36*, 4812.

(20) Yukawa, Y.; Aoyagi, K.; Kurihara, M.; Shinai, K.; Shimizu, K.; Mukaida, M.; Takeushi, T.; Kakihara, H. *Chem. Lett.* **1985**, 283.

(21) Che, C.-M.; Lai, T.-F.; Wong, K.-Y. *Inorg. Chem.* **1987**, *26*, 2289.

(22) Weaver, T. R.; Meyer, T. J.; Adeyemi, S. A.; Brown, G. M.; Eckberg, R. P.; Hatfield, W. E.; Johnson, E. C.; Murray, R. W.; Untereker, D. *J. Am. Chem. Soc.* **1975**, *97*, 3039.

(23) Aubern, P. R.; Dodsworth, E. S.; Haga, M.; Liu, W.; Nevin, W. A.; Lever, A. P. B. *Inorg. Chem.* **1991**, *30*, 3502.

(24) Shepherd, R. E.; Proctor, A.; Henderson, W. W.; Myser, T. K. *Inorg. Chem.* **1987**, *26*, 2440.

Chapter 3

Redox Behavior of Aqua Ruthenium Dioxolene Complexes Coupled with Acid-base Equilibrium of the Aqua Ligand

(Katsuaki Kobayashi, Hideki Ohtsu, Tohru Wada, and Koji Tanaka, *Chem. Lett.* 2002, 868.)

1, Introduction

Water molecules linked to a metal ion dissociates one or two protons to yield hydoroxo or oxo moieties. Meyer et al. synthesized series of high-valent oxoruthenium complexes with polypyridyl ligands by the deprotonation of aqua ligands coupled with the oxidation of a ruthenium ion.[1] Deprotonation of aqua ligand results in the increase of electron donation to central ruthenium ion from linked oxygen. Therefore, the oxidation of a ruthenium ion takes place in a relatively narrow potential range.

Deprotonation of aqua-Ru-dioxolene complex, $[Ru^{III}(trpy)(Bu_2SQ)(OH_2)](ClO_4)_2$ (**3**) in acetone have been briefly reported.[2] Addition of base such as KOBu to the acetone solution of complex **3** was reduced Ru-dioxolene moiety from Ru^{III}-semiquinone ($[Ru^{III}(SQ)]$) to Ru^{II}-semiquinone ($[Ru^{II}(SQ)]$). The change was monitored by the electronic absorption spectra and cyclic voltammetry. The spectral change finished upon the addition of ca. 1.7 equiv of base, and fully recovered the original spectrum by the addition of same equiv of acid. It indicated that the aqua ligand dissociated one or two protons coupled with the reduction of $[Ru^{III}(SQ)]$ moiety. Therefore it was presumed that the deprotonation of aqua/hydoroxo ligand causes electron transfer from the resultant OH^-/O^{2-} to $[Ru^{III}(SQ)]$ moiety yielding hydroxo radical ($OH^{\bullet}$)/oxyl radical ($O^{\bullet-}$) and $[Ru^{II}(SQ)]$. The details of the electronic structure of Ru^{II}-semiquinone hydroxo or oxyl radical complex, however, have remained unclear.

In this chapter, the author reports the detailed study of the electronic absorption and resonance Raman spectra, and redox behaviors (cyclic voltammetry) of aqua ruthenium complexes containing a dioxolene ligand, $[Ru^{III}(trpy)(Bu_2SQ)(OH_2)](ClO_4)_2$ (**3**) and

$[Ru^{III}(trpy)(4ClSQ)(OH_2)](ClO_4)_2$ (**4**).

2, Experimental Section

Materials. 2-Methoxyethanol solutions of *t*-BuOK and $HClO_4$ (0.1 M) were used as a base and an acid.

Electronic absorption spectra. Electronic absorption spectra were recorded on a Shimadzu UV-3100PC spectrometer at 298 K.

Cyclic Voltammetry. Cyclic voltammograms of the complexes were obtained in CH_2Cl_2 containing 0.1 M of tetra-*n*-butylammonium perchlorate (TBAP) as a supporting electrolyte at 298 K by using a three electrode system under deaerated conditions and a ALS/chi Electrochemical Analyzer Model 660. A glassy-carbon plate and platinum wire were used as a working electrode and a counter electrode, respectively. All potentials were recorded against an SCE reference electrode.

Resonance Raman spectra. Resonance Raman spectra were obtained using an excitation at 632.8 nm with He-Ne laser or at 704.3 nm with DCM dye laser, and detected with a JASCO NR-1800 triple polychromator equipped with a liquid-nitrogen-cooled Princeton Instruments CCD detector. Raman measurements were carried out with a spinning cell and the laser power was adjusted to 7 mW (632.8 excitation) and 30 mW (704.3 excitation) at the sample point. Raman shifts were calibrated using dichloromethane with the accuracy of the peak positions of the Raman bands being ± 1 cm^{-1}.

3, Results and Discussion

3-1 Electronic Absorption Spectra.

The electronic absorption spectra of $[Ru^{III}(trpy)(Bu_2SQ)(OH_2)](ClO_4)_2$ (**3**) in water at pH 3.2 showed a strong absorption band at λ_{max} = 600 nm (ε = 13800 $M^{-1}cm^{-1}$) (Figure 1A(a)). An increase of pH of the solution shifted the band maximum from 600 nm to 576 nm, and the absorbance at 576 nm reached the maximum at pH 7.1. Further alkalization of the solution resulted in an appearance of another band at 870 nm with decreasing the absorbance at the 576 nm band (Figure 1A). The intensity of 870 nm band observed at pH higher than 10 is much weaker than the 600 nm band of **3**, because of the insolubility of $[Ru^{II}(trpy)(Bu_2SQ)O^{\bullet-}]$ (**5**)**,** that is the doubly deprotonated form of **3**, in H_2O.

Although the solubility of **5** was too low to monitor the conversion from **3** to **5** in water, two successive equilibria of **3** were clearly observed in CH_2Cl_2 in the presence of various amounts of *t*-BuOK as a base (Figure 1B). A strong absorption band at 600 nm (ε = 16800 $M^{-1}cm^{-1}$) of **3** shifts to 576 nm upon a gradual addition of a 2-methoxyethanol solution of *t*-BuOK to the CH_2Cl_2 solution. The shift of the absorbance band around 600 nm reaches to 576 nm (ε = 16700 $M^{-1}cm^{-1}$) in the presence of 1.0 equiv of *t*-BuOK. Further addition of *t*-BuOK to the solution decreases the absorption of the 576 nm band, and a new band emerges at 870 nm. The 576 nm band almost disappeared in the presence of more than 3.0 equiv of *t*-BuOK. In addition, two isosbestic points are observed at 720 and 657 nm in these two-step spectral changes. Moreover, acidification by an addition of 3.0 equiv of $HClO_4$ in 2-methoxyethanol to

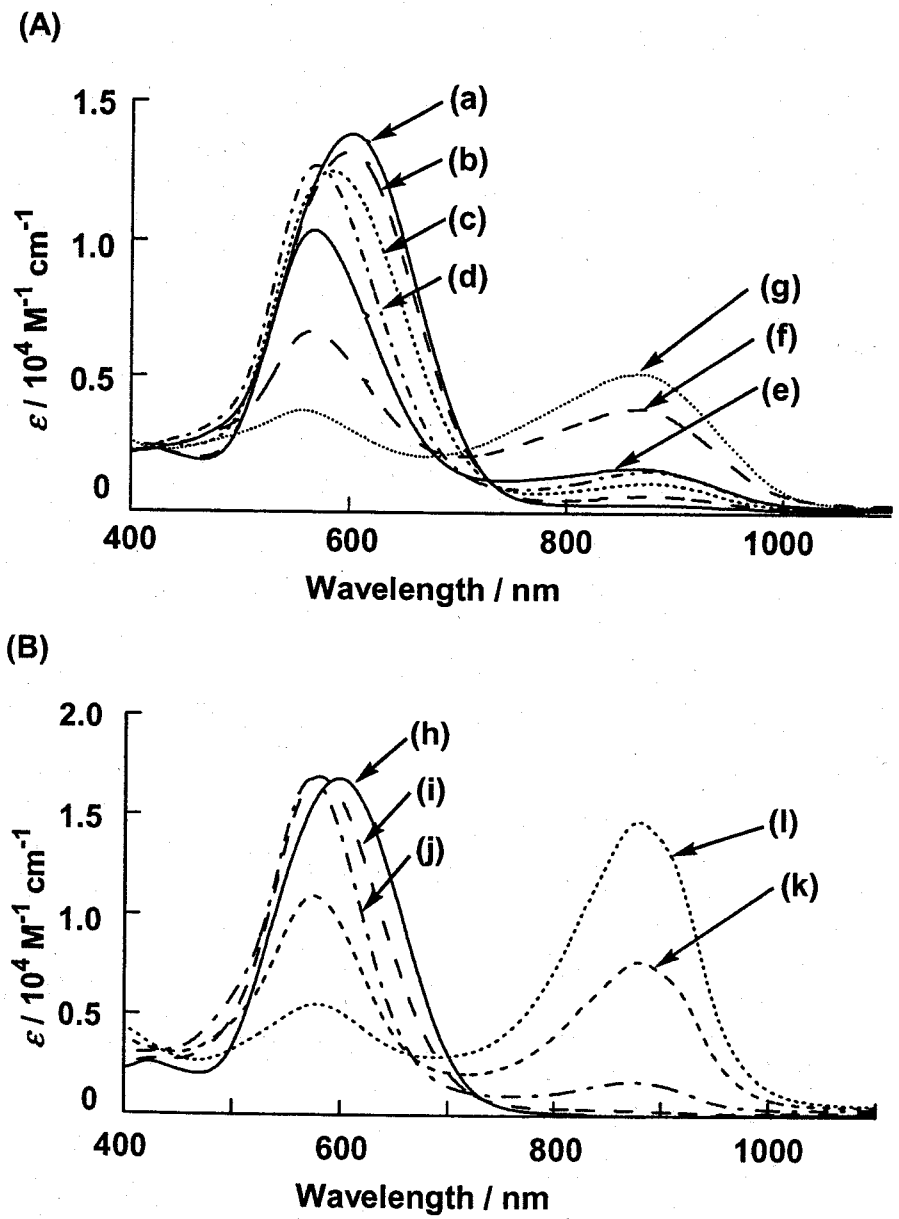

Figure 1. (A) pH dependent electronic absorption spectra of **3** (pH 3.2, (a); pH 4.5, (b); pH 5.6, (c); pH 7.1, (d); pH 10.1, (e); pH 11.0, (f); pH 12.0, (g)). (B) Electronic absorption spectra of **3** in the presence of various amounts of *t*-BuOK (0 equiv, (h); 0.5 equiv, (i); 1.0 equiv, (j); 2.0 equiv, (k); 3.0 equiv, (l)) in CH_2Cl_2.

the solution fully recovered the electronic absorption spectrum of **3** (λ_{max} = 600 nm, ε = 16800 M^{-1} cm^{-1}). Thus, the absorption maximum of **3** at 600 nm reversibly shifts to 576 nm and then to 870 nm in the presence of less than and more than 1.0 equiv of *t*-BuOK, respectively. Moreover, **5** obtained as single crystals also exhibited the same strong band at 870 nm in CH_2Cl_2, which completely disappeared by an addition of 2.0 equiv of $HClO_4$ and the 600 nm band of **3** was completely recovered.

The charge distribution between the $[Ru^{II}(Q)]$ and $[Ru^{III}(SQ)]$ frameworks (eq 1) and their one-electron reduced forms (eq 2) ($[Ru^{II}(SQ)]$ and $[Ru^{III}(Cat)]$) is associated with characteristic CT bands around 600 nm and 850 nm respectively.[3,4,5,6] In fact,

$$[Ru^{II}(Q)] \longleftrightarrow [Ru^{III}(SQ)] \quad (1)$$

$$[Ru^{II}(SQ)] \longleftrightarrow [Ru^{III}(Cat)] \quad (2)$$

$[Ru^{III}(trpy)(Bu_2SQ)Cl]^+$ and $[Ru^{III}(trpy)(Bu_2SQ)(OAc)]^+$ exhibit the CT bands at 592 nm (ε = 15500 $M^{-1}cm^{-1}$) and 584 nm (ε = 17000 $M^{-1}cm^{-1}$),[6] while $[Ru^{II}(bpy)_2(Bu_2SQ)]^+$ and $[Ru^{II}(trpy)(Bu_2SQ)(OAc)]$ show those bands at 843 nm (ε = 15500 $M^{-1}cm^{-1}$)[7a] and 883 nm (ε = 18600 $M^{-1}cm^{-1}$),[6] respectively. The shift of the CT band of **3** from 600 nm to 576 nm in the presence of less than 1.0 equiv of *t*-BuOK is simply explained by the formation of $[Ru^{III}(trpy)(Bu_2SQ)(OH^-)]^+$ (eq 3). Accordingly, the appearance of

$$\underset{\mathbf{3}}{[Ru^{III}(trpy)(Bu_2SQ)(OH_2)]^{2+}} \underset{+H^+}{\overset{-H^+}{\rightleftharpoons}} [Ru^{III}(trpy)(Bu_2SQ)(OH)]^+ \underset{+H^+}{\overset{-H^+}{\rightleftharpoons}} \underset{\mathbf{5}}{[Ru^{II}(trpy)(Bu_2SQ)O^{\bullet -}]} \quad (3)$$

the 870 nm band in the treatment of $[Ru^{III}(trpy)(Bu_2SQ)(OH_2)]^{2+}$ with more than 2.0 equiv of *t*-BuOK is indication of the occurrence of one-electron reduction of the $[Ru^{III}(Bu_2SQ)]$ core of **3** affording the $[Ru^{II}(Bu_2SQ)]$ one. The X ray analysis and XPS

of **5** demonstrated (Chapter 2) that the complex is expressed by $[Ru^{II}(trpy)(Bu_2SQ)O^{\bullet-}]$ (eq 3) rather than $[Ru^{III}(trpy)(Bu_2Cat)O^{\bullet-}]$.

One-electron reduction of the $[Ru^{III}(Bu_2SQ)]$ moiety of $[Ru^{III}(trpy)(Bu_2SQ)(OH^-)]^+$ coupled with dissociation of the hydroxo proton is caused by intra-molecular electron transfer from the resultant negatively charged oxo group to Ru-dioxolene moiety. Thus, Ru-dioxolene plays the key role as the electron reservoir in the acid-base equilibrium of the hydroxo ligand of $[Ru^{III}(trpy)(Bu_2SQ)(OH^-)]^+$ (eq 3).

The electronic absorption spectrum of $[Ru^{III}(trpy)(4ClSQ)(OH_2)](ClO_4)_2$ (**4**) in water at pH 2.0 shows an absorption band at λ_{max} = 570 nm (ε = 10000 $M^{-1}cm^{-1}$) (Figure 2A(a)). The absorption band at 570 nm is changed to 873 nm (ε = 5900 $M^{-1}cm^{-1}$) by the alkalization of the solution until pH 6.0. Further alkalization of solution, the absorption band at 873 nm is shifted to 775 nm (ε = 3300 $M^{-1}cm^{-1}$) with decreasing in intensity (Figure 2B). Two isosbestic points are observed at 681 and 745 nm in these two-step spectral changes.

The spectral change of **4** in CH_2Cl_2 is different from that of one in water. The absorption spectrum of **4** displays the strong CT band at 567 nm (ε = 5600 M^{-1} cm^{-1}) in CH_2Cl_2 (Figure 3A(a)). The absorbance at the 567 nm band is decreased by an addition of *t*-BuOK to the solution and a new absorption band assignable to the CT of the $[Ru^{III}(Cat)]$ or $[Ru^{II}(SQ)]$ moiety emerges at 870 nm (ε = 3700 $M^{-1}cm^{-1}$), which become almost constant in the presence of ca. 1.0 equiv of *t*-BuOK. The treatment of **4** with 1.0 equiv of *t*-BuOK shifted the CT band from 567 to 870 nm and no other strong absorption band was detected in the electronic absorption spectra. Further addition of more than 1 equiv of base to the solution did not induce any spectral changes, which were substantially different from the spectral changes observed in water.

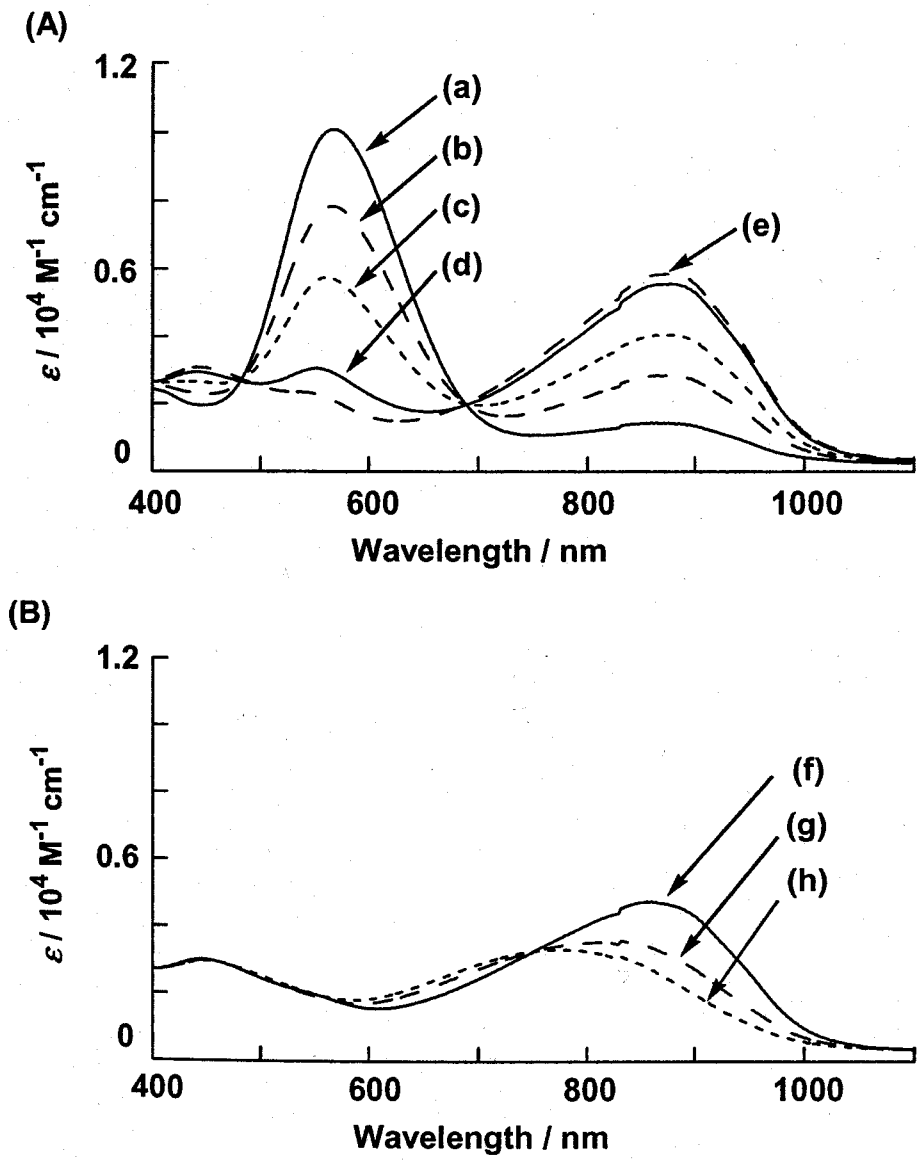

Figure 2. pH dependent electronic absorption spectra of **3**: (A) pH 2.0, (a); pH 3.1, (b); pH 4.2, (c); pH 5.1, (d); pH 6.0, (e): (B) pH 7.1, (f); pH 8.0, (g); pH 9.0, (g).

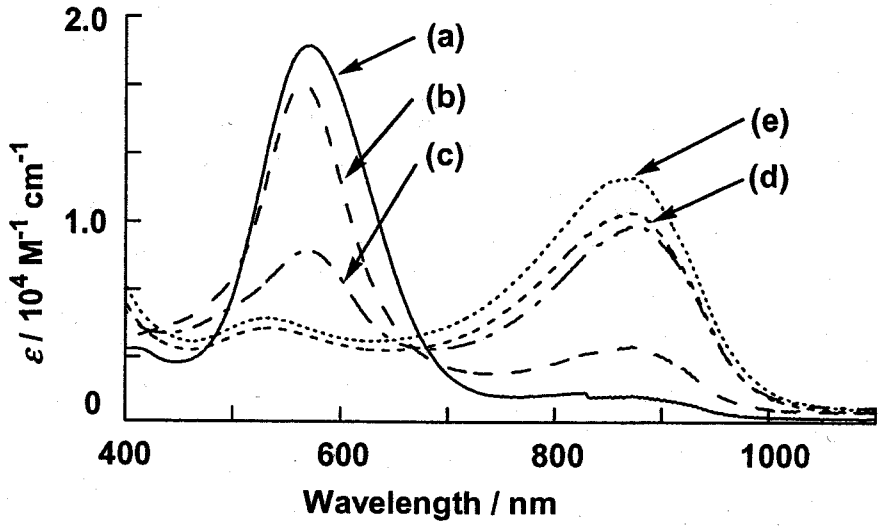

Figure 3. Electronic absorption spectra of **4** in the presence of various amounts of *t*-BuOK (0 equiv, (a); 0.25 equiv, (b); 0.5 equiv, (c); 0.75 equiv, (d); 1.0 equiv, (e)) in CH_2Cl_2.

Moreover, any isosbestic points are observed in CH_2Cl_2. These spectral changes are dramatically influenced by the solvents upon the second deprotonation. But, one-electron reduction of $[Ru^{III}(4ClSQ)]$ moiety of $[Ru^{III}(trpy)(4ClSQ)(OH_2)]^{2+}$ upon the deprotonation of an aqua ligand are observed in CH_2Cl_2 as well as in water. Therefore, the reduction of $[Ru^{III}(4ClSQ)]$ moiety of complex **4** is induced by the first deprotonation of the aqua ligand in contrast to the equilibrium of eq 2.

3-2 Resonance Raman Spectra.

3 and **4** have the strong CT band due to $[Ru^{III}(SQ)]$ moiety at 600 nm and 567 nm, respectively, in CH_2Cl_2. Resonance Raman (rR) spectrum of **3** in the same solvent with 632.8 nm excitation exhibit four strongly enhanced bands at 572, 590, 1167, and 1353 cm^{-1}, and five weakly enhanced peaks at 382, 440, 472, 524, and 1309 cm^{-1} (Figure 4A).

The rR pattern closely resembles that of $[Ru^{II}(bpy)_2(Bu_2Q)]^{2+}$ (516, 560, 585, 1072, 1125, and 1351 cm^{-1}).[7] According to the rR assignment of $[Ru^{II}(bpy)_2(Bu_2Q)]^{2+}$, the strong two bands at 572 and 590 cm^{-1} of **3** are correlated with Ru-O stretching modes coupled with the ν(C-C) and ring deformation modes, indicating strong electronic influence of the CT band on the Ru-O bonds ($[Ru^{II}(Bu_2Q)]$ or $[Ru^{III}(Bu_2SQ)]$). The remaining two enhanced peaks (1167 and 1353 cm^{-1}) are assigned to the stretching modes of the quinone ligand.[7] The Raman spectrum of **4** also is close to that of $[Ru^{II}(bpy)_2(Bu_2Q)]^{2+}$, but all observed peaks at 380, 440, 478, 521, 549, 590, 1160, and 1367 cm^{-1} are not so enhanced compared with the rR spectrum of **3**. This is because the wavelength of excitation laser of 632.8 nm is far from the CT band of **4** at 567 nm. The bands at 549 and 590 nm, and those at 1160 and 1367 cm^{-1} are also associated with

the stretching modes of Ru-O bonds and dioxolene ligands, respectively. Thus, the rR spectra of **3** and **4** also are identification of the resonance form of eq1.

As described in a previous section, **5** displays the strong CT band at 870 nm in CH_2Cl_2. No Raman peak of **5**, that was prepared by the reaction of **3** with 3.0 equiv of *t*-BuOK in CH_2Cl_2, was detected with 632.8 nm excitation, but the rR spectrum of **5** in the same solvent exhibited weakly enhanced 10 peaks at 503, 521, 556, 590, 1157, 1280, 1324, 1467, 1481, and 1497 cm^{-1} with 704.3 nm excitation (Figure 4B). The five bands at 1157, 1280, 1467, 1481, and 1497 cm^{-1} are tentatively associated with the stretching vibrations of the [Ru(trpy)] framework from the similarity of the rR spectra of $[Ru^{II}(trpy)_2](PF_6)_2$ which showed strong peaks as 1164, 1284, 1470, 1490, and 1549 cm^{-1} in CH_2Cl_2.[8] The four peaks at 503, 521, 556, and 590 cm^{-1} of **5** are correlated with the ν(Ru-O) bands coupled with the ν(C-C) bands of the ν(Bu_2SQ) by reference to the bands of Ru(II)-semiquinone complexes of $[Ru^{II}(bpy)_2(Bu_2SQ)]^+$ (519 and 551 cm^{-1})[7] and $[Ru^{II}(trpy)(Bu_2SQ)(OAc)]$ (**1**) (504, 521, 558, and 593 cm^{-1}). The remaining 1324 cm^{-1} peak of **5** is safely assigned to the ν(C-O) mode of the semiquinone, because the ν(C-O) bands of $[Ru^{II}(bpy)_2(Bu_2SQ)]$ and $[Ru^{II}(trpy)(Bu_2SQ)(OAc)]$ were observed at 1315 cm^{-1} and 1324 cm^{-1}, respectively. Similarly, the rR spectrum of **4** in CH_2Cl_2 in the presence of 3.0 equiv of *t*-BuOK exhibited quite weakly enhanced peaks at 467, 504, 533, and 1325 cm^{-1} due to the Ru(II)-semiquinone framework with 704.3 nm excitation, and the pattern was close to those of not only **5** but also $[Ru^{II}(bpy)_2(Bu_2SQ)]^+$ and $[Ru^{II}(trpy)(Bu_2SQ)(OAc)]$ in the same solvent.

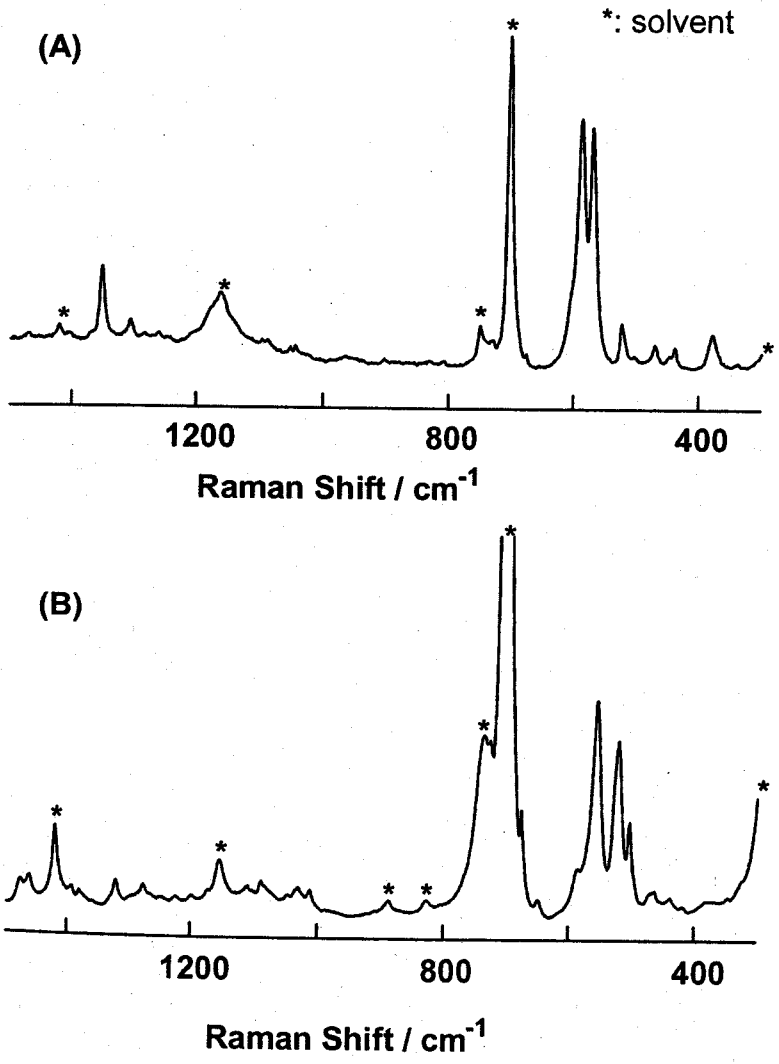

Figure 4. Resonance Raman spectra of **3** in CH_2Cl_2 at r.t.; 632.8 nm excitation (A) and 704.3 nm excitation (B) in the presence of 3.0 equiv of *t*-BuOK.

3-3 Electrochemistry.

The cyclic voltammograms (CVs) of **3** in the presence of various amounts of *t*-BuOK are shown in Figure 5. $E_{1/2}$ value and the rest potential (or equilibrium electrode potential) of the solution (E_{rest}) are summarized in Table 1.

The CV of **3** in CH_2Cl_2 exhibits two reversible redox waves at $E^{1a}{}_{1/2}$ = 0.31 V and $E^{1b}{}_{1/2}$ = –0.47 V (*vs.* SCE). Taking into account that **3**, the hydroxy complex and **5** have the $[Ru^{III}(Bu_2SQ)]$, $[Ru^{III}(Bu_2SQ)]$, and $[Ru^{II}(Bu_2SQ)]$ cores, respectively (eq 3), one electron reduction of **3** and the hydroxo complex is reasonably assumed to give the $[Ru^{II}(Bu_2SQ)]$ core rather than the $[Ru^{III}(Bu_2Cat)]$ one. The redox reactions of **3** at 0.31 V and –0.47 V, therefore, are associated with the $[Ru^{III}(Bu_2SQ)]^{2+}/[Ru^{II}(Bu_2SQ)]^{+}$ and $[Ru^{II}(Bu_2SQ)]^{+}/[Ru^{II}(Bu_2Cat)]$ couples. The addition of 1.0 equiv of *t*-BuOK into the solution resulted in disappearance of the $E^{1a}{}_{1/2}$ = 0.31 V and $E^{1b}{}_{1/2}$ = –0.47 V redox couples (Figure 5C). Instead, new two redox couples emerged at $E^{2a}{}_{1/2}$ = 0.07 V and $E^{2b}{}_{1/2}$ = –0.57 V assigned to the $[Ru^{III}(Bu_2SQ)]^{+}/[Ru^{II}(Bu_2SQ)]$ and the $[Ru^{II}(Bu_2SQ)]/[Ru^{II}(Bu_2Cat)]^{-}$ couples of $[Ru^{III}(trpy)(Bu_2SQ)(OH^{-})]^{+}$. The rest potential ($E_{rest}$) of **3** and $[Ru^{III}(trpy)(Bu_2SQ)(OH^{-})]^{+}$ in CH_2Cl_2 is 0.48 and 0.36 V, respectively, which also manifests the $[Ru^{III}(Bu_2SQ)]$ structure of both complexes, because the E_{rest} is located at potentials more positive than the $[Ru^{III}(Bu_2SQ)]^{2+}/[Ru^{II}(Bu_2SQ)]^{+}$ redox couple of both complexes ($E^{1a}{}_{1/2}$ = 0.31 V, $E^{2a}{}_{1/2}$ = 0.07 V). The redox couples at $E^{2a}{}_{1/2}$ = 0.07 V and $E^{2b}{}_{1/2}$ = –0.57 V of $[Ru^{III}(trpy)(Bu_2SQ)(OH^{-})]^{+}$ in CH_2Cl_2 were hardly influenced by the addition of more than 1.0 equiv of *t*-BuOK to the solution, but E_{rest} of the solution dramatically shifted from +0.48 to –0.17 V passing through the $[Ru^{III}(Bu_2SQ)]^{2+}/[Ru^{II}(Bu_2SQ)]^{+}$ redox couple at $E^{2a}{}_{1/2}$ = 0.07 V (Figure 5D). Unchanged redox potential upon the addition of

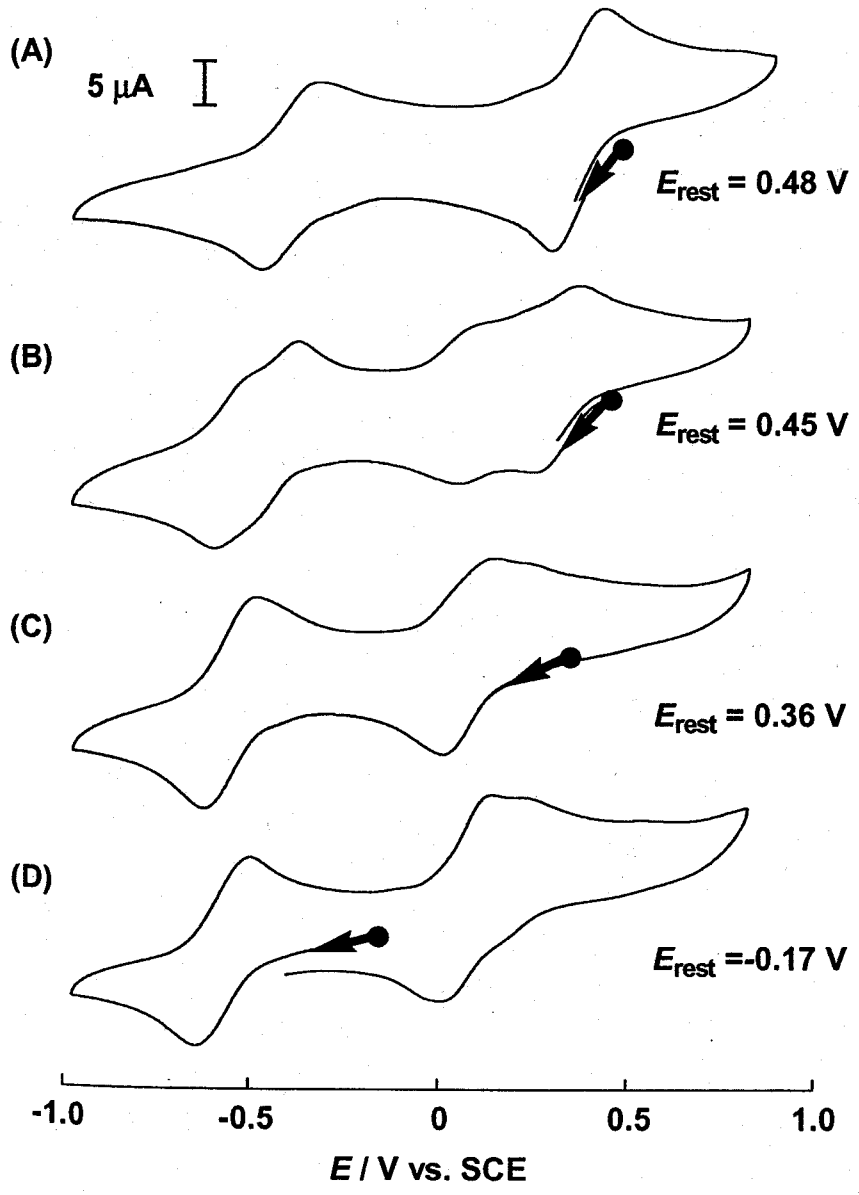

Figure 5. Cyclic voltammograms of **3** (1.0 mM) in the presence of various amounts of *t*-BuOK in CH_2Cl_2; 0 equiv, E_{rest} = 0.48 V (A); 0.5 equiv, E_{rest} = 0.45 V (B); 1.0 equiv, E_{rest} = 0.36 V (C); 3.0 equiv, E_{rest} = -0.17 V (D).

more than 1.0 eq of base indicated an anion ligand coordinated to Ru^{II}-dioxolene moiety, because the redox potential of $[Ru^{II}(Bu_2SQ)(Cl)]$ and $[Ru^{II}(Bu_2SQ)(OAc)]$, $E^{a}_{1/2}$ = 0.21 V and $E^{b}_{1/2}$ = –0.67 V for the farmer,[6] $E^{a}_{1/2}$ = 0.16 V and $E^{b}_{1/2}$ = –0.69 V for the latter,[6] which were quite nearly OH^- complex value. Such characteristic behavior is explained by the view that the first deprotonation of $[Ru^{III}(trpy)(Bu_2SQ)(OH_2)]^{2+}$ just converts the aqua ligand (OH_2) to the hydroxo one (OH^-), and the subsequent deprotonation of the hydroxo ligand (OH^-) of $[Ru^{III}(trpy)(Bu_2SQ)(OH^-)]^{+}$ causes electron transfer from the resultant O^{2-} to $[Ru^{III}(Bu_2SQ)]$ yielding oxyl radical ($O^{\bullet-}$) and $[Ru^{II}(Bu_2SQ)]$ of **5** (Scheme 1A). Indeed, **5** generated by deprotonation of $[Ru^{III}(trpy)(Bu_2SQ)(OH^-)]^{+}$ exhibits the characteristic CT band of the $[Ru^{II}(Bu_2SQ)]$ framework at 870 nm. The Ru-OH_2 complex **3**, Ru-OH complex $[Ru^{III}(trpy)(Bu_2SQ)(OH^-)]^{+}$, and Ru-$O^{\bullet-}$ one show their own electronic spectra. On the other hand, the redox potentials of the $[Ru^{III}(Bu_2SQ)]^{2+}/[Ru^{II}(Bu_2SQ)]^{+}$ and the $[Ru^{II}(Bu_2SQ)]^{+}/[Ru^{II}(Bu_2Cat)]$ couples of $[Ru^{III}(trpy)(Bu_2SQ)(OH^-)]^{+}$ closely resembles those of **5**, suggesting that OH^- and $O^{\bullet-}$ give the similar electronic influence on the redox reaction of the Ru-dioxolene moiety. Moreover, the redox potentials of **5** was hardly influenced by the presence of free *t*-BuOK, because **5** isolated as reddish purple crystals displayed the same CV as that of **3** in the presence of 3.0 equiv of *t*-BuOK in CH_2Cl_2.

The CV of **4** in CH_2Cl_2 also showed the two reversible redox waves at $E^{1a}_{1/2}$ = 0.60 V and $E^{1b}_{1/2}$ = –0.14 V (*vs.* SCE). The electronic structures of the acetato complex **2**, aqua complex **4**, and the oxo complex derived from double deprotonation of **4** are described as $[Ru^{II}(trpy)(4ClSQ)(OAc)]$, $[Ru^{III}(trpy)(4ClSQ)(OH_2)]^{2+}$, and $[Ru^{II}(trpy)(4ClSQ)(O^{\bullet-})]$, respectively, suggesting that one electron reduction of **4** take

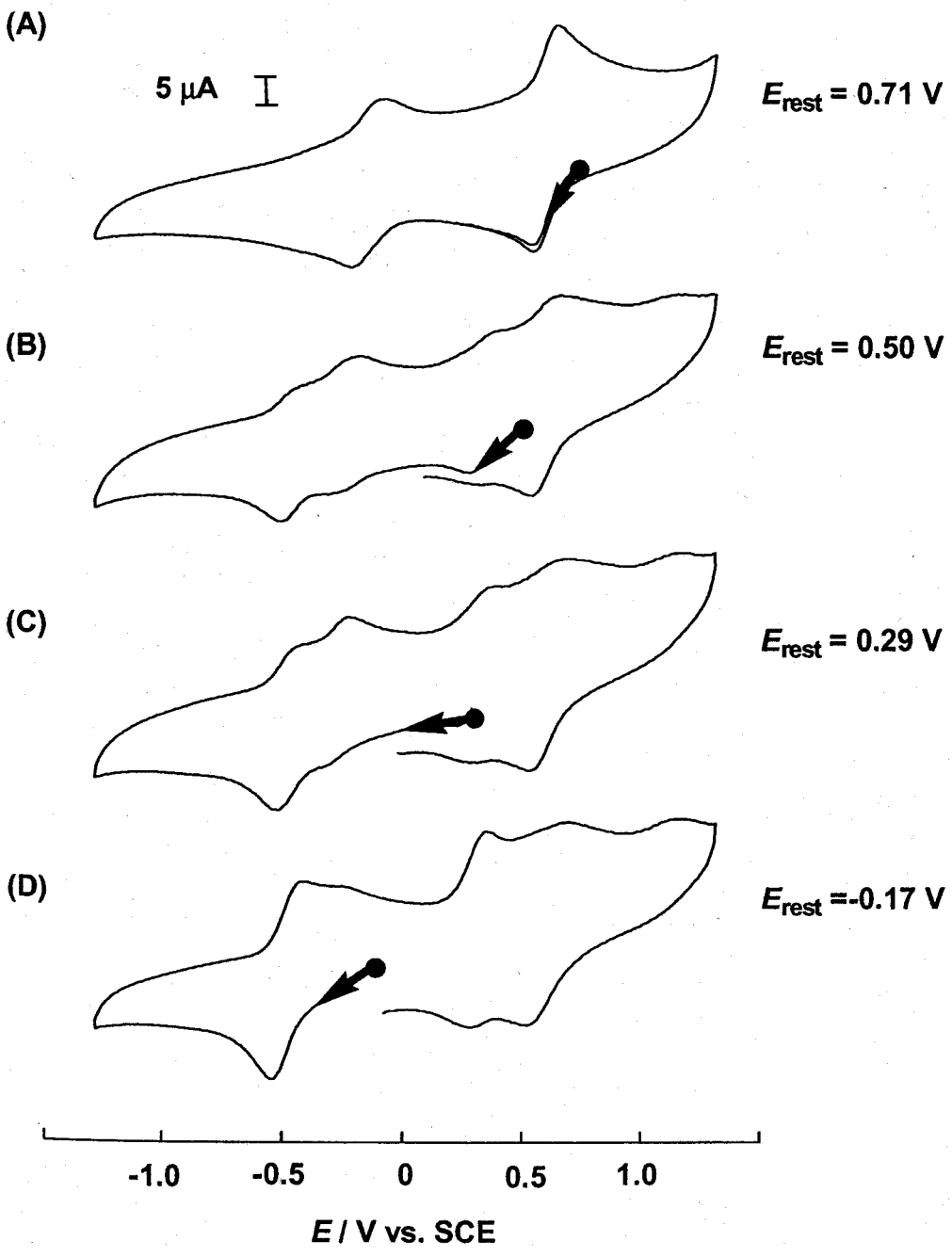

Figure 6. Cyclic voltammograms of **4** (1.0 mM) in the presence of various amounts of *t*-BuOK in CH_2Cl_2; 0 equiv, E_{rest} = 0.71 V (A); 0.5 equiv, E_{rest} = 0.50 V (B); 1.0 equiv, E_{rest} = 0.29 V (C); 2.0 equiv, E_{rest} = -0.17 V (D).

place on the central metal. The redox reactions at 0.60 V and –0.14 V, therefore would be ascribed to the $[Ru^{III}(4ClSQ)]^{2+}/[Ru^{II}(4ClSQ)]^{+}$ and $[Ru^{II}(4ClSQ)]^{+}/[Ru^{II}(4ClCat)]$ couples, respectively (Figure 6A). Instead, one quasi-reversible and one reversible redox couple of the corresponding hydroxo complex appeared at $E^{2a}_{1/2}$ = 0.29 V and $E^{2b}_{1/2}$ = –0.48 V (*vs.* SCE), respectively. At the same time, the rest potential negatively shifted from 0.71 V to –0.17 V passing through the quasi-reversible couple of the hydroxy complex at $E^{2a}_{1/2}$ = 0.29 V. The change of CV almost ceased after addition of 2.0 equiv of *t*-BuOK, though the absorption spectra of **4** did not change upon the addition of more than 1.0 equiv of *t*-BuOK in CH_2Cl_2. The second deprotonation of **4**, that was observed in the absorption spectra in water, also occurred in CH_2Cl_2. Deprotonation of the aqua ligand of **4**, therefore, produces probably $[Ru^{II}(trpy)(4ClSQ)(OH^{\bullet})]^{+}$ rather than $[Ru^{III}(trpy)(4ClSQ)(OH^{-})]^{+}$ (Scheme 1B).

In contrast to the equilibrium of eq 3, the deprotonation of the aqua ligand of **4** induces intra-molecular electron transfer from OH^{-} to the $[Ru^{III}(4ClSQ)]$ framework giving $[Ru^{II}(trpy)(4ClSQ)(OH^{\bullet})]^{+}$. The absence of an isosbestic point in the conversion from **4** to $[Ru^{II}(trpy)(4ClSQ)(OH^{\bullet})]^{+}$ (Figure 3) may be associated with a concomitant inter-molecular electron transfer from the resultant $[Ru^{II}(trpy)(4ClSQ)(OH^{\bullet})]^{+}$ to unreacted $[Ru^{III}(trpy)(4ClSQ)(OH_2)]^{2+}$ (eq 4).

$$[Ru^{II}(trpy)(4ClSQ)(OH^{\bullet})]^{+} + [Ru^{III}(trpy)(4ClSQ)(OH_2)]^{2+} \rightarrow [Ru^{III}(trpy)(4ClSQ)(OH^{\bullet})]^{2+} + [Ru^{II}(trpy)(4ClSQ)(OH_2)]^{+} \quad (4)$$

Table 1. Redox Potentials (V vs. SCE) and Rest Potentials (V) for Complexes **3** and **4** under Various Conditions

	$Ru^{III}(R_nSQ)/Ru^{II}(R_nSQ)$	$Ru^{II}(R_nSQ)/Ru^{II}(R_nCat)$	E_{rest}
3	0.31	–0.47	0.48
3 + 1.0 equiv *t*-BuOK	0.07	–0.57	0.36
3 + 3.0 equiv *t*-BuOK	0.07	–0.57	–0.17
4	0.60	–0.14	0.71
4 + 1.0 equiv *t*-BuOK	0.29	–0.48	–0.17

Scheme 1.

(A) $[Ru^{III}(trpy)(Bu_2SQ)(OH_2)]^{2+}$

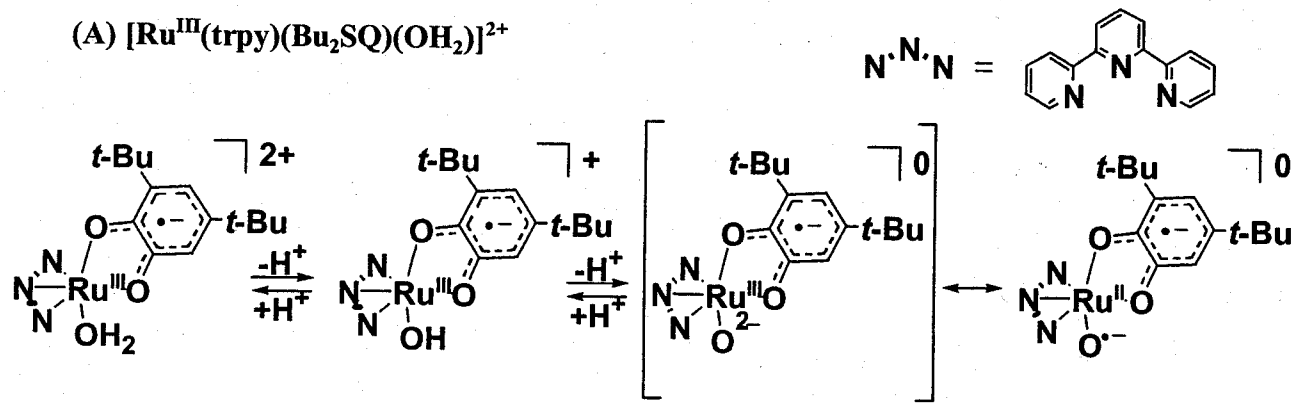

(B) $[Ru^{III}(trpy)(4ClSQ)(OH_2)]^{2+}$

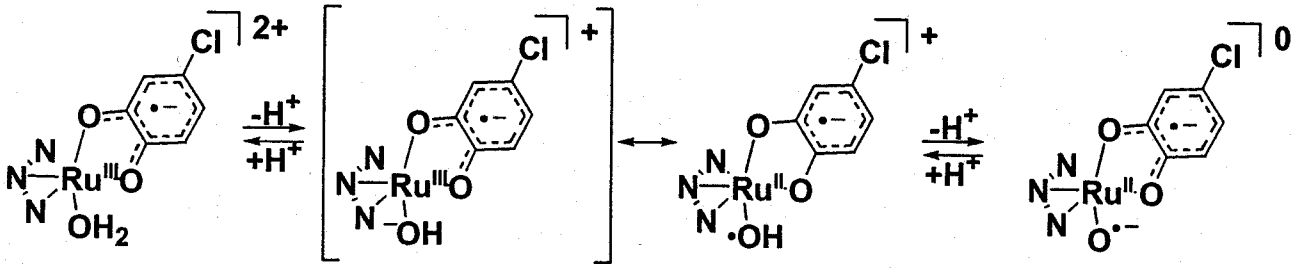

4, References

(1) (a) Moyer, B. A.; Meyer, T. J. *Inorg. Chem.* **1981**, *20*, 436. (b) Takeuchi, K. J.; Thompson, M. S.; Pipes, D. W.; Meyer, T. J. *Inorg. Chem.* **1984**, *23*, 1845.

(2) K. Tsuge, K. Tanaka, *Chem. Lett.*, **1998**, 1069; K. Tsuge, M. Kurihara, K. Tanaka, *Bull. Chem. So. Jpn.*, **2000**, *73*, 607.

(3) (a) Pierpont, C. G.; Buchanan, R. M. *Coord. Chem. Rev.* **1981**, *38*, 45. (b) Pierpont, C. G.; Lange, C. W. *Prog. Inorg. Chem.* **1994**, *41*, 331.

(4) (a) Haga, M.; Dodsworth, E. S.; Lever, A. P. B.; Boone, S. R.; Pierpont, C. G. *J. Am. Chem. Soc.* **1986**, *108*, 7413. (b) Boone, S. R.; Pierpont, C. G. *Inorg. Chem.* **1987**, *26*, 1769. (c) Bhattacharya, S.; Pierpont, C. G. *Inorg. Chem.* **1991**, *30*, 1511. (d) Bhattacharya, S.; Pierpont, C. G. *Inorg. Chem.* **1992**, *31*, 35. (e) Bhattacharya, S.; Pierpont, C. G. *Inorg. Chem.* **1994**, *33*, 6038. (f) Sugimoto, H.; Tanaka, K. *J. Organomet. Chem.* **2001**, *622*, 280.

(5) (a) Haga, M.; Dodsworth, E. S.; Lever, A. P. B. *Inorg. Chem.* **1986**, *25*, 447. (b) Ebadi, M.; Lever, A. P. B. *Inorg. Chem.* **1999**, *38*, 467 (c) Lever, A. P. B.; Auburn, P. R.; Dodsworth, E. S.; Haga, M.; Liu, W.; Melnik, M.; Nevin, W. A. *J. Am. Chem. Soc.* **1988**, *110*, 8076. (d) Auburn, P. R.; Dodsworth, E. S.; Haga, M.; Liu, W.; Nevin, W. A.; Lever, A. P. B. *Inorg. Chem.* **1991**, *30*, 3502.

(6) Kurihara, M.; Daniele, S.; Tsuge, K.; Sugimoto, H.; Tanaka, K. *Bull. Chem. Soc. Jpn.* **1998**, *71*, 867.

(7) Stufkens, D. J.; Snoeck, Th. L.; Lever, A. P. B. *Inorg. Chem.* **1988**, *27*, 953.

(8) Coe, B. J.; Tompson, D. W.; Culbertson, C. T.; Schoonover, J. R.; Meyer, T. J. *Inorg. Chem.* **1995**, *34*, 3385.

Chapter 4

Characterization of the Oxyl Radical Ligand

(Katsuaki Kobayashi, Hideki Ohtsu, Tohru Wada, and Koji Tanaka, *Chem. Lett.* 2002, 868.)

1, Introduction

Electronic absorption, rR spectra and CV demonstrated that one electron reduction of the $[Ru^{III}(SQ)]$ moiety of the aqua-Ru-dioxolene ($[Ru^{III}(SQ)(OH_2)]^{2+}$) complex was induced by the dissociation of one or two protons of the aqua ligand. The absorption spectrum of the reduced complex generated by deprotonation fully recovered that of the $[Ru^{III}(SQ)]$ moiety upon the addition of acid (Chapter 3). Such reversible change is explained as follows; i) successive deprotonation of the aqua ligand yields OH^- and O^{2-} ligands, ii) the resultant electron rich OH^- and O^{2-} reduced the $[Ru^{III}(SQ)]$ moiety through the intramolecular electron transfer to form the $[Ru^{II}(SQ)]$ moiety with generating oxyl radical complex ($[Ru^{II}SQ(O^{\bullet-})]$). The electronic structure of the the Ru-dioxolene moiety can be estimated by the electronic absorption spectra and electrochemical study. Resonance Raman spectra are expected to give the information of Ru-$O^{\bullet-}$ bond character of $[Ru^{II}SQ(O^{\bullet-})]$. The vibration mode assignable to the Ru-$O^{\bullet-}$ bond, however, could not be observed even after the rR measurements of $H_2{}^{18}O$ complex ($[Ru^{III}(SQ)(^{18}OH_2)]^{2+}$).

In addition the spin trapping technique, to confirm the oxyl radical complex, ESR measurements were conducted at low temperatures to get the better understanding about the ruthenium semiquinone oxyl radical complexes ($[Ru^{II}(SQ)(O^{\bullet-})]$).

2, Experimental Section

Materials. Dichloromethane solutions of DMPO (5,5-dimethyl-1-pyrroline N-oxide)(0.1 M) were used as a stock solution of spin trapping reagents.

ESR Spectra. The ESR spectra at 193 K were measured with a JEOL X-band spectrometer (JES-RE1XE) using an attached VT (Variable Temperature) apparatus. The *g* values were calibrated precisely with a Mn^{2+} marker which was used as a reference. Frozen state ESR spectra at low temperatures were measured on Brüker X-band spectrometer (Brüker ESP300E) with a cryostat (Oxford ESR900) and a temperature controller (Oxford Model ITC4). The *g* values were calculated from the magnetic field and the microwave frequency, measured by an NMR tesla meter (Brüker ER035M) and a microwave frequency counter (HEWLETT PACKERD 5352B), respectively. Both of measurements were demonstrated under nonsaturating microwave power conditions.

ESI Mass Spectra. Electron spray mass spectra were obtained on a JEOL JMS-T100L attached a syringe pomp apparatus (Harvard Apparatus model 22). The ion spray interface was adjusted to 2.0 kV, then sample solutions were loaded to the sprayer through glass capillary (ϕ = 100 μm) by 10 μL/sec. Nebulization of solutions were performed by compressed N_2. TOF detector was employed to the ion detection in positive detection mode, whose detection range is 250-1000 (*m/z*). Orifice potential was maintained at 25 V.

3, Results and Discussion

3-1 Spin Trapping Experiments.

The ESR spectrum of a mixture of $[Ru^{III}(trpy)(Bu_2SQ)(OH_2)](ClO_4)_2$ (**3**) and more than 1.0 equiv of *t*-BuOK in CH_2Cl_2 displayed an isotropic broad signal without a hyperfine structure (g = 2.030, ΔH_{msl} = 8.0 mT) at 193 K (Figure 1A). The intensity of the signal linearly increased with an increase of the amount of *t*-BuOK and became almost constant in the presence of 3.0 equiv of the base. The isotropic broad signal centered at g = 2.029 would be correlated with the triplet signal at Δm_s = 1 region, together with disappearance of hyperfine structures because of the solution state experiment (vide infra). The broad signal at g = 2.030 merely implies the involvement of two radicals in **5**, that is the doubly deprotonated form of **3**. Technique of spin trapping using 5,5-dimethyl-1-pyrroline *N*-oxide (DMPO) was applied for detection and identification of the oxyl radical moiety of $[Ru^{II}(trpy)(Bu_2SQ)O^{\bullet -}]$, that is produced in the reaction of **3** with 3.0 equiv of *t*-BuOK in CH_2Cl_2. Indeed, 12-line sharp signals centered at g = 2.006 together with the isotropic broad signal without hyperfine structure (g = 2.029, ΔH_{msl} = 7.3 mT) are detected in the ESR spectrum of a CH_2Cl_2 solution containing **3**, 3.0 equivs of *t*-BuOK and of DMPO (Figure 1B).

The signal with hyperfine structure increased linearly with an increase in the DMPO concentration, which indicated that DMPO was trapped with radical species. The appearance of the 12-line sharp signals demonstrates the spin adduct formation between $[Ru^{II}(trpy)(Bu_2SQ)O^{\bullet -}]$ (**5**) and DMPO, since the isotropic ESR signal of $[Ru^{II}(trpy)(Bu_2SQ)(OAc)]$ in CH_2Cl_2 (g = 2.030, ΔH_{msl} = 8.0 mT) were not influenced by the presence of a large excess of DMPO. Therefore, DMPO can not trap the

semiquinone radical linked a ruthenium ion, but generate the spin adduct with the oxyl radical. Moreover, a mixture of recrystallized **5** and excess amounts of DMPO also showed the same 12-line sharp signals in CH_2Cl_2. The hyperfine coupling constants for the 12-line signals were determined as $a_N^{\alpha} = 1.35$, $a_H^{\beta} = 0.66$ and $a_H^{\gamma} = 0.15$ mT by the computer simulation (Figure 2), and the assignment of the ESR signal of the spin adduct, $[Ru^{II}(trpy)(Bu_2SQ)(O\text{-}DMPO)]$ is depicted in Figure 2.

Shown in Figure 3A is the ESR spectrum of $[Ru^{III}(trpy)(4ClSQ)(OH_2)](ClO_4)_2$ (**4**) in CH_2Cl_2 containing 3.0 equiv of *t*-BuOK at 193 K. An isotropic broad signal expected from the triplet signal was not detected. On the other hand, 12-line signals of the spin adduct were also observed in the ESR spectra of a mixture of **4**, 3.0 equivs of *t*-BuOK and of DMPO in CH_2Cl_2 at 193 K (Figures 3B). The hyperfine coupling constants were also estimated as $a_N^{\alpha} = 1.30$, $a_H^{\beta} = 0.63$, and $a_H^{\gamma} = 0.21$ mT by the computer simulation (Figure 4). Moreover, $[Ru^{II}(trpy)(4ClSQ)(OAc)]$ did not exhibit an ESR signal either in CH_2Cl_2.

The a_N^{α}, a_H^{β}, and a_H^{γ} values of the spin adducts are also summarized in Table 4. The a_N^{α} values of the spin adducts of Ru oxyl radical complexes are close to those of other spin adducts such as DMPO-OH (1.4-1.5 mT), though the a_H^{β} and a_H^{γ} values are largely influenced by parent radicals (Table 1).[1,2,3]

The 1:1 adduct formation between **5** and DMPO is further demonstrated by electron spray ionization mass spectroscopy (ESI mass). The mass spectrum of a CH_2Cl_2 solution containing **3**, 3.0 equiv of *t*-BuOK and 100 equiv of DMPO (Figure 5A) well coincides with the simulated isotope pattern of $[Ru^{II}(trpy)(Bu_2SQ)(^{16}O\text{-}DMPO)]^+$ (Figure 5C). The labeling experiment using $[Ru^{III}(trpy)(Bu_2SQ)(^{18}OH_2)](ClO_4)_2$ under otherwise the same conditions also exhibited the expected signal at *m*/*z* 686 of

$[Ru^{II}(trpy)(Bu_2SQ)(^{18}O\text{-}DMPO)]^+$ (Figure 5B). These observations also indicate the spin adduct formation between the oxyl radical of $[Ru^{II}(trpy)(Bu_2SQ)O^{\bullet-}]$ and DMPO.

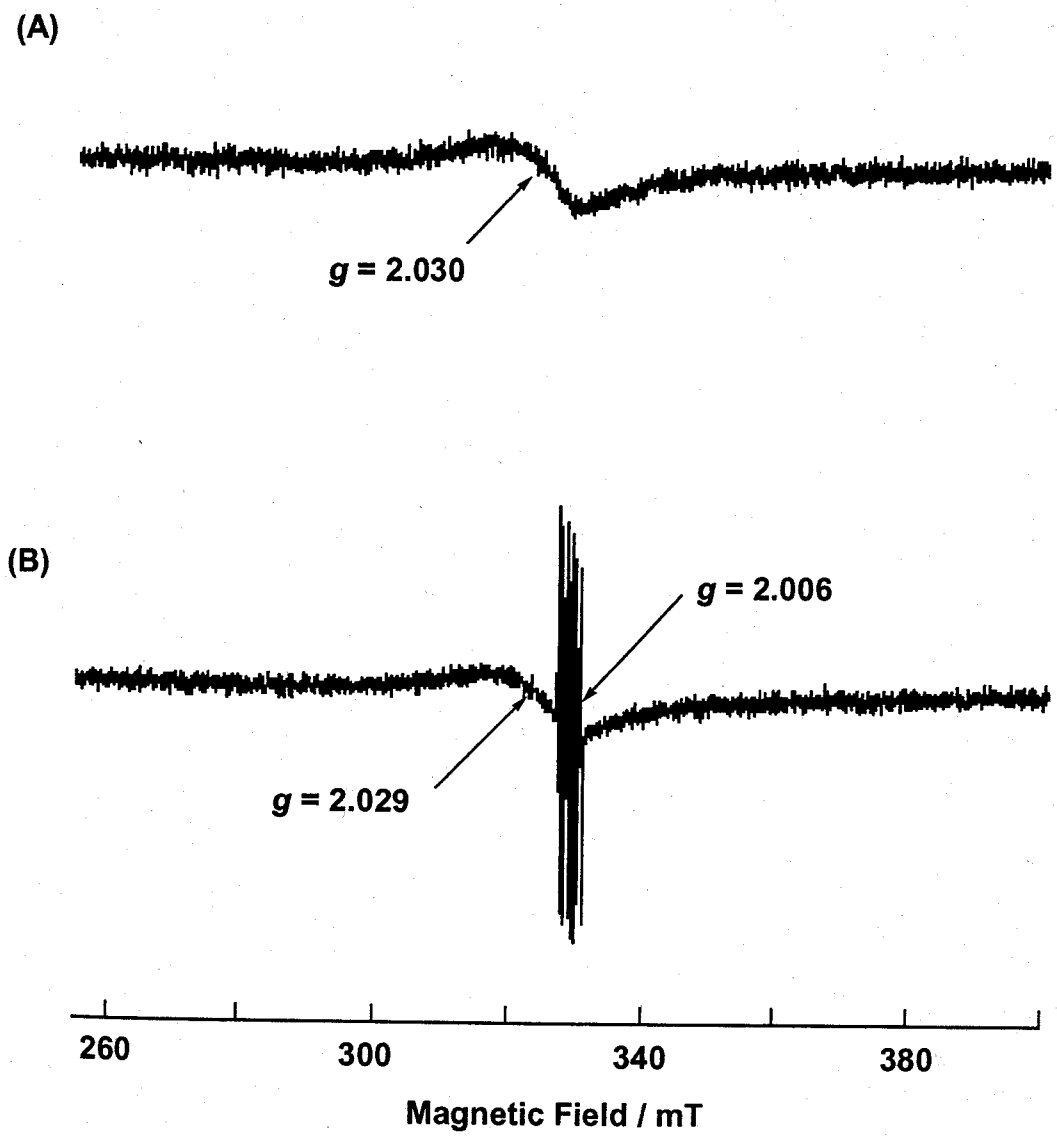

Figure 1. (A) ESR spectrum obtained upon the addition of 3.0 equivs of *t*-BuOK to a CH_2Cl_2 solution of **3** (2.0 mM). (B) ESR spectrum obtained upon the addition of 3.0 equivs of *t*-BuOK and DMPO to a CH_2Cl_2 solution of **3** (2.0 mM). All spectra were obtained at 193 K. Microwave power is 1.0 mW and modulation amplitude is 0.14 mT.

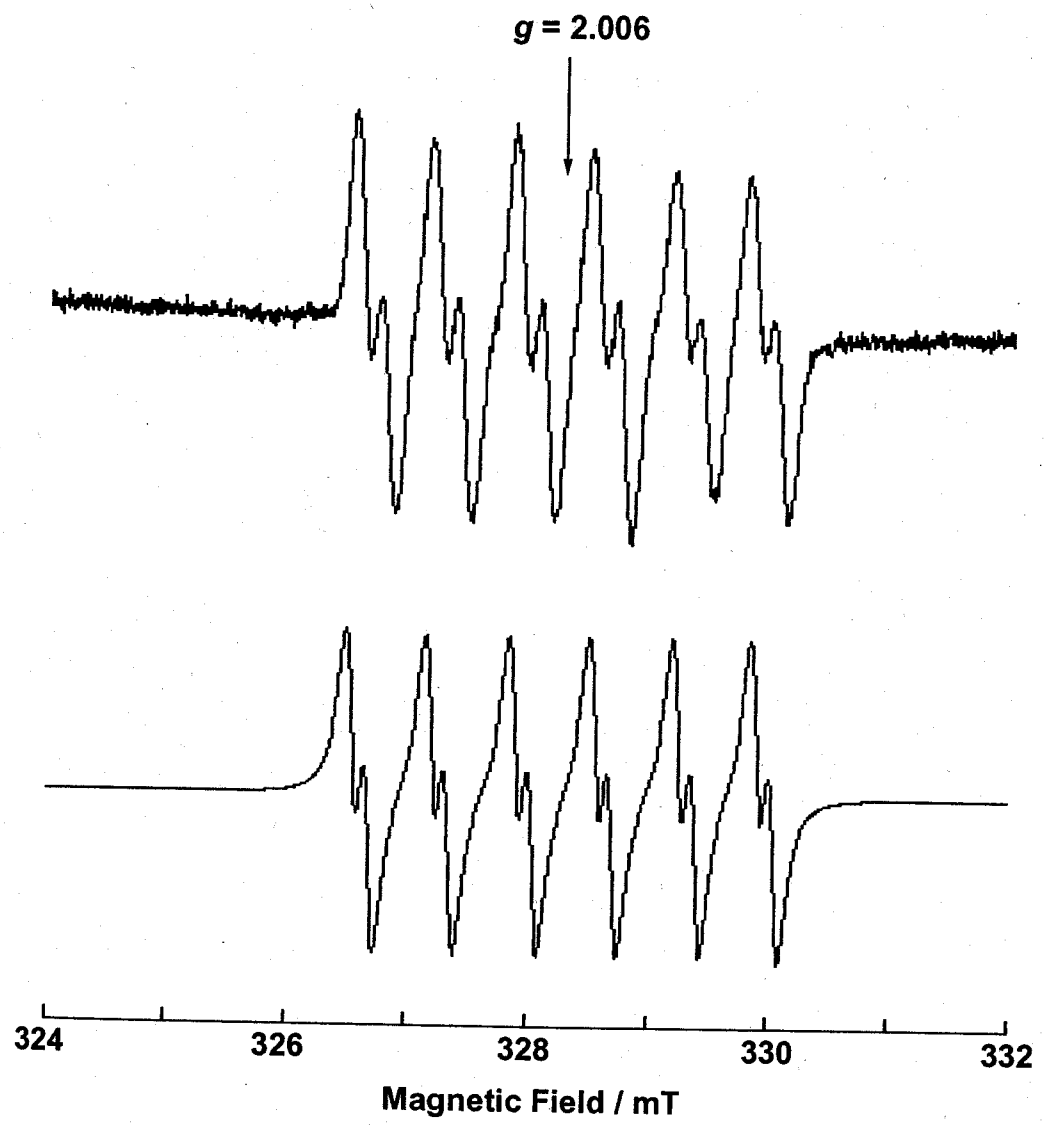

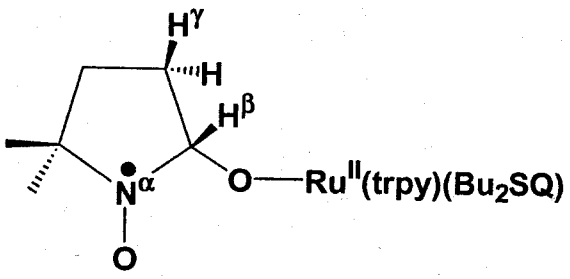

Figure 2. (A) ESR spectra obtained upon the addition of 3.0 equivs of *t*-BuOK and of DMPO to a CH_2Cl_2 solution of **3** (2.0 mM) at 193 K. (B) Computer simulation of [Ru^{II}(trpy)(Bu_2SQ)(O-DMPO)] (g = 2.006, a_N^{α} = 1.35, a_H^{β} = 0.66, and a_H^{γ} = 0.15 mT). The proposal structure of [Ru^{II}(trpy)(Bu_2SQ)(O-DMPO)] is shown in (C). Microwave power is 1.0 mW and modulation amplitude is 0.14 mT.

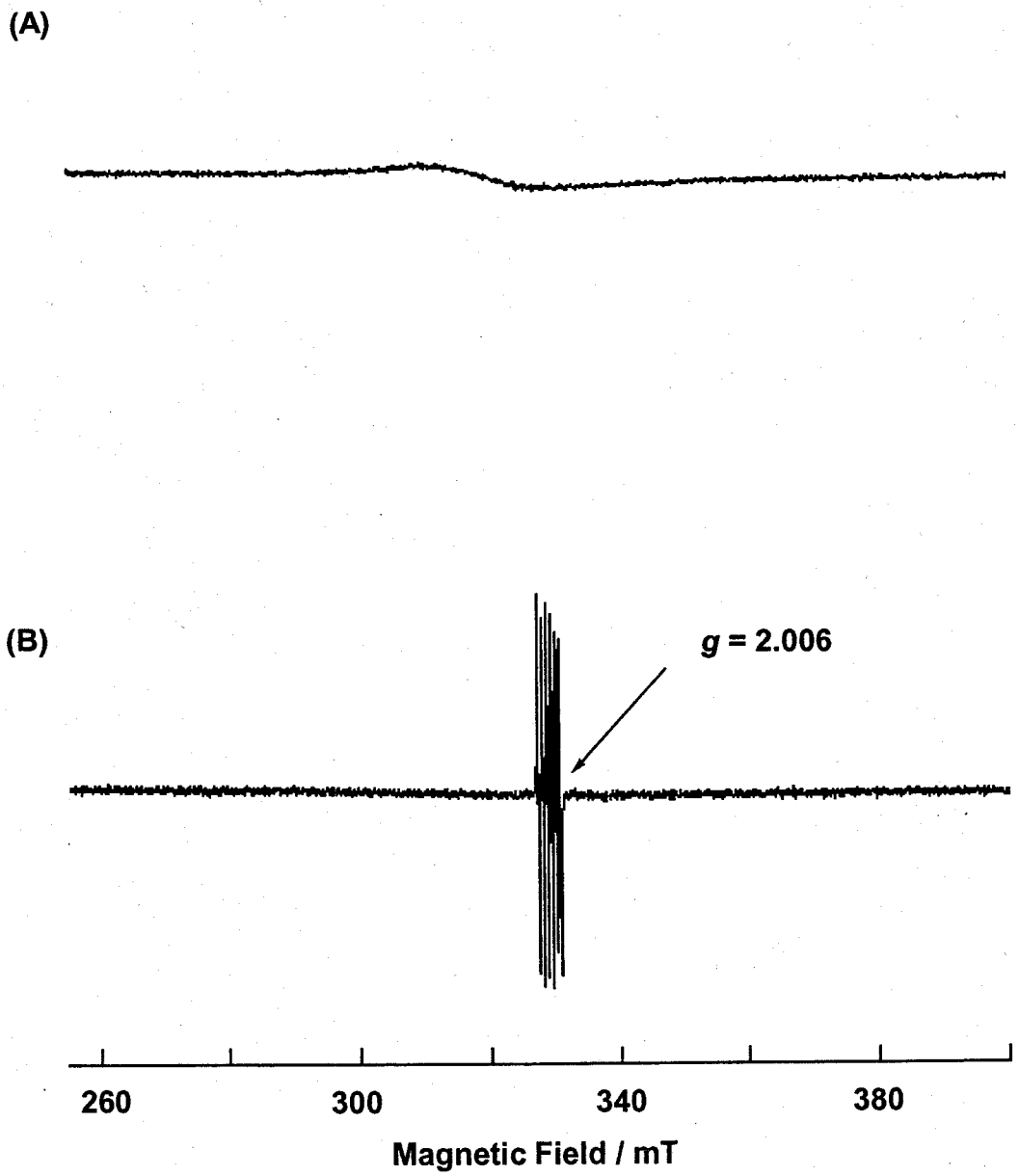

Figure 3. (A) ESR spectrum obtained upon the addition of 3.0 equivs of *t*-BuOK to a CH_2Cl_2 solution of **4** (2.0 mM). (B) ESR spectrum obtained upon the addition of 3.0 equivs of *t*-BuOK and DMPO to a CH_2Cl_2 solution of **4** (2.0 mM). All spectra were obtained at 193 K. Microwave power is 1.0 mW and modulation amplitude is 0.14 mT.

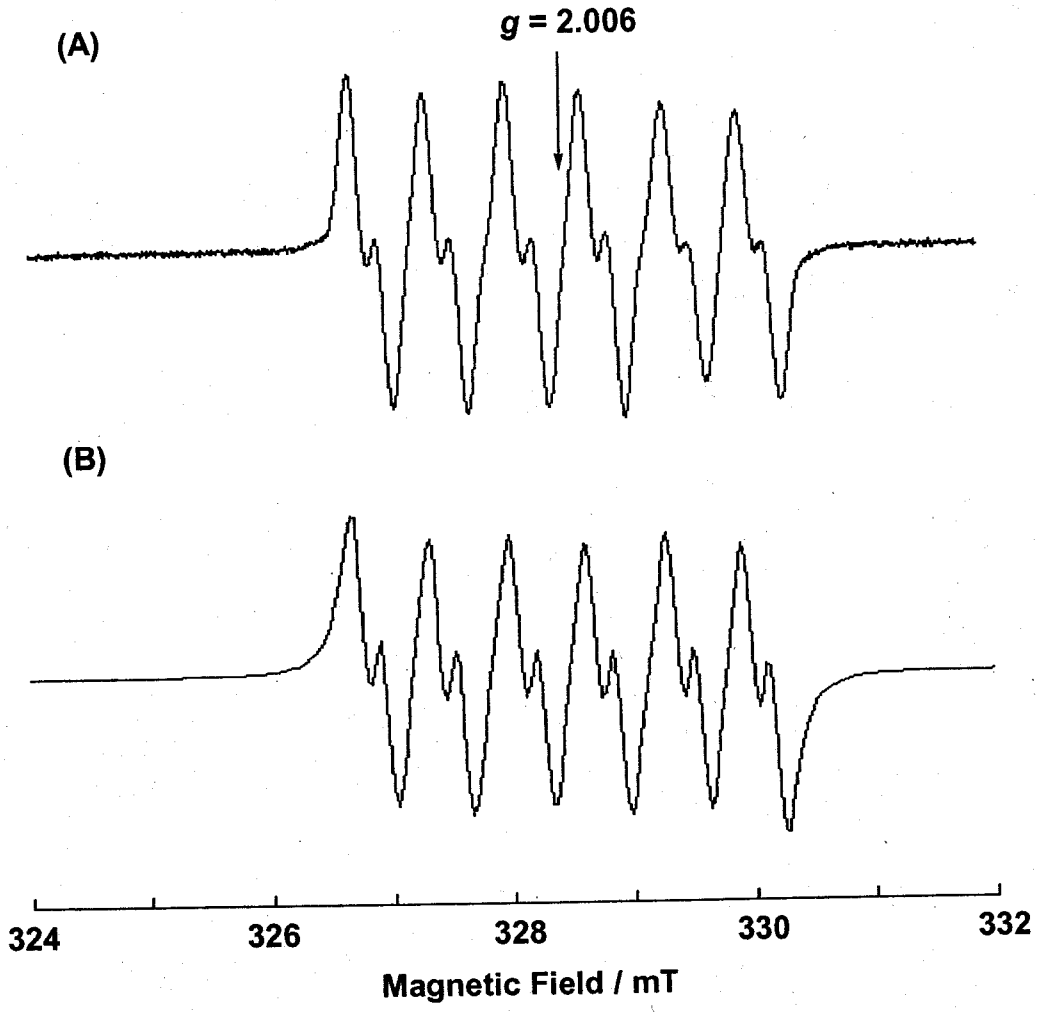

(C)

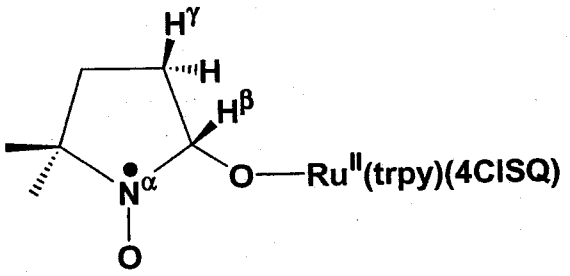

Figure 4. (A) ESR spectra obtained upon the addition of 3.0 equivs of *t*-BuOK and of DMPO to a CH_2Cl_2 solution of **4** (2.0 mM) at 193 K. (B) Computer simulation of [Ru^{II}(trpy)(4ClSQ)(O-DMPO)] (g = 2.006, a_N^{α} = 1.30, a_H^{β} = 0.63, and a_H^{γ} = 0.21 mT). The proposal structure of [Ru^{II}(trpy)(4ClSQ)(O-DMPO)] is shown in (C). Microwave power is 1.0 mW and modulation amplitude is 0.14 mT.

Table 1. Hyperfine Coupling Constants (mT) of DMPO Spin Adducts

Parent radical	a_N^{α}	a_H^{β}	a_H^{γ}	ref.
$[Ru^{II}(trpy)(Bu_2SQ)(O^{\bullet-})]$	1.35	0.66	0.15	*a*
$[Ru^{II}(trpy)(4ClSQ)(O^{\bullet-})]$	1.30	0.63	0.21	*a*
·OH	1.53	0.06		1
·OOH	1.43	1.17	0.13	1
$\cdot CH_2OH$	1.60	2.27		2
$CH_3\cdot CHOH$	1.58	2.28		2
$\cdot CH_2CO_2H$	1.61	2.28		3
$\cdot CH_2CO_2^-$	1.61	2.28		3

[a] This work.

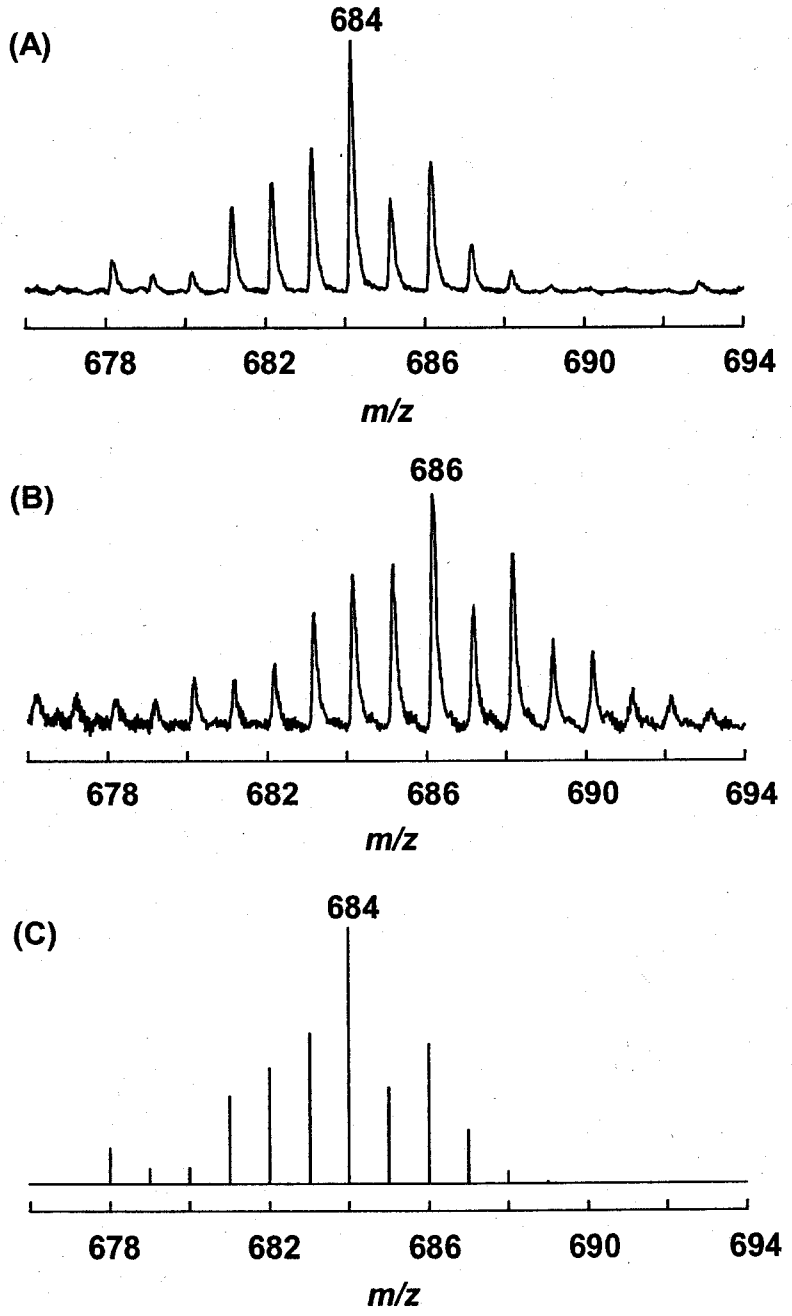

Figure 5. ESI mass spectra observed upon the addition of 3.0 equiv of *t*-BuOK and 100 equiv of DMPO into CH_2Cl_2 solution of **3** (10 mM) containing small amount of water ($H_2{}^{16}O$ (A) and $H_2{}^{18}O$ (B)). Computer simulation of [Ru^{II}(trpy)(Bu_2SQ)(^{16}O-DMPO)] (C).

3-2 ESR Spectra at 3.9 K (g = 2).

Both **3** and **4** in CH_2Cl_2 did not show any ESR signals at 3.9 K. The ESR spectrum of a mixture of **3** and 3.0 equiv of *t*-BuOK at 3.9 K exhibited an isotropic broad signal with hyperfine structure of zero field splitting of triplet state at Δm_s = 1 region (Figure 6A).[4-7] The splitting can not be observed clearly because of the large signal line width of signal. Computer simulation curve of triplet signal at Δm_s = 1 region using WINEPR SimFonia ver. 1.25 with $g_{xx} = g_{yy} = g_{zz} = 2.054$ and $|D| = 0.020$ cm^{-1}, $|E| = 0.005$ cm^{-1} gives good agreement with the observed spectrum (Figure 6B). If D is assumed to involve only dipolar interaction, $|D|$ (cm^{-1}) is expressed by eq 1, where r (Å) is the spin-spin distance.[6] Calculation of eq 1 using $|D| = 0.020$ cm^{-1} and g = 2.054

$$D = -3g\beta/2r^3 \qquad (1)$$

revealed the spin-spin distance is 5.09 Å. The distance between oxyl radical and the center of dioxolene ring is 4.91 Å based on the X-ray structural analysis of **5**, which is close to the value obtained from ESR experiment (Scheme 1).

The ESR spectrum of **4** in the presence of 3.0 equiv of *t*-BuOK in frozen CH_2Cl_2 exhibited an anisotropic broad signal with a hyperfine structure of zero field splitting at 3.9 K (Figure 7A). Computer simulation curve with $g_{xx} = g_{yy} = 2.150$, $g_{zz} = 2.060$, $|D| = 0.038$ cm^{-1}, and $|E| = 0.011$ cm^{-1} gives reasonable agreement with the observed spectrum (Figure 7B). The r value calculated from eq 1 using $g_{av} = 2.11$[8] and $|D| = 0.038$ cm^{-1} is 4.23 Å, which is close to the distance between oxyl radical and the center of O-C-C-O skeleton linked to Ru, 3.90 Å, based on the structure of **5**. The electronic structure of the oxo complex (or hydroxy) derived from **4**, therefore, is expressed by [Ru^{II}(trpy)(4ClSQ)$O^{\bullet -}$] (or [Ru^{II}(trpy)(4ClSQ)$OH^{\bullet}$]) with a minor contribution of the [Ru^{III}(4ClCat)] core (Scheme 1). The resonance of the oxo complexes derived from

double deprotonation of **4** slightly lies to the right ([Ru^{III}(Cat)]) of eq 2. Such a difference is reasonably ascribed to the strong electron withdrawing ability of 4ClSQ compared with Bu_2SQ. Moreover, the grate difference between g_{xx}, g_{yy} and g_{zz} of [Ru^{II}(trpy)(4ClSQ)$O^{\bullet-}$] was probably induced by the Ru(III) contribution of [Ru^{III}(Cat)].

$$[Ru^{II}(SQ)] \quad \leftrightarrow \quad [Ru^{III}(Cat)] \qquad (2)$$

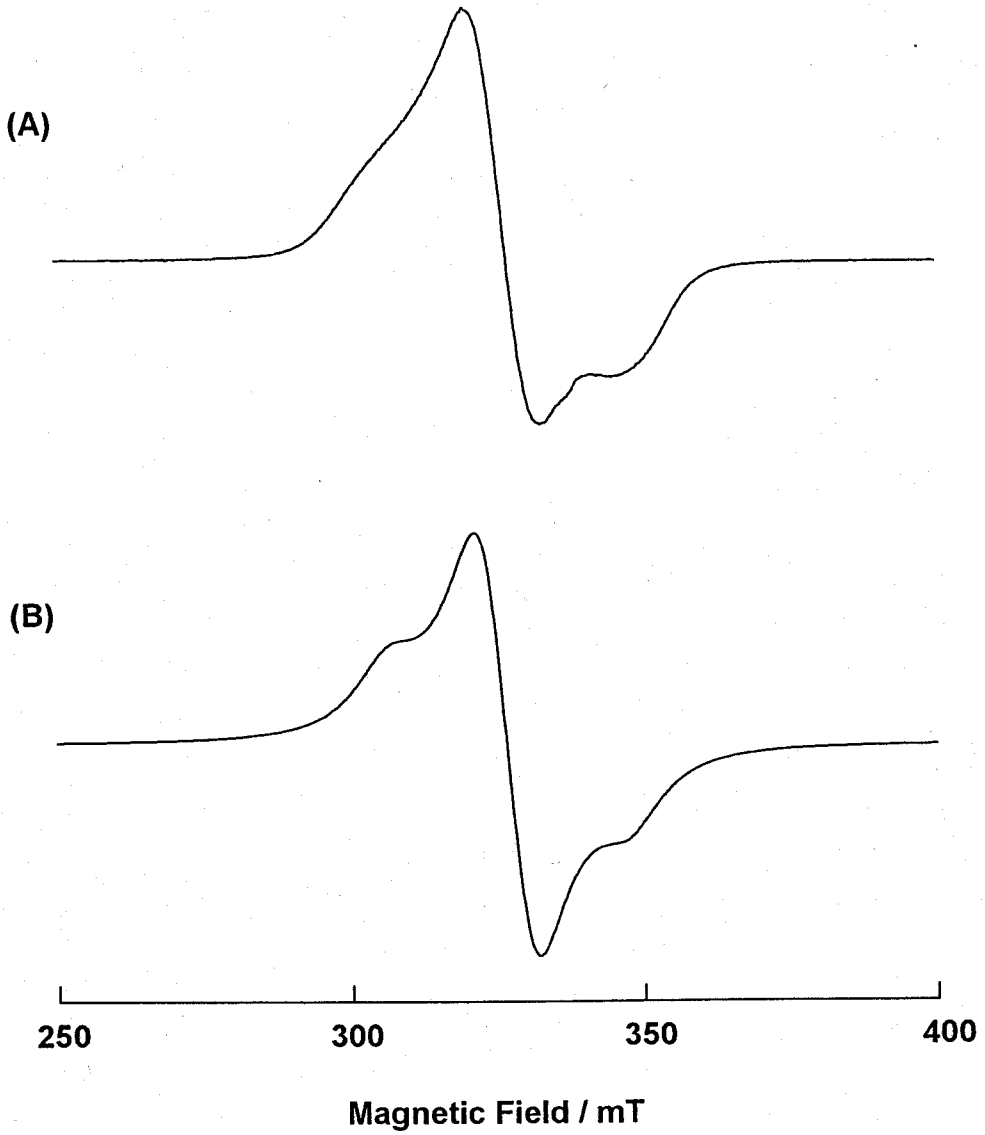

Figure 6. ESR spectra obtained upon the addition of 3.0 equiv of *t*-BuOK to a CH_2Cl_2 solution of **3** (A) and simulation curve using $|D| = 0.020$ cm^{-1}, $|E| = 0.005$ cm^{-1}, and $g_{xx} = g_{yy} = g_{zz} = 2.054$.

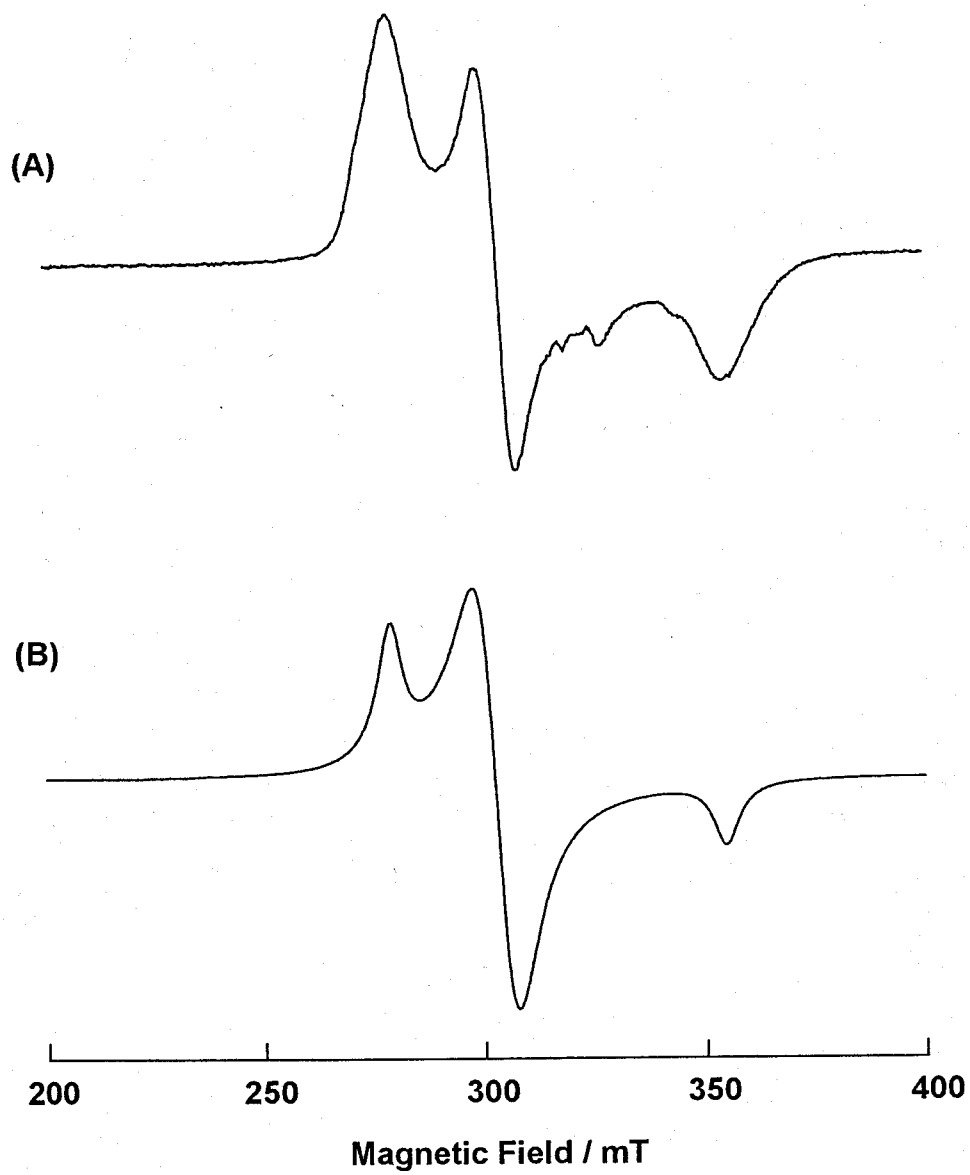

Figure 7. ESR spectra obtained upon the addition of 3.0 equiv of *t*-BuOK to a CH_2Cl_2 solution of **4** (A) and simulation curve using $|D| = 0.038$ cm^{-1}, $|E| = 0.011$ cm^{-1}, $g_{xx} = g_{yy} = 2.150$, and $g_{zz} = 2.060$.

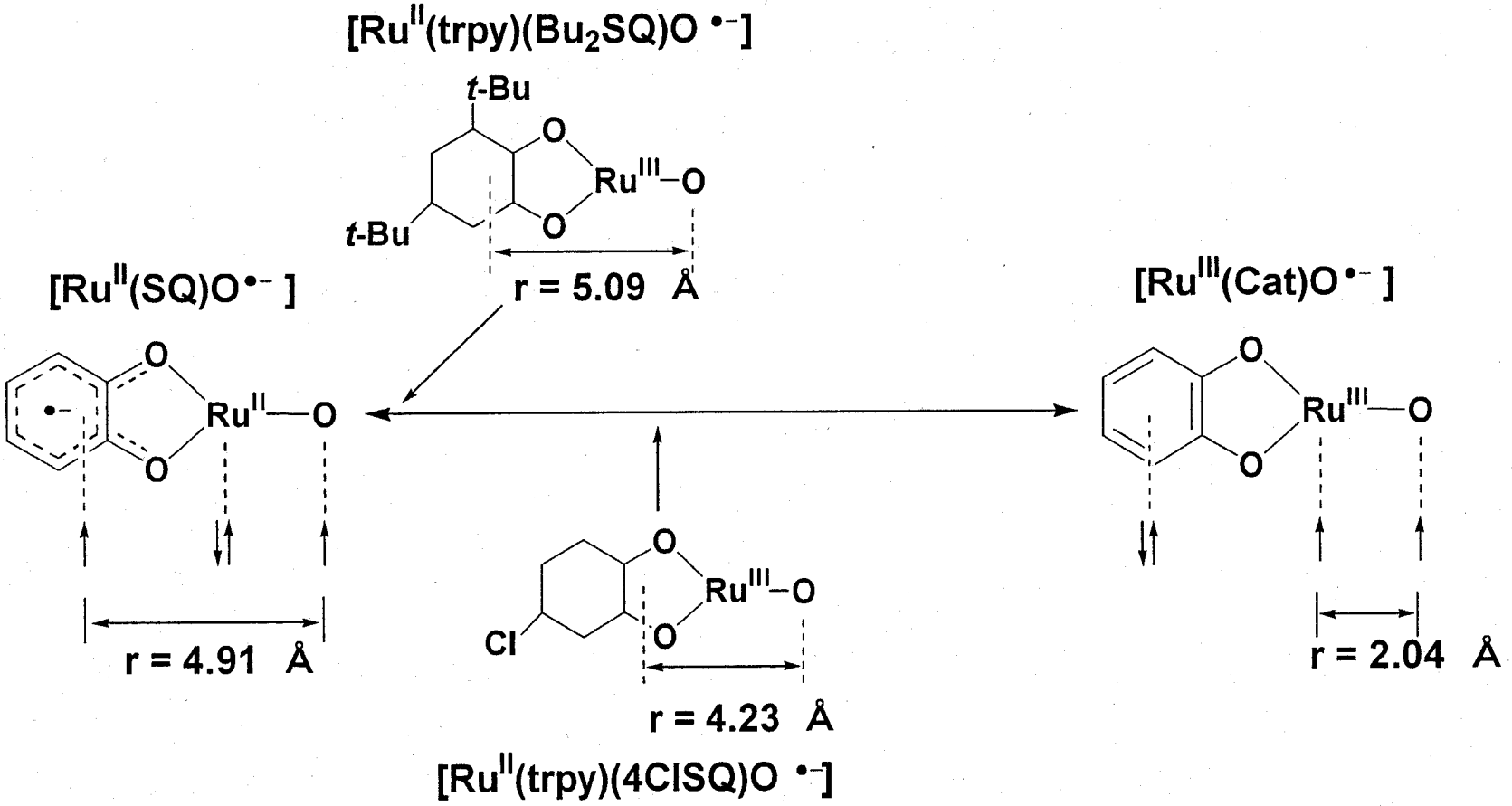
[Ru^II(trpy)(Bu2SQ)O •−]
t-Bu
t-Bu
O
O
Ru^III–O
r = 5.09 Å
[Ru^II(SQ)O•−]
O
O
Ru^II–O
r = 4.91 Å
[Ru^III(Cat)O•−]
O
O
Ru^III–O
r = 2.04 Å
Cl
O
O
Ru^III–O
r = 4.23 Å
[Ru^II(trpy)(4ClSQ)O •−]

3-3 Temperature Dependent ESR Spectra (g = 4).

The ESR spectra of **3** and **4** in the presence of 3.0 equiv of *t*-BuOK in frozen CH_2Cl_2 exhibited a signal at g = 4.18 and g = 4.65, respectively, due to the intra-molecular ferromagnetic coupling between [Ru^{II}(SQ)] and oxyl radical. The intensity of the signal of **3** and **4** with base decrease with an increase of temperature (Figure 8 and 9).

The splitting energy 2J between the triplet and singlet is determined from the temperature dependence of intensities (IT vs. T) by a fitting procedure to the Boltzmann function IT = const.$(3 + \exp(-2J/kT))^{-1}$ ($H = -2JS_1S_2$) (Figure 10).[7] 2J values of **5** (**3** in the presence of 3.0 equiv of *t*-BuOK) and [Ru^{II}(trpy)(4ClSQ)$O^{\bullet-}$] are –0.67 cm^{-1} and –1.97 cm^{-1}, respectively.[9] The difference in the antiferromagnetic interaction between the [Ru^{II}(trpy)(4ClSQ)$O^{\bullet-}$] framework (2J = -1.97 cm^{-1}) and the [Ru^{II}(trpy)(Bu_2SQ)$O^{\bullet-}$] one (2J = -0.67 cm^{-1}) is correlated the short the spin-spin distance of [Ru^{II}(trpy)(4ClSQ)$O^{\bullet-}$] compared with that of [Ru^{II}(trpy)(Bu_2SQ)$O^{\bullet-}$].

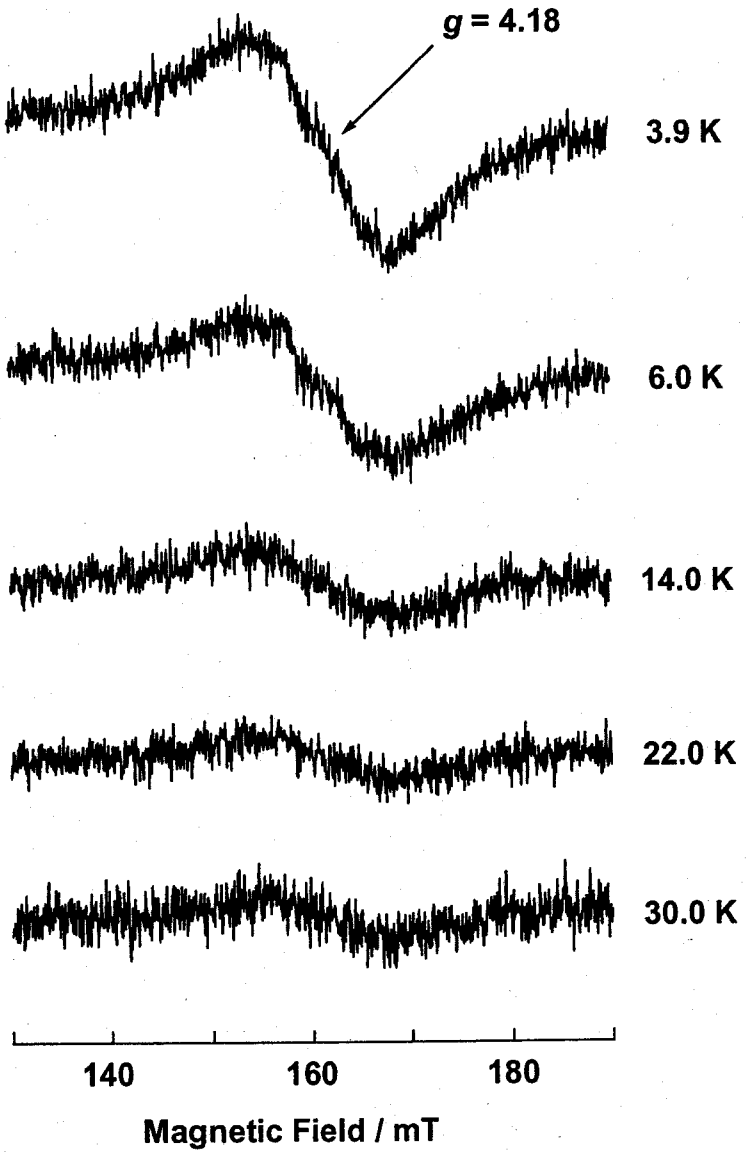

Figure 8. Temperature dependent ESR spectra of a CH_2Cl_2 solution of **3** containing 3.0 equiv of *t*-BuOK.

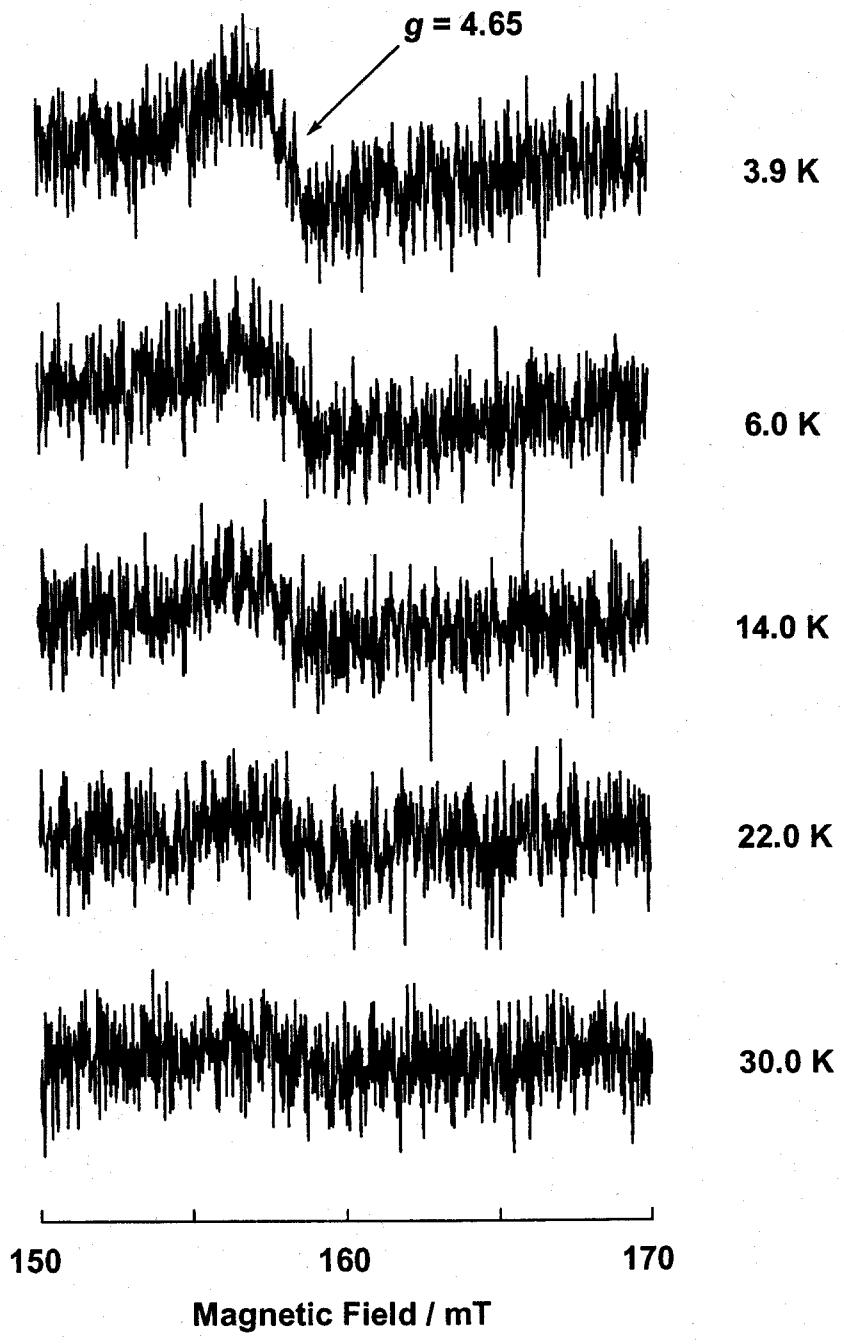

Figure 9. Temperature dependent ESR spectra of a CH_2Cl_2 solution of **4** containing 3.0 equiv of *t*-BuOK.

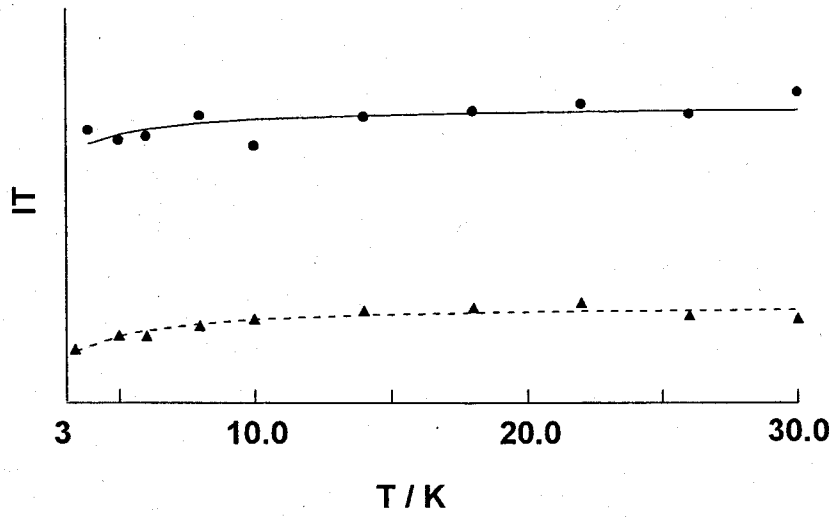

Figure 10. IT-T plot of the ESR spectra of **3** (closed circles) and **4** (closed triangles) in CH_2Cl_2 containing 3.0 equiv of *t*-BuOK. Simulation curves for **3** (solid line) and for **4** (dashed line).

4, References

(1) Harbour, J. R.; Chow, V.; Bolton, J. R. *Can. J. Chem.* **1974**, *52*, 3549.

(2) Finkelstein, E.; Rosen, G. M.; Rauckman, E. J. *Arch. Biochem. Biophys.* **1980**, *200*, 1.

(3) Taniguchi, H.; Madden, K. P. *J. Phys. Chem.* **1998**, *102*, 6753.

(4) A CH_2Cl_2/2-methoxyethanol (10:1 v/v) solution of **5** also showed the ESR signal of Figure 10A at 3.9 K.

(5) (a) Sheltz, D. A.; Bodnar, S. H. *Inorg. Chem.* **1999**, *38*, 591. (b) Shultz, D. A.; Lee, H.; Gawltney, K. P. *J. Org. Chem.* **1998**, *63*, 7584.

(6) Eaton, S. A.; More, K. M.; Sawant, B. M.; Eaton, G. R. *J. Am. Chem. Soc.* **1983**, *105*, 6560.

(7) (a) Gambarelli, S.; Jaouen, D.; Rassat, A. *J. Phys. Chem.* **1996**, *100*, 9605. (b) Pezeshk, A.; Coffman, R. E. *J. Phys. Chem.* **1986**, *90*, 6638.

(8) $g_{av}^2 = (g_{xx}^2 + g_{yy}^2 + g_{zz}^2)/3$

(9) *J* values obtained from the ESR signal intensities around $g = 2$ of **5** and $[Ru^{II}(trpy)(4ClSQ)O^{\bullet -}]$ were essentially consistent with those of the values determined from signals around $g = 4$.

Chapter 5

General Conclusion

Ru-OH_2 complexes containing a quinone ligand (**3**, **4**) reversibly dissociate protons to afford Ru-OH (or Ru-$OH^{\bullet}$) and Ru-$O^{\bullet-}$ (**5**) complexes. The Ru-$O^{\bullet-}$ complex **5** was isolated as single crystals by slow evaporation of CH_3OH of a CH_3OH/H_2O solution of **3** under strong basic conditions. X-ray crystal structure revealed that **5** is the first terminal metal-O complex with a single bond length. Dissociation of hydroxyl (or aqua) proton of **3** (or **4**) gave rise to the intra-molecular electron transfer from O^{2-} (or OH^-) to the [Ru^{III}(SQ)] moiety, which resulted in the formation of oxyl radical $O^{\bullet-}$ (or hydroxyl radical $OH^{\bullet}$) and the [Ru^{II}(SQ)] core. The resulted Ru-oxyl radical complexes showed antiferromagnetic behavior, and the ruthenium oxyl radical frameworks were characterized by spin trapping techniques. Ru-dioxolene plays the key roles in not only dissociation of hydroxyl proton as the electron reservoir, but also stabilization of the triplet state of the [Ru^{II}(SQ)] framework and oxyl radical ligand. This work is the first example of the metal complexes with an oxyl radical ligand, and may shed light on the development of a new type of electrocatalysts.

Appendix

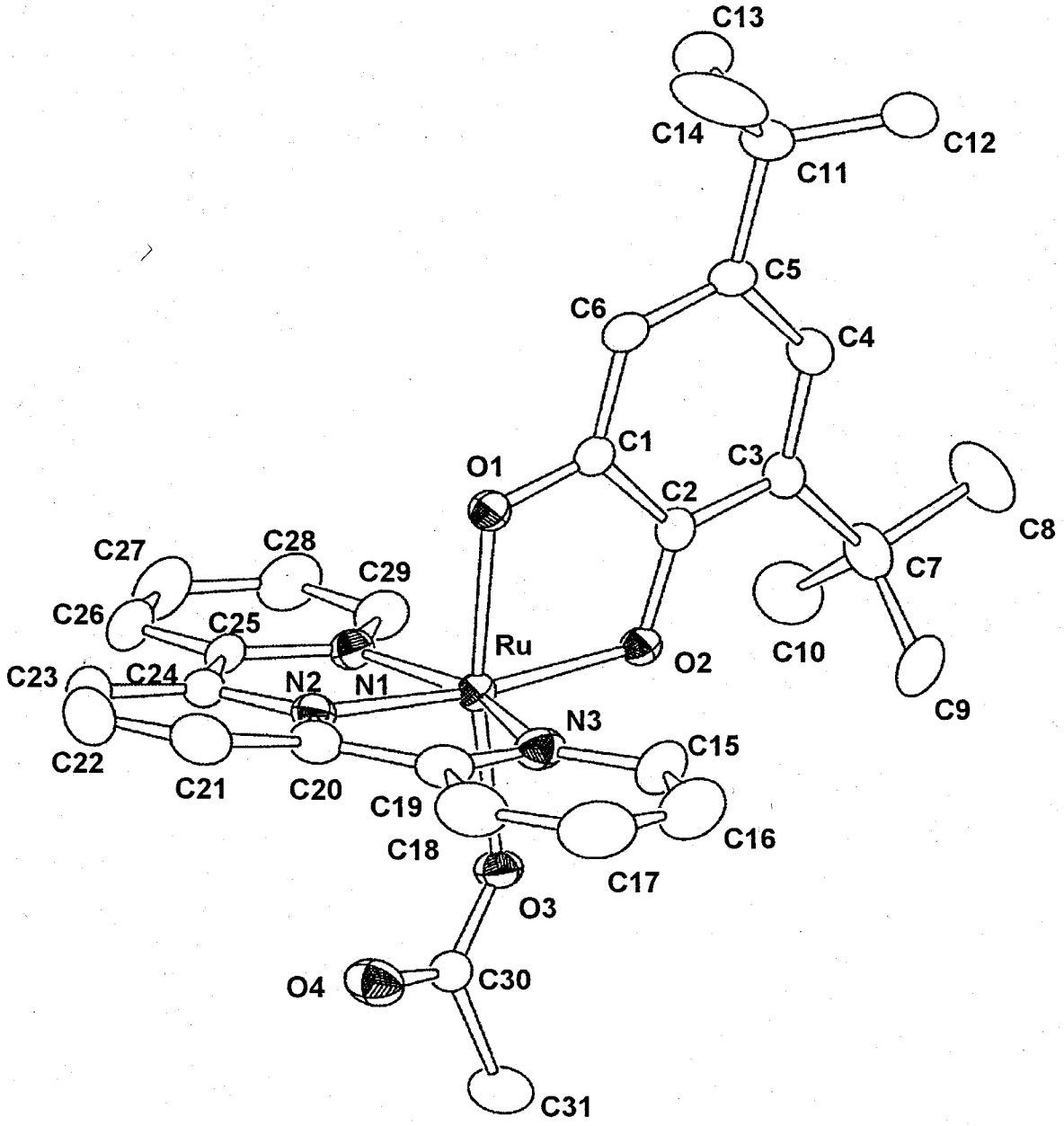

Figure A1. Crystal structures of [Ru^{II}(trpy)(Bu_2SQ)(OAc)] and the atom-numbering scheme. All hydrogen atoms are omitted for clarity.

Table A1. Crystal Data, Data Collection `Parameters, and Structure Refinement for $[Ru^{II}(trpy)(Bu_2SQ)(OAc)]\cdot MeOH$ (**1**·MeOH)

Crystal Data	
formula	$C_{32}H_{37}N_3O_5Ru$
formula weight	644.73
color	violet
crystal size / mm	0.50 × 0.30 × 0.20
crystal system	triclinic
space group	P-1
a / Å	8.391(5)
b / Å	9.318(6)
c / Å	21.46(2)
α / deg	86.59(2)
β / deg	81.85(2)
γ / deg	65.66(1)
V / Å^3	1513(1)
Z	2
D_{calc} / g cm^{-3}	1.415
F(000) / e	668.00
Data Collection	
Diffractometer Used	Rigaku/MSC Mercury CCD
radiation	Mo Kα (λ = 0.71070 Å)
μ / cm^{-1}	5.62
Voltage, Current	50 kV, 100 mA
T / K	173
Collimator Size	0.5 mm
Data Images	720 exposures @ 10.0 sec
Detector Aperture	70 mm x 70 mm
ω oscillation Range (χ=45.0, ϕ=0.0)	70.0
Detector Swing Angle	19.58º
Detector Position	45.08 mm
$2\theta_{max}$ / deg	55.0

Table A1 (continued) . Crystal Data, Data Collection `Parameters, and Structure Refinement for [Ru^{II}(trpy)(Bu_2SQ)(OAc)]·MeOH (**1**·MeOH)

No. of Reflections Measured	Total: 6557 Unique: 6557 (R_{int} = 0.029)

Structure Solution and Refinement

Structure Solution	Patterson Methods (DIRDIF94 PATTY)
Refinement	Full matrix least
Function Minimized	Σ w (|Fo|-|Fc|)^2
Least Squares Weights	$w = 1/\sigma^2(Fo) = 4Fo^2/\sigma^2(Fo^2)$
p factor	0.0500
Anomalous Dispersion	All non hydrogen atoms
reflections used (I>0.00σ(I), 2θ < 54.97^o)	6545
no. of variables	370
reflection / parameter ratio	17.69
GOF	1.890
R ($I > 2\sigma(I)$)	0.050,where $R = \Sigma[\|Fo\| - \|Fc\|]/\Sigma\|Fo\|$
R_w ($I > 2\sigma(I)$)	0.073, where $R_w = [(\Sigma w(\|Fo\| - \|Fc\|)^2/\Sigma w(\|Fo\|^2))^{1/2}$
Max Shift/Error in Final Cycle	0.039
Maximum peak in Final Diff. Map	1.72 $e^-/Å^3$
Minimum peak in Final Diff. Map	1.69 $e^-/Å^3$

Table A2. Fractional Atomic Coordination Including Hydrogen Atoms and Isotropic Thermal Parameters of $[Ru^{II}(trpy)(Bu_2SQ)(OAc)]\cdot MeOH$ (**1**·MeOH)

atom	x	y	z	B_{eq} [c]
Ru(1)	0.13436(4)	0.41442(3)	0.18950(1)	1.414(7)
O(1)	-0.0528(3)	0.5586(3)	0.2553(1)	1.71(5)
O(2)	0.2901(3)	0.4128(3)	0.2534(1)	1.61(5)
O(3)	0.3608(3)	0.2665(3)	0.1357(1)	1.88(5)
O(4)	0.2511(4)	0.1582(4)	0.0725(1)	2.59(6)
O(5)	0.2756(5)	0.1780(5)	0.8015(2)	4.59(9)
N(1)	0.1440(4)	0.6002(4)	0.1354(1)	1.70(6)
N(2)	-0.0392(4)	0.4392(4)	0.1334(1)	1.63(6)
N(3)	0.0649(5)	0.2324(4)	0.2203(2)	2.06(7)
C(1)	0.0142(5)	0.5772(4)	0.3051(2)	1.59(7)
C(2)	0.2014(5)	0.4990(4)	0.3038(2)	1.53(7)
C(3)	0.2836(5)	0.5205(5)	0.3538(2)	1.78(7)
C(4)	0.1732(5)	0.6119(5)	0.4044(2)	1.98(8)
C(5)	-0.0148(5)	0.6849(4)	0.4077(2)	1.78(7)
C(6)	-0.0907(5)	0.6665(4)	0.3573(2)	1.78(7)
C(7)	0.5659(6)	0.5058(7)	0.2934(2)	3.5(1)
C(8)	0.5508(6)	0.2651(6)	0.3461(2)	3.4(1)
C(9)	0.5464(6)	0.4782(9)	0.4100(2)	4.8(1)
C(10)	0.4847(5)	0.4442(6)	0.3509(2)	2.64(9)
C(11)	-0.0442(7)	0.7324(6)	0.5254(2)	3.19(10)
C(12)	-0.3100(8)	0.7850(9)	0.4755(3)	5.3(2)
C(13)	-0.1443(8)	0.9572(6)	0.4505(2)	3.7(1)
C(14)	-0.1258(6)	0.7871(5)	0.4646(2)	2.27(8)
C(15)	0.2434(5)	0.6786(5)	0.1410(2)	2.20(8)
C(16)	0.2328(6)	0.8082(6)	0.1043(2)	3.1(1)
C(17)	0.1201(6)	0.8557(6)	0.0585(2)	3.2(1)
C(18)	0.0178(5)	0.7741(5)	0.0516(2)	2.40(8)
C(19)	0.0292(5)	0.6479(5)	0.0910(2)	1.75(7)
C(20)	-0.0784(5)	0.5570(5)	0.0906(2)	1.88(7)
C(21)	-0.2108(6)	0.5864(5)	0.0536(2)	2.60(9)
C(22)	-0.3086(6)	0.4944(6)	0.0643(2)	3.1(1)
C(23)	-0.2704(6)	0.3759(6)	0.1089(2)	2.72(9)

Table A2 (continued). Fractional Atomic Coordination Including Hydrogen Atoms and Isotropic Thermal Parameters of $[Ru^{II}(trpy)(Bu_2SQ)(OAc)]\cdot MeOH$ (**1**·MeOH)

atom	x	y	z	B_{eq} [c]
C(24)	-0.1279(5)	0.3443(5)	0.1424(2)	2.03(8)
C(25)	-0.0627(5)	0.2236(5)	0.1903(2)	2.08(8)
C(26)	-0.1202(7)	0.1024(6)	0.2044(2)	3.1(1)
C(27)	-0.0483(7)	-0.0054(6)	0.2504(3)	3.7(1)
C(28)	0.0762(8)	0.0044(6)	0.2814(3)	3.7(1)
C(29)	0.1313(6)	0.1261(5)	0.2657(2)	2.67(9)
C(30)	0.3727(5)	0.1711(4)	0.0932(2)	1.70(7)
C(31)	0.5632(6)	0.0633(6)	0.0688(2)	3.3(1)
C(32)	0.4417(8)	0.0981(8)	0.7705(3)	5.2(1)
H(1)	0.2271	0.6260	0.4386	2.4
H(2)	-0.2164	0.7157	0.3575	2.1
H(3)	0.5242	0.6187	0.2965	4.3
H(4)	0.5322	0.4832	0.2559	4.3
H(5)	0.6910	0.4613	0.2905	4.3
H(6)	0.5152	0.2400	0.3096	3.9
H(7)	0.6768	0.2184	0.3425	3.9
H(8)	0.5041	0.2258	0.3823	3.9
H(9)	0.6721	0.4288	0.4071	6.0
H(10)	0.4986	0.4371	0.4465	6.0
H(11)	0.5080	0.5881	0.4149	6.0
H(12)	-0.0290	0.6263	0.5348	3.8
H(13)	0.0725	0.7334	0.5202	3.8
H(14)	-0.1127	0.7981	0.5595	3.8
H(15)	-0.2997	0.6787	0.4851	6.1
H(16)	-0.3686	0.8186	0.4388	6.1
H(17)	-0.3820	0.8503	0.5099	6.1
H(18)	-0.0295	0.9583	0.4445	4.4
H(19)	-0.1993	0.9959	0.4139	4.4
H(20)	-0.2123	1.0236	0.4854	4.4
H(21)	0.3257	0.6439	0.1715	2.7
H(22)	0.3017	0.8653	0.1101	3.4
H(23)	0.1149	0.9418	0.0316	3.8
H(24)	0.0592	0.8047	0.0193	2.9

Table A2 (continued). Fractional Atomic Coordination Including Hydrogen Atoms and Isotropic Thermal Parameters of $[Ru^{II}(trpy)(Bu_2SQ)(OAc)]\cdot MeOH$ (**1**·MeOH)

atom	x	y	z	B_{eq} [c]
H(25)	-0.2346	0.6668	0.0219	3.1
H(26)	-0.4056	0.5166	0.0406	3.6
H(27)	-0.3410	0.3166	0.1171	3.3
H(28)	-0.2092	0.0970	0.1826	3.6
H(29)	-0.0849	-0.0909	0.2593	4.4
H(30)	0.1255	-0.0691	0.3138	4.3
H(31)	0.2171	0.1356	0.2882	3.2
H(32)	0.6263	0.1246	0.0508	3.8
H(33)	0.5661	-0.0056	0.0369	3.8
H(34)	0.6225	0.0012	0.1021	3.8
H(35)	0.4682	0.1575	0.7361	6.0
H(36)	0.4497	0.0003	0.7528	6.0
H(37)	0.5301	0.0690	0.7977	6.0

[a] Numbers in parentheses are the estimated standard deviation in the last significant digit.

[b] The hydrogen atoms were placed at the calculated position and not refined.

[c] $B_{eq} = 8\pi^2/3(U_{11}(aa^*)^2+U_{22}(bb^*)^2+U_{33}(cc^*)^2+2U_{12}(aa^*bb^*)\cos\gamma+2U_{13}(aa^*cc^*)\cos\beta+2U_{23}(bb^*cc^*)\cos\alpha)$

Table A3. Anisotropic Thermal Parameters for Non-hydrogen Atoms in $[Ru^{II}(trpy)(Bu_2SQ)(OAc)]\cdot MeOH$ (**1**·MeOH)

atom	U_{11}	U_{22}	U_{33}	U_{12}	U_{13}	U_{23}
Ru(1)	0.0161(2)	0.0178(2)	0.0185(2)	-0.0054(1)	-0.0024(1)	-0.0004(1)
O(1)	0.016(1)	0.025(1)	0.022(1)	-0.005(1)	-0.0027(9)	-0.003(1)
O(2)	0.016(1)	0.021(1)	0.021(1)	-0.004(1)	-0.0023(9)	-0.0024(10)
O(3)	0.019(1)	0.022(1)	0.026(1)	-0.005(1)	-0.001(1)	-0.006(1)
O(4)	0.029(2)	0.037(2)	0.035(2)	-0.015(1)	-0.003(1)	-0.012(1)
O(5)	0.050(2)	0.041(2)	0.058(2)	0.005(2)	-0.003(2)	0.005(2)
N(1)	0.021(2)	0.020(2)	0.022(1)	-0.006(1)	-0.001(1)	0.000(1)
N(2)	0.023(2)	0.019(2)	0.020(1)	-0.008(1)	-0.001(1)	-0.003(1)
N(3)	0.031(2)	0.018(2)	0.027(2)	-0.008(1)	0.001(1)	-0.001(1)
C(1)	0.022(2)	0.014(2)	0.021(2)	-0.005(1)	-0.003(1)	0.002(1)
C(2)	0.022(2)	0.018(2)	0.020(2)	-0.010(1)	-0.004(1)	0.004(1)
C(3)	0.019(2)	0.028(2)	0.021(2)	-0.010(2)	-0.003(1)	0.001(1)
C(4)	0.021(2)	0.030(2)	0.025(2)	-0.011(2)	-0.005(1)	-0.004(2)
C(5)	0.022(2)	0.018(2)	0.023(2)	-0.006(1)	0.003(1)	-0.003(1)
C(6)	0.019(2)	0.019(2)	0.026(2)	-0.004(1)	0.000(1)	-0.001(1)
C(7)	0.029(2)	0.060(3)	0.046(3)	-0.024(2)	0.005(2)	-0.004(2)
C(8)	0.024(2)	0.047(3)	0.039(3)	0.004(2)	-0.005(2)	0.010(2)
C(9)	0.025(2)	0.116(6)	0.038(3)	-0.022(3)	-0.008(2)	-0.024(3)
C(10)	0.019(2)	0.056(3)	0.024(2)	-0.014(2)	-0.004(1)	-0.004(2)
C(11)	0.048(3)	0.031(2)	0.027(2)	-0.003(2)	0.002(2)	-0.005(2)
C(12)	0.042(3)	0.102(5)	0.059(4)	-0.036(3)	0.029(3)	-0.051(4)
C(13)	0.065(3)	0.026(2)	0.037(3)	-0.006(2)	-0.005(2)	-0.004(2)
C(14)	0.032(2)	0.024(2)	0.027(2)	-0.010(2)	0.002(2)	-0.006(2)
C(15)	0.024(2)	0.025(2)	0.036(2)	-0.012(2)	-0.001(2)	0.001(2)
C(16)	0.037(3)	0.029(2)	0.052(3)	-0.015(2)	-0.002(2)	0.005(2)
C(17)	0.032(2)	0.032(2)	0.052(3)	-0.012(2)	-0.002(2)	0.015(2)
C(18)	0.024(2)	0.027(2)	0.031(2)	-0.003(2)	-0.001(2)	0.008(2)
C(19)	0.018(2)	0.020(2)	0.022(2)	-0.001(1)	-0.003(1)	0.001(1)
C(20)	0.024(2)	0.021(2)	0.019(2)	-0.002(2)	-0.003(1)	-0.003(1)
C(21)	0.027(2)	0.035(2)	0.031(2)	-0.004(2)	-0.010(2)	-0.003(2)
C(22)	0.027(2)	0.053(3)	0.039(2)	-0.014(2)	-0.015(2)	-0.010(2)
C(23)	0.031(2)	0.039(3)	0.041(2)	-0.020(2)	-0.004(2)	-0.012(2)

Table A3 (continued). Anisotropic Thermal Parameters for Non-hydrogen Atoms in $[Ru^{II}(trpy)(Bu_2SQ)(OAc)]\cdot MeOH$ (**1**·MeOH)

atom	U_{11}	U_{22}	U_{33}	U_{12}	U_{13}	U_{23}
C(16)	0.037(3)	0.029(2)	0.052(3)	-0.015(2)	-0.002(2)	0.005(2)
C(17)	0.032(2)	0.032(2)	0.052(3)	-0.012(2)	-0.002(2)	0.015(2)
C(18)	0.024(2)	0.027(2)	0.031(2)	-0.003(2)	-0.001(2)	0.008(2)
C(19)	0.018(2)	0.020(2)	0.022(2)	-0.001(1)	-0.003(1)	0.001(1)
C(20)	0.024(2)	0.021(2)	0.019(2)	-0.002(2)	-0.003(1)	-0.003(1)
C(21)	0.027(2)	0.035(2)	0.031(2)	-0.004(2)	-0.010(2)	-0.003(2)
C(22)	0.027(2)	0.053(3)	0.039(2)	-0.014(2)	-0.015(2)	-0.010(2)
C(23)	0.031(2)	0.039(3)	0.041(2)	-0.020(2)	-0.004(2)	-0.012(2)
C(24)	0.019(2)	0.030(2)	0.029(2)	-0.012(2)	0.000(1)	-0.008(2)
C(25)	0.022(2)	0.027(2)	0.031(2)	-0.014(2)	0.006(1)	-0.006(2)
C(26)	0.049(3)	0.034(3)	0.046(3)	-0.029(2)	0.006(2)	-0.007(2)
C(27)	0.053(3)	0.035(3)	0.054(3)	-0.025(2)	0.014(2)	-0.002(2)
C(28)	0.053(3)	0.031(3)	0.048(3)	-0.015(2)	0.008(2)	0.013(2)
C(29)	0.031(2)	0.027(2)	0.034(2)	-0.005(2)	0.001(2)	0.008(2)
C(30)	0.022(2)	0.020(2)	0.019(2)	-0.006(1)	-0.001(1)	0.001(1)
C(31)	0.026(2)	0.050(3)	0.042(3)	-0.007(2)	-0.001(2)	-0.020(2)
C(32)	0.040(3)	0.046(4)	0.086(5)	0.003(3)	0.002(3)	0.022(3)

[a] Numbers in parentheses are the estimated standard deviation in the last significant digit.

[b] The general temperature factor expression:

$\exp(-2\pi^2(a^{*2}h^2U_{11}+b^{*2}k^2U_{22}+c^{*2}l^2U_{33}+2a^*b^*hkU_{12}+2a^*c^*hlU_{13}+2b^*c^*klU_{23}))$

Table A4. Bond Distances and Bond Angles of $[Ru^{II}(trpy)(Bu_2SQ)(OAc)]\cdot MeOH$ (**1**·MeOH)

Bond Distances (Å)

atom	atom	distance	atom	atom	distance
Ru(1)	O(1)	2.030(3)	Ru(1)	O(2)	2.019(3)
Ru(1)	O(3)	2.062(3)	Ru(1)	N(1)	2.050(3)
Ru(1)	N(2)	1.952(3)	Ru(1)	N(3)	2.056(3)
O(1)	C(1)	1.328(4)	O(2)	C(2)	1.324(4)
O(3)	C(30)	1.276(4)	O(4)	C(30)	1.221(5)
O(5)	C(32)	1.371(7)	N(1)	C(15)	1.336(5)
N(1)	C(19)	1.375(5)	N(2)	C(20)	1.351(5)
N(2)	C(24)	1.362(5)	N(3)	C(25)	1.357(5)
N(3)	C(29)	1.352(6)	C(1)	C(2)	1.430(5)
C(1)	C(6)	1.396(5)	C(2)	C(3)	1.421(5)
C(3)	C(4)	1.392(5)	C(3)	C(10)	1.531(5)
C(4)	C(5)	1.430(5)	C(5)	C(6)	1.383(5)
C(5)	C(14)	1.533(5)	C(7)	C(10)	1.522(7)
C(8)	C(10)	1.532(7)	C(9)	C(10)	1.532(6)
C(11)	C(14)	1.521(6)	C(12)	C(14)	1.538(7)
C(13)	C(14)	1.543(7)	C(15)	C(16)	1.380(6)
C(16)	C(17)	1.388(7)	C(17)	C(18)	1.386(7)
C(18)	C(19)	1.385(6)	C(19)	C(20)	1.472(6)
C(20)	C(21)	1.382(6)	C(21)	C(22)	1.402(7)
C(22)	C(23)	1.381(7)	C(23)	C(24)	1.401(6)
C(24)	C(25)	1.461(6)	C(25)	C(26)	1.403(6)
C(26)	C(27)	1.378(8)	C(27)	C(28)	1.352(8)
C(28)	C(29)	1.398(7)	C(30)	C(31)	1.530(6)

Bond Angles (deg)

atom	atom	atom	angle	atom	atom	atom	angle
O(1)	Ru(1)	O(2)	80.7(1)	O(1)	Ru(1)	O(3)	167.8(1)
O(1)	Ru(1)	N(1)	92.6(1)	O(1)	Ru(1)	N(2)	92.3(1)
O(1)	Ru(1)	N(3)	90.1(1)	O(2)	Ru(1)	O(3)	87.1(1)

Table A4 (continued). Bond Distances and Bond Angles of [Ru^{II}(trpy)(Bu_2SQ)(OAc)]·MeOH (**1**·MeOH)

atom	atom	atom	angle	atom	atom	atom	angle
O(2)	Ru(1)	N(1)	98.9(1)	O(2)	Ru(1)	N(2)	172.8(1)
O(2)	Ru(1)	N(3)	102.1(1)	O(3)	Ru(1)	N(1)	89.1(1)
O(3)	Ru(1)	N(2)	99.9(1)	O(3)	Ru(1)	N(3)	92.6(1)
N(1)	Ru(1)	N(2)	79.4(1)	N(1)	Ru(1)	N(3)	159.0(1)
N(2)	Ru(1)	N(3)	79.7(1)	Ru(1)	O(1)	C(1)	112.6(2)
Ru(1)	O(2)	C(2)	113.3(2)	Ru(1)	O(3)	C(30)	127.1(2)
Ru(1)	N(1)	C(15)	126.7(3)	Ru(1)	N(1)	C(19)	114.0(3)
C(15)	N(1)	C(19)	119.2(4)	Ru(1)	N(2)	C(20)	119.6(3)
Ru(1)	N(2)	C(24)	118.3(3)	C(20)	N(2)	C(24)	121.9(3)
Ru(1)	N(3)	C(25)	113.7(3)	Ru(1)	N(3)	C(29)	127.3(3)
C(25)	N(3)	C(29)	119.0(4)	O(1)	C(1)	C(2)	116.9(3)
O(1)	C(1)	C(6)	122.6(3)	C(2)	C(1)	C(6)	120.5(3)
O(2)	C(2)	C(1)	116.5(3)	O(2)	C(2)	C(3)	123.3(3)
C(1)	C(2)	C(3)	120.1(3)	C(2)	C(3)	C(4)	116.9(3)
C(2)	C(3)	C(10)	120.3(3)	C(4)	C(3)	C(10)	122.8(3)
C(3)	C(4)	C(5)	123.5(3)	C(4)	C(5)	C(6)	118.2(3)
C(4)	C(5)	C(14)	119.9(3)	C(6)	C(5)	C(14)	121.8(3)
C(1)	C(6)	C(5)	120.6(3)	C(3)	C(10)	C(7)	109.2(4)
C(3)	C(10)	C(8)	109.6(4)	C(3)	C(10)	C(9)	112.1(4)
C(7)	C(10)	C(8)	109.5(4)	C(7)	C(10)	C(9)	109.2(4)
C(8)	C(10)	C(9)	107.1(4)	C(5)	C(14)	C(11)	113.1(4)
C(5)	C(14)	C(12)	110.3(3)	C(5)	C(14)	C(13)	107.9(3)
C(11)	C(14)	C(12)	107.3(4)	C(11)	C(14)	C(13)	108.8(4)
C(12)	C(14)	C(13)	109.3(5)	N(1)	C(15)	C(16)	122.2(4)
C(15)	C(16)	C(17)	119.1(4)	C(16)	C(17)	C(18)	119.3(4)
C(17)	C(18)	C(19)	119.3(4)	N(1)	C(19)	C(18)	120.8(4)
N(1)	C(19)	C(20)	114.6(3)	C(18)	C(19)	C(20)	124.6(4)
N(2)	C(20)	C(19)	112.3(3)	N(2)	C(20)	C(21)	121.3(4)
C(19)	C(20)	C(21)	126.3(4)	C(20)	C(21)	C(22)	117.5(4)
C(21)	C(22)	C(23)	121.0(4)	C(22)	C(23)	C(24)	119.3(4)
N(2)	C(24)	C(23)	118.8(4)	N(2)	C(24)	C(25)	112.8(3)

Table A4 (continued). Bond Distances and Bond Angles of [Ru^{II}(trpy)(Bu_2SQ)(OAc)]·MeOH (**1**·MeOH)

atom	atom	atom	angle	atom	atom	atom	angle
C(23)	C(24)	C(25)	128.3(4)	N(3)	C(25)	C(24)	115.2(3)
N(3)	C(25)	C(26)	120.6(4)	C(24)	C(25)	C(26)	124.1(4)
C(25)	C(26)	C(27)	118.9(5)	C(26)	C(27)	C(28)	120.9(4)
C(27)	C(28)	C(29)	118.6(5)	N(3)	C(29)	C(28)	122.0(5)
O(3)	C(30)	O(4)	126.9(4)	O(3)	C(30)	C(31)	113.3(3)
O(4)	C(30)	C(31)	119.8(3)				

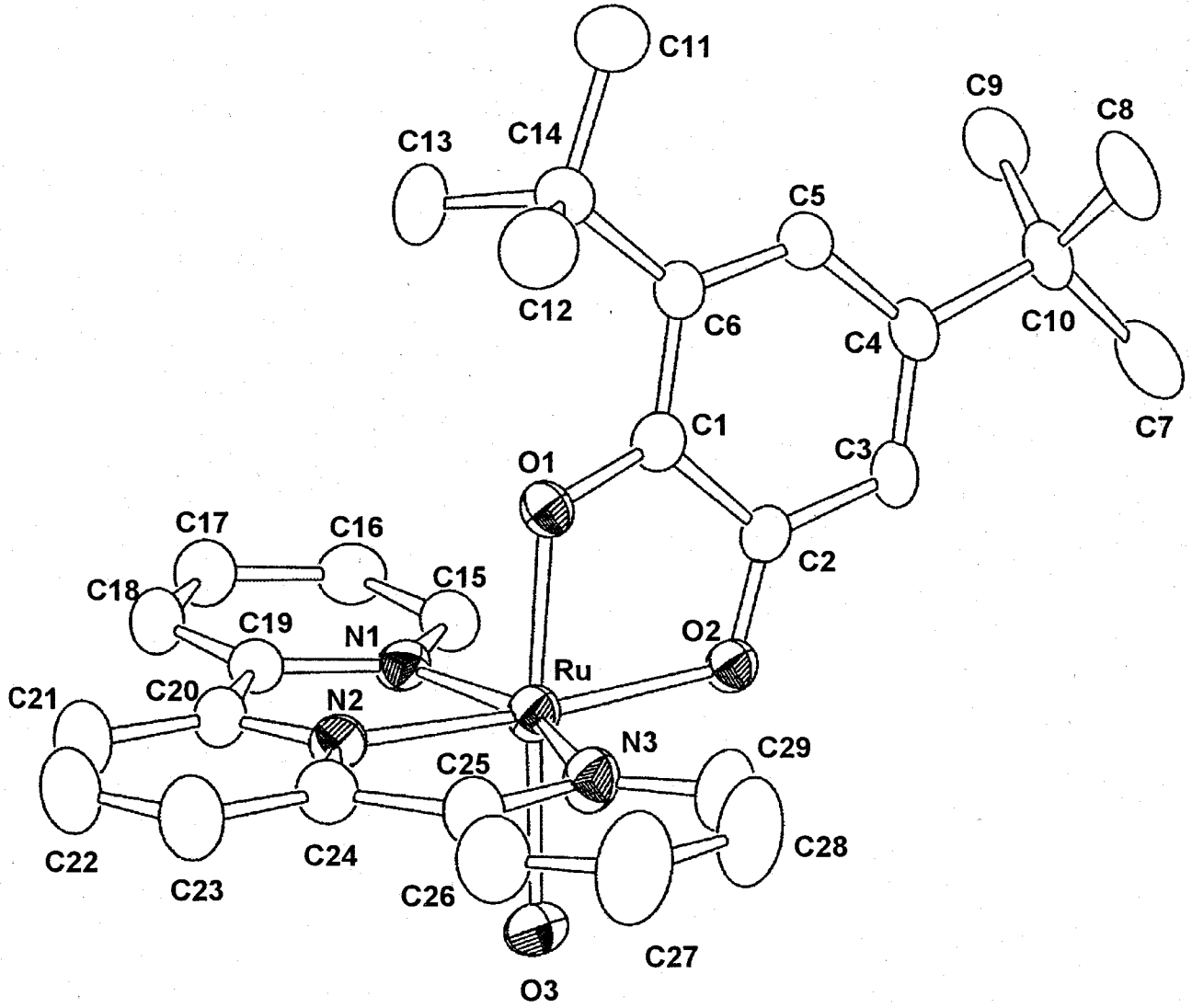

Figure A2. Crystal structures of $[Ru^{II}(trpy)(Bu_2SQ)(OH_2)]^{2+}$ cation and the atom-numbering scheme. All hydrogen atoms are omitted for clarity.

Table A5. Crystal Data, Data Collection `Parameters, and Structre Refinement for $[Ru^{III}(trpy)(Bu_2SQ)(OH_2)](ClO_4)_2 \cdot H_2O$ (**3**$\cdot H_2O$)

Crystal Data	
formula	$C_{29}H_{31}N_3O_{12}RuCl_2$
formula weight	785.55
color	Blue
crystal size / mm	0.20 × 0.06 × 0.06
crystal system	triclinic
space group	P-1
a / Å	10.989(2)
b / Å	11.062(2)
c / Å	15.058(2)
α / deg	91.681(4)
β / deg	103.517(5)
γ / deg	109.252(6)
V / Å^3	1668.9(5)
Z	2
D_{calc} / g cm^{-3}	1.563
F(000) / e	800.00
Data Collection	
Diffractometer Used	Rigaku/MSC Mercury CCD
radiation	Mo Kα (λ = 0.71070 Å)
μ / cm^{-1}	6.95
Voltage, Current	60 kV, 250 mA
T / K	173
Collimator Size	0.5 mm
Data Images	720 exposures @ 50.0 sec
Detector Aperture	70 mm x 70 mm
ω oscillation Range (χ=45.0, ϕ=0.0)	70.0
Detector Swing Angle	19.61º
Detector Position	45.05 mm
$2\theta_{max}$ / deg	55.0

Table A5 (continued). Crystal Data, Data Collection `Parameters, and Structre Refinement for $[Ru^{III}(trpy)(Bu_2SQ)(OH_2)](ClO_4)_2 \cdot H_2O$ (**3**$\cdot H_2O$)

No. of Reflections Measured	Total: 7303 Unique: 7303 (R_{int} = 0.035)
Structure Solution and Refinement	
Structure Solution	Direct Methods (SIR88)
Refinement	Full matrix least-squares
Function Minimized	Σ w (|Fo|-|Fc|)^2
Least Squares Weights	$1/\sigma^2(Fo) = 4Fo^2/\sigma^2(Fo^2)$
p factor	0.0500
Anomalous Dispersion	All non hydrogen atoms
reflections used	7214
($I>0.00\sigma(I)$, $2\theta < 54.97^o$)	
no. of variables	424
reflection / parameter ratio	17.01
GOF	1.61
R^a ($I > 2\sigma(I)$)	0.064
$R_w{}^a$ ($I > 2\sigma(I)$)	0.074
Max Shift/Error in Final Cycle	0.766
Maximum peak in Final Diff. Map	1.61 $e^-/Å^3$
Minimum peak in Final Diff. Map	-0.83 $e^-/Å^3$

Table A6. Fractional Atomic Coordination Including Hydrogen Atoms and Isotropic Thermal Parameters of $[Ru^{III}(trpy)(Bu_2SQ)(OH_2)](ClO_4)_2 \cdot H_2O$ (**3**$\cdot H_2O$)

atom	x	y	z	B_{eq} [c]
Ru(1)	0.27626(4)	0.29042(3)	0.84917(3)	2.236(8)
Cl(1)	0.5421(1)	0.2809(1)	0.34465(9)	2.67(2)
Cl(2)	0.7684(2)	0.3333(1)	0.8976(1)	4.08(3)
O(1)	0.0971(3)	0.2201(3)	0.7641(2)	2.17(6)
O(2)	0.2353(3)	0.4543(3)	0.8261(2)	2.11(6)
O(3)	0.4692(3)	0.3847(3)	0.9336(2)	2.87(7)
O(4)	0.5141(4)	0.1513(3)	0.3625(3)	4.4(1)
O(5)	0.6636(5)	0.3286(5)	0.3196(4)	5.4(1)
O(6)	0.4367(5)	0.2871(6)	0.2695(3)	6.0(1)
O(7)	0.5471(5)	0.3582(4)	0.4233(3)	4.8(1)
O(8)	0.739(1)	0.2070(6)	0.8706(5)	17.0(4)
O(9)	0.7803(7)	0.3548(5)	0.9937(4)	6.8(2)
O(10)	0.8799(7)	0.4125(8)	0.8772(5)	10.2(2)
O(11)	0.6646(7)	0.3774(9)	0.8486(5)	10.1(2)
O(12)	0.5233(4)	0.3300(4)	0.1043(3)	3.91(9)
N(1)	0.3599(4)	0.2766(3)	0.7418(3)	2.11(7)
N(2)	0.3022(4)	0.1245(3)	0.8637(3)	2.25(8)
N(3)	0.2088(4)	0.2458(4)	0.9648(3)	2.69(9)
C(1)	0.0448(5)	0.3028(4)	0.7295(3)	1.99(9)
C(2)	0.1244(5)	0.4369(4)	0.7671(3)	2.07(9)
C(3)	0.0779(5)	0.5377(4)	0.7361(3)	2.21(9)
C(4)	-0.0386(5)	0.5069(4)	0.6700(3)	2.08(9)
C(5)	-0.1144(5)	0.3727(4)	0.6345(3)	2.25(9)
C(6)	-0.0783(5)	0.2699(4)	0.6611(3)	2.06(9)
C(7)	-0.0036(6)	0.7428(5)	0.6722(4)	3.6(1)
C(8)	-0.2322(6)	0.5826(6)	0.6463(4)	3.9(1)
C(9)	-0.1067(6)	0.6009(5)	0.5261(4)	3.2(1)
C(10)	-0.0939(5)	0.6101(5)	0.6307(3)	2.6(1)
C(11)	-0.0745(6)	0.0749(5)	0.5746(4)	3.5(1)
C(12)	-0.1902(6)	0.0479(5)	0.7008(4)	3.9(1)
C(13)	-0.2857(6)	0.1169(6)	0.5537(5)	4.6(1)
C(14)	-0.1570(5)	0.1290(4)	0.6229(3)	2.60(10)

Table A6 (continued). Fractional Atomic Coordination Including Hydrogen Atoms and Isotropic Thermal Parameters of $[Ru^{III}(trpy)(Bu_2SQ)(OH_2)](ClO_4)_2 \cdot H_2O$ (**3**$\cdot H_2O$)

atom	x	y	z	B_{eq} [c]
C(15)	0.3799(5)	0.3597(4)	0.6797(3)	2.45(9)
C(16)	0.4210(5)	0.3330(5)	0.6031(3)	2.60(10)
C(17)	0.4398(5)	0.2177(5)	0.5912(4)	2.8(1)
C(18)	0.4208(5)	0.1317(5)	0.6560(4)	2.9(1)
C(19)	0.3800(5)	0.1613(4)	0.7307(3)	2.26(9)
C(20)	0.3530(5)	0.0778(4)	0.8034(3)	2.46(10)
C(21)	0.3760(6)	-0.0371(5)	0.8136(4)	3.5(1)
C(22)	0.3442(7)	-0.1030(5)	0.8882(4)	4.1(1)
C(23)	0.2935(7)	-0.0537(5)	0.9502(4)	3.7(1)
C(24)	0.2723(5)	0.0618(5)	0.9364(3)	2.7(1)
C(25)	0.2173(6)	0.1317(5)	0.9938(3)	2.9(1)
C(26)	0.1776(7)	0.0881(6)	1.0712(4)	4.2(1)
C(27)	0.1228(9)	0.1593(7)	1.1169(5)	5.6(2)
C(28)	0.1112(9)	0.2707(6)	1.0863(5)	5.2(2)
C(29)	0.1573(7)	0.3131(5)	1.0103(4)	3.6(1)
H(1)	0.1271	0.6247	0.7618	2.7
H(2)	-0.1969	0.3543	0.5888	2.8
H(3)	0.0824	0.7585	0.6613	4.3
H(4)	0.0057	0.7517	0.7364	4.3
H(5)	-0.0384	0.8056	0.6452	4.3
H(6)	-0.2275	0.5842	0.7105	4.6
H(7)	-0.2708	0.6437	0.6217	4.6
H(8)	-0.2904	0.4980	0.6169	4.6
H(9)	-0.1434	0.6624	0.4986	4.0
H(10)	-0.1653	0.5164	0.4976	4.0
H(11)	-0.0222	0.6159	0.5143	4.0
H(12)	0.0085	0.0816	0.6179	4.2
H(13)	-0.0529	0.1238	0.5257	4.2
H(14)	-0.1208	-0.0126	0.5512	4.2
H(15)	-0.1085	0.0520	0.7446	4.7
H(16)	-0.2412	0.0786	0.7323	4.7
H(17)	-0.2381	-0.0406	0.6772	4.7
H(18)	-0.3402	0.1497	0.5809	5.5

Table A6 (continued). Fractional Atomic Coordination Including Hydrogen Atoms and Isotropic Thermal Parameters of $[Ru^{III}(trpy)(Bu_2SQ)(OH_2)](ClO_4)_2 \cdot H_2O$ (**3**$\cdot H_2O$)

atom	x	y	z	B_{eq} [c]
H(19)	-0.3344	0.0296	0.5287	5.5
H(20)	-0.2665	0.1662	0.5035	5.5
H(21)	0.3661	0.4403	0.6884	2.9
H(22)	0.4359	0.3941	0.5592	3.1
H(23)	0.4650	0.1967	0.5382	3.3
H(24)	0.4362	0.0521	0.6490	3.4
H(25)	0.4137	-0.0709	0.7711	4.1
H(26)	0.3589	-0.1835	0.8963	4.8
H(27)	0.2733	-0.0977	1.0015	4.4
H(28)	0.1878	0.0111	1.0932	4.9
H(29)	0.0892	0.1291	1.1679	6.2
H(30)	0.0752	0.3206	1.1174	6.0
H(31)	0.1509	0.3930	0.9900	4.2

[a] Numbers in parentheses are the estimated standard deviation in the last significant digit.

[b] The hydrogen atoms were placed at the calculated position and not refined.

[c] $Beq = 8\pi^2/3(U_{11}(aa^*)^2+U_{22}(bb^*)^2+U_{33}(cc^*)^2+2U_{12}(aa^*bb^*)\cos\gamma+2U_{13}(aa^*cc^*)\cos\beta+2U_{23}(bb^*cc^*)\cos\alpha)$

Table A7. Anisotropic Thermal Parameters for Non-hydrogen Atoms in $[Ru^{III}(trpy)(Bu_2SQ)(OH_2)](ClO_4)_2 \cdot H_2O$ (**3**·H_2O)

atom	U_{11}	U_{22}	U_{33}	U_{12}	U_{13}	U_{23}
Ru(1)	0.0388(2)	0.0230(2)	0.0240(2)	0.0134(2)	0.0055(1)	0.0050(1)
Cl(1)	0.0409(7)	0.0285(5)	0.0383(6)	0.0138(5)	0.0191(5)	0.0095(5)
Cl(2)	0.068(1)	0.0402(7)	0.0544(9)	0.0197(7)	0.0268(8)	0.0166(6)
O(1)	0.033(2)	0.023(1)	0.028(2)	0.013(1)	0.006(1)	0.008(1)
O(2)	0.034(2)	0.022(1)	0.024(2)	0.011(1)	0.004(1)	0.003(1)
O(3)	0.038(2)	0.034(2)	0.031(2)	0.011(1)	-0.002(1)	-0.003(1)
O(4)	0.063(3)	0.026(2)	0.076(3)	0.010(2)	0.020(2)	0.011(2)
O(5)	0.055(3)	0.070(3)	0.082(3)	0.006(2)	0.045(3)	0.010(3)
O(6)	0.079(4)	0.115(4)	0.053(3)	0.057(3)	0.015(3)	0.031(3)
O(7)	0.101(4)	0.043(2)	0.053(3)	0.027(2)	0.043(3)	0.004(2)
O(8)	0.53(2)	0.068(4)	0.100(6)	0.123(8)	0.157(9)	0.038(4)
O(9)	0.152(6)	0.071(3)	0.059(3)	0.053(4)	0.046(3)	0.022(3)
O(10)	0.103(5)	0.159(7)	0.130(6)	0.015(5)	0.079(5)	0.045(5)
O(11)	0.084(5)	0.209(8)	0.098(5)	0.071(5)	0.007(4)	0.024(5)
O(12)	0.055(3)	0.039(2)	0.044(2)	0.014(2)	-0.004(2)	0.010(2)
N(1)	0.031(2)	0.021(2)	0.025(2)	0.008(1)	0.002(2)	0.001(1)
N(2)	0.038(2)	0.025(2)	0.022(2)	0.012(2)	0.004(2)	0.007(1)
N(3)	0.048(3)	0.025(2)	0.031(2)	0.016(2)	0.009(2)	0.007(2)
C(1)	0.033(2)	0.024(2)	0.022(2)	0.009(2)	0.012(2)	0.008(2)
C(2)	0.035(2)	0.023(2)	0.023(2)	0.012(2)	0.009(2)	0.003(2)
C(3)	0.034(2)	0.023(2)	0.035(2)	0.014(2)	0.017(2)	0.008(2)
C(4)	0.030(2)	0.027(2)	0.029(2)	0.015(2)	0.014(2)	0.009(2)
C(5)	0.029(2)	0.027(2)	0.030(2)	0.011(2)	0.008(2)	0.005(2)
C(6)	0.030(2)	0.025(2)	0.027(2)	0.011(2)	0.010(2)	0.004(2)
C(7)	0.053(3)	0.046(3)	0.054(3)	0.033(3)	0.015(3)	0.026(3)
C(8)	0.049(3)	0.055(3)	0.066(4)	0.037(3)	0.030(3)	0.023(3)
C(9)	0.051(3)	0.045(3)	0.038(3)	0.027(3)	0.014(2)	0.017(2)
C(10)	0.041(3)	0.032(2)	0.038(3)	0.024(2)	0.015(2)	0.013(2)
C(11)	0.057(4)	0.028(2)	0.054(3)	0.019(2)	0.019(3)	-0.001(2)
C(12)	0.044(3)	0.031(3)	0.066(4)	-0.001(2)	0.021(3)	0.013(3)
C(13)	0.051(4)	0.038(3)	0.069(4)	0.014(3)	-0.012(3)	-0.005(3)
C(14)	0.034(3)	0.027(2)	0.036(3)	0.011(2)	0.004(2)	0.006(2)

Table A7 (continued). Anisotropic Thermal Parameters for Non-hydrogen Atoms in $[Ru^{III}(trpy)(Bu_2SQ)(OH_2)](ClO_4)_2 \cdot H_2O$ (**3**$\cdot H_2O$)

atom	U_{11}	U_{22}	U_{33}	U_{12}	U_{13}	U_{23}
C(15)	0.035(3)	0.022(2)	0.036(3)	0.009(2)	0.008(2)	0.010(2)
C(16)	0.035(3)	0.033(2)	0.029(2)	0.007(2)	0.010(2)	0.011(2)
C(17)	0.040(3)	0.038(3)	0.034(3)	0.015(2)	0.014(2)	0.005(2)
C(18)	0.044(3)	0.031(2)	0.038(3)	0.019(2)	0.010(2)	0.002(2)
C(19)	0.035(2)	0.025(2)	0.026(2)	0.013(2)	0.004(2)	0.004(2)
C(20)	0.040(3)	0.025(2)	0.029(2)	0.015(2)	0.006(2)	0.003(2)
C(21)	0.061(4)	0.035(3)	0.045(3)	0.026(3)	0.018(3)	0.011(2)
C(22)	0.078(5)	0.040(3)	0.053(4)	0.036(3)	0.018(3)	0.017(3)
C(23)	0.076(4)	0.035(3)	0.043(3)	0.028(3)	0.023(3)	0.021(2)
C(24)	0.045(3)	0.030(2)	0.030(2)	0.015(2)	0.009(2)	0.011(2)
C(25)	0.054(3)	0.037(3)	0.030(2)	0.023(2)	0.015(2)	0.011(2)
C(26)	0.087(5)	0.049(3)	0.039(3)	0.034(3)	0.025(3)	0.023(3)
C(27)	0.131(7)	0.060(4)	0.053(4)	0.048(4)	0.058(5)	0.030(3)
C(28)	0.120(6)	0.055(4)	0.054(4)	0.048(4)	0.053(4)	0.021(3)
C(29)	0.076(4)	0.036(3)	0.037(3)	0.028(3)	0.020(3)	0.007(2)

[a] Numbers in parentheses are the estimated standard deviation in the last significant digit.

[b] The general temperature factor expression:

$\exp(-2\pi^2(a^{*2}h^2U_{11}+b^{*2}k^2U_{22}+c^{*2}l^2U_{33}+2a^*b^*hkU_{12}+2a^*c^*hlU_{13}+2b^*c^*klU_{23}))$

Table A8. Bond Distances and Bond Angles of $[Ru^{III}(trpy)(Bu_2SQ)(OH_2)](ClO_4)_2 \cdot H_2O$ (**3**$\cdot H_2O$)

Bond Distances (Å)

atom	atom	distance	atom	atom	distance
Ru(1)	O(1)	1.968(3)	Ru(1)	O(2)	2.028(3)
Ru(1)	O(3)	2.099(3)	Ru(1)	N(1)	2.063(4)
Ru(1)	N(2)	1.959(4)	Ru(1)	N(3)	2.059(4)
Cl(1)	O(4)	1.412(4)	Cl(1)	O(5)	1.410(4)
Cl(1)	O(6)	1.439(5)	Cl(1)	O(7)	1.420(4)
Cl(2)	O(8)	1.353(6)	Cl(2)	O(9)	1.428(5)
Cl(2)	O(10)	1.359(6)	Cl(2)	O(11)	1.442(7)
Cl(2)	O(10)	1.359(6)	Cl(2)	O(11)	1.442(7)
N(1)	C(15)	1.333(6)	N(1)	C(19)	1.376(6)
N(2)	C(20)	1.343(6)	N(2)	C(24)	1.360(6)
N(3)	C(25)	1.371(6)	N(3)	C(29)	1.332(7)
C(1)	C(2)	1.466(6)	C(1)	C(6)	1.423(6)
C(2)	C(3)	1.420(6)	C(3)	C(4)	1.357(7)
C(4)	C(5)	1.454(6)	C(4)	C(10)	1.533(6)
C(5)	C(6)	1.365(6)	C(6)	C(14)	1.528(6)
C(7)	C(10)	1.492(8)	C(8)	C(10)	1.525(7)
C(9)	C(10)	1.545(7)	C(11)	C(14)	1.533(7)
C(12)	C(14)	1.537(8)	C(13)	C(14)	1.510(8)
C(15)	C(16)	1.391(7)	C(16)	C(17)	1.371(7)
C(17)	C(18)	1.387(7)	C(18)	C(19)	1.373(7)
C(19)	C(20)	1.473(6)	C(20)	C(21)	1.382(7)
C(21)	C(22)	1.407(8)	C(22)	C(23)	1.376(8)
C(23)	C(24)	1.386(7)	C(24)	C(25)	1.492(7)
C(25)	C(26)	1.383(7)	C(26)	C(27)	1.390(9)
C(27)	C(28)	1.363(9)	C(28)	C(29)	1.390(8)

Bond Angles (deg)

atom	atom	atom	angle	atom	atom	atom	angle
O(1)	Ru(1)	O(2)	79.2(1)	O(1)	Ru(1)	O(3)	173.6(1)

Table A8 (continued). Bond Distances and Bond Angles of $[Ru^{III}(trpy)(Bu_2SQ)(OH_2)](ClO_4)_2 \cdot H_2O$ (**3**$\cdot H_2O$)

atom	atom	atom	angle	atom	atom	atom	angle
O(1)	Ru(1)	N(1)	89.9(1)	O(1)	Ru(1)	N(2)	96.1(1)
O(1)	Ru(1)	N(3)	94.2(2)	O(2)	Ru(1)	O(3)	95.0(1)
O(2)	Ru(1)	N(1)	99.8(1)	O(2)	Ru(1)	N(2)	175.3(1)
O(2)	Ru(1)	N(3)	100.6(1)	O(3)	Ru(1)	N(1)	88.6(1)
O(3)	Ru(1)	N(2)	89.7(1)	O(3)	Ru(1)	N(3)	89.3(2)
N(1)	Ru(1)	N(2)	79.5(2)	N(1)	Ru(1)	N(3)	159.5(1)
N(2)	Ru(1)	N(3)	80.1(2)	O(4)	Cl(1)	O(5)	111.0(3)
O(4)	Cl(1)	O(6)	108.5(3)	O(4)	Cl(1)	O(7)	110.0(3)
O(5)	Cl(1)	O(6)	108.5(3)	O(5)	Cl(1)	O(7)	109.9(3)
O(6)	Cl(1)	O(7)	108.8(3)	O(8)	Cl(2)	O(9)	111.1(4)
O(8)	Cl(2)	O(10)	113.7(6)	O(8)	Cl(2)	O(11)	110.4(7)
O(9)	Cl(2)	O(10)	109.6(4)	O(9)	Cl(2)	O(11)	108.1(4)
O(10)	Cl(2)	O(11)	103.5(5)	Ru(1)	O(1)	C(1)	116.7(3)
Ru(1)	O(2)	C(2)	114.1(3)	Ru(1)	N(1)	C(15)	126.3(3)
Ru(1)	N(1)	C(19)	113.3(3)	C(15)	N(1)	C(19)	120.0(4)
Ru(1)	N(2)	C(20)	119.2(3)	Ru(1)	N(2)	C(24)	119.1(3)
C(20)	N(2)	C(24)	121.7(4)	Ru(1)	N(3)	C(25)	113.6(3)
Ru(1)	N(3)	C(29)	127.1(4)	C(25)	N(3)	C(29)	119.3(4)
O(1)	C(1)	C(2)	113.8(4)	O(1)	C(1)	C(6)	124.4(4)
C(2)	C(1)	C(6)	121.8(4)	O(2)	C(2)	C(1)	115.8(4)
O(2)	C(2)	C(3)	124.3(4)	C(1)	C(2)	C(3)	119.8(4)
C(2)	C(3)	C(4)	118.6(4)	C(3)	C(4)	C(5)	119.8(4)
C(3)	C(4)	C(10)	121.9(4)	C(5)	C(4)	C(10)	118.3(4)
C(4)	C(5)	C(6)	125.5(4)	C(1)	C(6)	C(5)	114.4(4)
C(1)	C(6)	C(14)	120.1(4)	C(5)	C(6)	C(14)	125.5(4)
C(4)	C(10)	C(7)	112.0(4)	C(4)	C(10)	C(8)	108.9(4)
C(4)	C(10)	C(9)	108.2(4)	C(7)	C(10)	C(8)	110.8(4)
C(7)	C(10)	C(9)	108.1(4)	C(8)	C(10)	C(9)	108.7(5)
C(6)	C(14)	C(11)	109.8(4)	C(6)	C(14)	C(12)	110.5(4)
C(6)	C(14)	C(13)	110.8(4)	C(11)	C(14)	C(12)	108.8(4)
C(11)	C(14)	C(13)	108.2(5)	C(12)	C(14)	C(13)	108.7(5)
N(1)	C(15)	C(16)	121.6(4)	C(15)	C(16)	C(17)	118.7(4)

Table A8 (continued). Bond Distances and Bond Angles of $[Ru^{III}(trpy)(Bu_2SQ)(OH_2)](ClO_4)_2 \cdot H_2O$ (**3**·H_2O)

atom	atom	atom	angle	atom	atom	atom	angle
C(16)	C(17)	C(18)	119.9(5)	C(17)	C(18)	C(19)	119.7(4)
N(1)	C(19)	C(18)	120.1(4)	N(1)	C(19)	C(20)	114.5(4)
C(18)	C(19)	C(20)	125.3(4)	N(2)	C(20)	C(19)	113.1(4)
N(2)	C(20)	C(21)	120.4(5)	C(19)	C(20)	C(21)	126.5(4)
C(20)	C(21)	C(22)	118.1(5)	C(21)	C(22)	C(23)	121.1(5)
C(22)	C(23)	C(24)	118.2(5)	N(2)	C(24)	C(23)	120.5(5)
N(2)	C(24)	C(25)	112.2(4)	C(23)	C(24)	C(25)	127.3(5)
N(3)	C(25)	C(24)	115.0(4)	N(3)	C(25)	C(26)	121.0(5)
C(24)	C(25)	C(26)	123.9(5)	C(25)	C(26)	C(27)	118.6(5)
C(26)	C(27)	C(28)	120.1(6)	C(27)	C(28)	C(29)	119.1(6)
N(3)	C(29)	C(28)	121.8(5)				

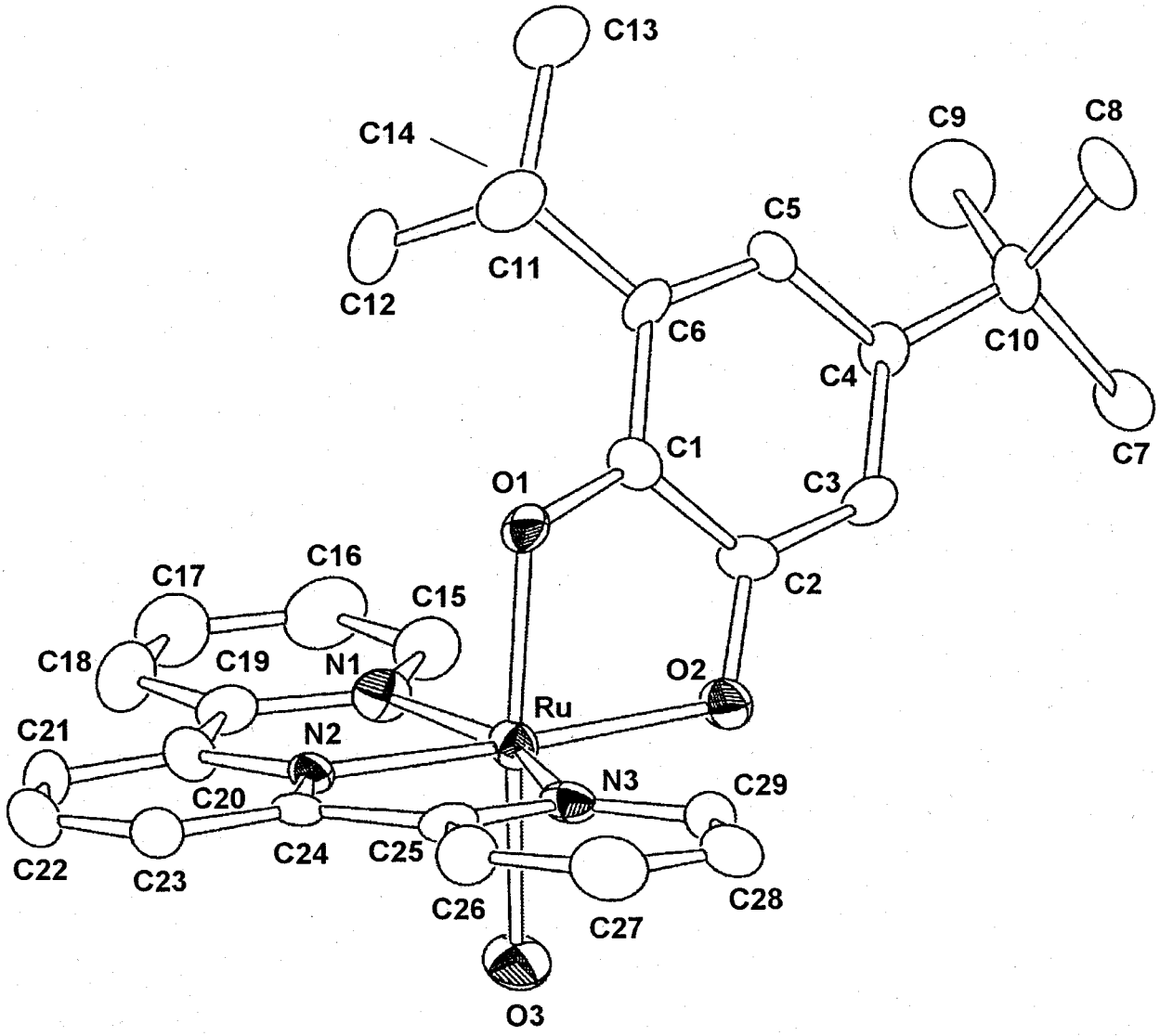

Figure A3. Crystal structures of [Ru^{II}(trpy)(Bu_2SQ)($O^{\bullet-}$)] and the atom-numbering scheme. All hydrogen atoms are omitted for clarity.

Table A9. Crystal Data, Data Collection `Parameters, and Structre Refinement for $[Ru^{II}(trpy)(Bu_2SQ)(O^{\bullet -})]\cdot 3H_2O$ (**5**·$3H_2O$)

Crystal Data	
formula	$C_{29}H_{31}N_3O_7Ru$
formula weight	634.65
color	Reddish purple
crystal size / mm	0.20 × 0.10 × 0.10
crystal system	tetragonal
space group	I-4
a / Å	24.688(2)
b / Å	24.688(2)
c / Å	10.0934(9)
α / deg	90
β / deg	90
γ / deg	90
V / Å^3	6152.0(8)
Z	8
D_{calc} / g cm^{-3}	1.370
F(000) / e	2608.00
Data Collection	
Diffractometer Used	Rigaku/MSC Mercury CCD
radiation	Mo Kα (λ = 0.71070 Å)
μ / cm^{-1}	5.57
Voltage, Current	60 kV, 250 mA
T / K	173
Collimator Size	0.5 mm
Data Images	720 exposures @ 40.0 sec
Detector Aperture	70 mm x 70 mm
ω oscillation Range (χ=45.0, ϕ=0.0)	70.0
Detector Swing Angle	19.59o
Detector Position	45.09 mm
$2\theta_{max}$ / deg	55.0

Table A9 (continued). Crystal Data, Data Collection `Parameters, and Structre Refinement for $[Ru^{II}(trpy)(Bu_2SQ)(O^{\bullet -})]\cdot 3H_2O$ (**5**$\cdot 3H_2O$)

No. of Reflections Measured	Total: 3723
	Unique: 3723 (Rint = 0.035)

Structure Solution and Refinement

Structure Solution	Direct Methods (SIR92)
Refinement	Full matrix least-squares
Function Minimized	Σ w $(\|Fo\|-\|Fc\|)^2$
Least Squares Weights	$1/\sigma^2(Fo) = 4Fo^2/\sigma^2(Fo^2)$
p factor	0.0500
Anomalous Dispersion	All non hydrogen atoms
reflections used	3707
$(I>0.00\sigma(I), 2\theta < 54.97o)$	
no. of variables	352
reflection / parameter ratio	10.53
GOF	0.855
R^a $(I > 2\sigma(I))$	0. 048, where
	$R = \Sigma[\|Fo\| - \|Fc\|]/\Sigma\|Fo\|$
$R_w{}^a$ $(I > 2\sigma(I))$	0. 057, where
	$R_w = [(\Sigma w(\|Fo\| - \|Fc\|)^2/\Sigma w(\|Fo\|^2))^{1/2}$
Max Shift/Error in Final Cycle	0.076
Maximum peak in Final Diff. Map	1.61 e^-/Å3
Minimum peak in Final Diff. Map	-1.11 e^-/Å3

Table A10. Fractional Atomic Coordination Including Hydrogen Atoms and Isotropic Thermal Parameters of $[Ru^{II}(trpy)(Bu_2SQ)(O^{\bullet -})]\cdot 3H_2O$ (**5**$\cdot 3H_2O$)

atom	x	y	z	B_{eq} [c]
Ru(1)	0.31931(3)	0.14954(3)	0.86264(8)	1.51(2)
O(1)	0.2401(3)	0.1364(3)	0.8754(7)	1.7(1)
O(2)	0.3062(3)	0.1179(3)	0.6768(6)	1.8(2)
O(3)	0.4011(3)	0.1540(3)	0.8347(8)	2.7(2)
O(4)	0.5768(3)	0.1191(3)	0.9895(7)	2.8(2)
O(5)	0.4519(3)	0.0633(3)	0.7244(9)	3.9(2)
O(6)	0.4650(5)	0.1238(7)	0.049(1)	10.4(5)
N(1)	0.3314(3)	0.0792(3)	0.9703(9)	1.8(2)
N(2)	0.3278(3)	0.1799(3)	1.0392(8)	1.7(2)
N(3)	0.3102(3)	0.2304(3)	0.8221(8)	1.6(2)
C(1)	0.2228(4)	0.1017(4)	0.7813(10)	1.5(2)
C(2)	0.2581(4)	0.0931(4)	0.6713(10)	1.7(2)
C(3)	0.2423(4)	0.0603(4)	0.566(1)	1.7(2)
C(4)	0.1931(4)	0.0339(4)	0.5661(10)	1.7(2)
C(5)	0.1593(4)	0.0419(4)	0.6753(10)	1.6(2)
C(6)	0.1717(4)	0.0735(4)	0.7848(10)	1.6(2)
C(7)	0.2175(4)	-0.0083(5)	0.344(1)	2.9(3)
C(8)	0.1229(5)	0.0194(5)	0.391(1)	2.9(3)
C(9)	0.1617(6)	-0.0612(5)	0.508(1)	4.0(3)
C(10)	0.1738(5)	-0.0030(5)	0.453(1)	2.4(3)
C(11)	0.1163(5)	0.1348(5)	0.927(1)	2.7(3)
C(12)	0.1669(6)	0.0584(5)	1.027(1)	2.8(3)
C(13)	0.0860(5)	0.0417(5)	0.893(1)	3.0(3)
C(14)	0.1353(4)	0.0773(4)	0.9069(10)	1.6(2)
C(15)	0.3301(4)	0.0274(4)	0.927(1)	2.3(3)
C(16)	0.3361(5)	-0.0167(5)	1.010(1)	3.1(3)
C(17)	0.3462(5)	-0.0070(4)	1.143(2)	3.3(3)
C(18)	0.3476(5)	0.0452(5)	1.189(1)	2.8(3)
C(19)	0.3403(4)	0.0876(4)	1.104(1)	1.9(2)
C(20)	0.3380(3)	0.1468(4)	1.142(1)	1.8(2)
C(21)	0.3466(4)	0.1680(5)	1.2687(10)	1.9(2)
C(22)	0.3420(4)	0.2226(5)	1.284(1)	2.5(3)

Table A10 (continued). Fractional Atomic Coordination Including Hydrogen Atoms and Isotropic Thermal Parameters of $[Ru^{II}(trpy)(Bu_2SQ)(O^{\bullet-})]\cdot 3H_2O$ (**5**$\cdot 3H_2O$)

atom	x	y	z	B_{eq} [c]
C(23)	0.3303(4)	0.2563(4)	1.182(1)	2.0(2)
C(24)	0.3229(4)	0.2343(4)	1.056(1)	1.5(2)
C(25)	0.3116(4)	0.2623(4)	0.932(1)	1.6(2)
C(26)	0.3033(4)	0.3183(4)	0.920(1)	2.1(2)
C(27)	0.2942(5)	0.3404(4)	0.799(1)	2.8(3)
C(28)	0.2940(4)	0.3088(5)	0.688(1)	2.4(3)
C(29)	0.3018(4)	0.2530(5)	0.702(1)	2.1(2)
H(1)	0.2667	0.0556	0.4912	2.3
H(2)	0.1248	0.0229	0.6758	2.2
H(3)	0.2495	-0.0233	0.3846	4.1
H(4)	0.2250	0.0249	0.3063	4.1
H(5)	0.2055	-0.0336	0.2776	4.1
H(6)	0.1274	0.0538	0.3553	3.7
H(7)	0.1079	-0.0047	0.3257	3.7
H(8)	0.0949	0.0219	0.4612	3.7
H(9)	0.1475	-0.0869	0.4422	5.4
H(10)	0.1342	-0.0610	0.5785	5.4
H(11)	0.1930	-0.0789	0.5464	5.4
H(12)	0.1448	0.1602	0.9323	3.5
H(13)	0.0950	0.1468	0.8444	3.5
H(14)	0.0915	0.1400	0.9970	3.5
H(15)	0.1801	0.0221	1.0144	3.2
H(16)	0.1973	0.0816	1.0400	3.2
H(17)	0.1450	0.0589	1.1046	3.2
H(18)	0.0627	0.0425	0.9684	3.6
H(19)	0.0646	0.0520	0.8166	3.6
H(20)	0.0956	0.0036	0.8787	3.6
H(21)	0.3249	0.0208	0.8330	2.8
H(22)	0.3338	-0.0543	0.9743	4.3
H(23)	0.3565	-0.0355	1.2039	4.0
H(24)	0.3494	0.0540	1.2852	3.3
H(25)	0.3569	0.1443	1.3444	2.3
H(26)	0.3447	0.2384	1.3731	2.6

Table A10 (continued). Fractional Atomic Coordination Including Hydrogen Atoms and Isotropic Thermal Parameters of $[Ru^{II}(trpy)(Bu_2SQ)(O^{\bullet -})]\cdot 3H_2O$ (**5**·$3H_2O$)

atom	x	y	z	B_{eq} [c]
H(27)	0.3275	0.2951	1.1990	2.2
H(28)	0.3015	0.3406	0.9999	2.6
H(29)	0.2882	0.3788	0.7914	3.0
H(30)	0.2881	0.3259	0.6036	2.5
H(31)	0.3010	0.2293	0.6224	2.7

[a] Numbers in parentheses are the estimated standard deviation in the last significant digit.

[b] The hydrogen atoms were placed at the calculated position and not refined.

[c] $Beq = 8\pi^2/3(U_{11}(aa^*)^2+U_{22}(bb^*)^2+U_{33}(cc^*)^2+2U_{12}(aa^*bb^*)\cos\gamma+2U_{13}(aa^*cc^*)\cos\beta+2U_{23}(bb^*cc^*)\cos\alpha)$

Table A11. Anisotropic Thermal Parameters for Non-hydrogen Atoms in $[Ru^{II}(trpy)(Bu_2SQ)(O^{\bullet -})]\cdot 3H_2O$ (**5**·$3H_2O$)

atom	U_{11}	U_{22}	U_{33}	U_{12}	U_{13}	U_{23}
Ru(1)	0.0195(5)	0.0183(5)	0.0196(3)	0.0004(4)	-0.0011(4)	-0.0043(4)
O(1)	0.024(4)	0.023(4)	0.018(4)	-0.001(3)	0.003(3)	-0.007(4)
O(2)	0.020(4)	0.026(4)	0.024(4)	-0.005(3)	-0.001(3)	-0.008(3)
O(3)	0.020(4)	0.044(5)	0.038(5)	0.010(3)	0.001(4)	-0.009(4)
O(4)	0.042(5)	0.036(5)	0.028(4)	0.002(4)	0.003(4)	0.005(4)
O(5)	0.047(6)	0.039(5)	0.062(6)	-0.001(4)	-0.010(5)	-0.005(5)
O(6)	0.055(8)	0.28(2)	0.062(8)	-0.02(1)	-0.010(6)	-0.02(1)
N(1)	0.024(5)	0.015(5)	0.029(5)	0.000(4)	0.000(4)	0.003(4)
N(2)	0.019(5)	0.026(5)	0.017(4)	-0.003(4)	0.002(4)	-0.007(4)
N(3)	0.018(5)	0.019(5)	0.023(5)	-0.004(4)	-0.002(4)	-0.002(4)
C(1)	0.023(6)	0.011(5)	0.021(5)	0.002(4)	-0.004(5)	0.003(4)
C(2)	0.022(5)	0.013(5)	0.028(6)	0.000(4)	0.000(4)	-0.002(4)
C(3)	0.025(6)	0.015(5)	0.026(6)	-0.001(4)	0.004(5)	0.001(5)
C(4)	0.033(6)	0.012(5)	0.018(5)	-0.005(5)	-0.001(5)	-0.005(4)
C(5)	0.021(5)	0.016(5)	0.023(6)	-0.003(4)	-0.008(4)	0.008(4)
C(6)	0.025(6)	0.015(5)	0.020(5)	0.001(4)	0.008(5)	0.006(4)
C(7)	0.035(6)	0.051(7)	0.024(7)	-0.012(6)	0.006(6)	-0.029(6)
C(8)	0.040(7)	0.048(8)	0.022(7)	-0.009(6)	-0.014(5)	-0.015(6)
C(9)	0.08(1)	0.012(6)	0.058(9)	-0.011(6)	0.003(8)	-0.011(6)
C(10)	0.034(7)	0.036(7)	0.023(6)	-0.001(5)	-0.006(5)	0.002(5)
C(11)	0.030(7)	0.035(7)	0.038(7)	0.000(5)	0.014(6)	-0.001(6)
C(12)	0.060(9)	0.031(7)	0.015(6)	-0.008(6)	0.001(6)	0.006(5)
C(13)	0.030(7)	0.040(7)	0.044(9)	-0.005(5)	0.009(6)	0.006(6)
C(14)	0.015(5)	0.025(6)	0.021(5)	-0.001(4)	0.004(4)	-0.004(4)
C(15)	0.037(7)	0.017(6)	0.035(6)	0.000(5)	0.002(5)	-0.006(5)
C(16)	0.040(8)	0.021(6)	0.059(9)	0.002(6)	0.012(7)	0.007(6)
C(17)	0.051(8)	0.027(6)	0.046(7)	0.004(5)	0.003(8)	0.006(7)
C(18)	0.040(7)	0.037(7)	0.030(6)	0.004(6)	0.003(6)	0.010(6)
C(19)	0.024(6)	0.021(6)	0.028(7)	0.000(4)	0.003(5)	0.001(5)
C(20)	0.017(5)	0.021(5)	0.031(5)	0.004(4)	-0.007(5)	0.008(7)
C(21)	0.026(6)	0.032(7)	0.015(5)	0.000(5)	-0.004(5)	0.003(5)
C(22)	0.023(6)	0.045(8)	0.026(6)	0.003(5)	0.000(5)	-0.013(6)

Table A11 (continued). Anisotropic Thermal Parameters for Non-hydrogen Atoms in $[Ru^{II}(trpy)(Bu_2SQ)(O^{\bullet-})]\cdot 3H_2O$ (**5**·$3H_2O$)

atom	U_{11}	U_{22}	U_{33}	U_{12}	U_{13}	U_{23}
C(23)	0.026(6)	0.030(6)	0.019(5)	-0.002(5)	0.001(5)	-0.004(5)
C(24)	0.010(5)	0.022(6)	0.024(6)	0.000(4)	0.001(4)	-0.002(5)
C(25)	0.012(5)	0.018(5)	0.031(6)	0.000(4)	0.006(5)	-0.006(5)
C(26)	0.027(6)	0.023(6)	0.030(6)	0.006(5)	0.000(5)	-0.001(5)
C(27)	0.037(7)	0.017(6)	0.054(8)	0.002(5)	-0.006(6)	0.006(6)
C(28)	0.021(6)	0.033(7)	0.037(7)	0.000(5)	-0.008(5)	0.013(6)
C(29)	0.022(6)	0.030(6)	0.026(6)	-0.002(5)	-0.005(5)	0.004(5)

[a] Numbers in parentheses are the estimated standard deviation in the last significant digit.

[b] The general temperature factor expression:

$\exp(-2\pi^2(a^{*2}h^2U_{11}+b^{*2}k^2U_{22}+c^{*2}l^2U_{33}+2a^*b^*hkU_{12}+2a^*c^*hlU_{13}+2b^*c^*klU_{23}))$

Table A12. Bond Distances and Bond Angles of $[Ru^{II}(trpy)(Bu_2SQ)(O^{\bullet -})]\cdot 3H_2O$ (**5**$\cdot 3H_2O$)

Bond Distances (Å)

atom	atom	distance	atom	atom	distance
Ru(1)	O(1)	1.985(6)	Ru(1)	O(2)	2.058(6)
Ru(1)	O(3)	2.043(7)	Ru(1)	N(1)	2.071(8)
Ru(1)	N(2)	1.945(8)	Ru(1)	N(3)	2.050(9)
O(1)	C(1)	1.35(1)	O(2)	C(2)	1.34(1)
N(1)	C(15)	1.35(1)	N(1)	C(19)	1.38(1)
N(2)	C(20)	1.34(1)	N(2)	C(24)	1.36(1)
N(3)	C(25)	1.36(1)	N(3)	C(29)	1.35(1)
C(1)	C(2)	1.43(1)	C(1)	C(6)	1.44(1)
C(2)	C(3)	1.39(1)	C(3)	C(4)	1.38(1)
C(4)	C(5)	1.39(1)	C(4)	C(10)	1.53(1)
C(5)	C(6)	1.39(1)	C(6)	C(14)	1.53(1)
C(7)	C(10)	1.55(2)	C(8)	C(10)	1.51(2)
C(9)	C(10)	1.57(2)	C(11)	C(14)	1.51(1)
C(12)	C(14)	1.51(2)	C(13)	C(14)	1.51(1)
C(15)	C(16)	1.38(2)	C(16)	C(17)	1.39(2)
C(17)	C(18)	1.37(2)	C(18)	C(19)	1.37(1)
C(19)	C(20)	1.51(1)	C(20)	C(21)	1.40(1)
C(21)	C(22)	1.36(2)	C(22)	C(23)	1.36(2)
C(23)	C(24)	1.39(1)	C(24)	C(25)	1.46(1)
C(25)	C(26)	1.40(1)	C(26)	C(27)	1.36(2)
C(27)	C(28)	1.37(2)	C(28)	C(29)	1.40(1)

Bond Angles (deg)

atom	atom	atom	angle	atom	atom	atom	angle
O(1)	Ru(1)	O(2)	80.9(3)	O(1)	Ru(1)	O(3)	172.4(3)
O(1)	Ru(1)	N(1)	88.3(3)	O(1)	Ru(1)	N(2)	96.3(3)
O(1)	Ru(1)	N(3)	93.6(3)	O(2)	Ru(1)	O(3)	92.9(3)
O(2)	Ru(1)	N(1)	100.5(3)	O(2)	Ru(1)	N(2)	177.1(3)
O(2)	Ru(1)	N(3)	99.8(3)	O(3)	Ru(1)	N(1)	88.6(3)
O(3)	Ru(1)	N(2)	90.0(3)	O(3)	Ru(1)	N(3)	91.7(3)

Table A12 (continued). Bond Distances and Bond Angles of $[Ru^{II}(trpy)(Bu_2SQ)(O^{\bullet -})]\cdot 3H_2O$ (**5**$\cdot 3H_2O$)

atom	atom	atom	angle	atom	atom	atom	angle
N(1)	Ru(1)	N(2)	80.1(4)	N(1)	Ru(1)	N(3)	159.6(3)
N(2)	Ru(1)	N(3)	79.6(3)	Ru(1)	O(1)	C(1)	111.7(6)
Ru(1)	O(2)	C(2)	110.6(6)	Ru(1)	N(1)	C(15)	128.3(7)
Ru(1)	N(1)	C(19)	114.1(7)	C(15)	N(1)	C(19)	117.5(9)
Ru(1)	N(2)	C(20)	119.4(7)	Ru(1)	N(2)	C(24)	119.2(7)
C(20)	N(2)	C(24)	121.4(9)	Ru(1)	N(3)	C(25)	113.6(6)
Ru(1)	N(3)	C(29)	126.8(7)	C(25)	N(3)	C(29)	119.6(9)
O(1)	C(1)	C(2)	116.7(9)	O(1)	C(1)	C(6)	124.6(9)
C(2)	C(1)	C(6)	118.7(9)	O(2)	C(2)	C(1)	116.2(8)
O(2)	C(2)	C(3)	123.1(9)	C(1)	C(2)	C(3)	120.7(9)
C(2)	C(3)	C(4)	121.3(9)	C(3)	C(4)	C(5)	117.4(9)
C(3)	C(4)	C(10)	123.5(9)	C(5)	C(4)	C(10)	119.1(9)
C(4)	C(5)	C(6)	125.3(9)	C(1)	C(6)	C(5)	116.4(9)
C(1)	C(6)	C(14)	120.3(9)	C(5)	C(6)	C(14)	123.2(9)
C(4)	C(10)	C(7)	111.2(9)	C(4)	C(10)	C(8)	110.4(9)
C(4)	C(10)	C(9)	109.8(9)	C(7)	C(10)	C(8)	108.7(9)
C(7)	C(10)	C(9)	107.8(10)	C(8)	C(10)	C(9)	108.8(10)
C(6)	C(14)	C(11)	110.4(8)	C(6)	C(14)	C(12)	108.7(8)
C(6)	C(14)	C(13)	111.5(9)	C(11)	C(14)	C(12)	110.1(9)
C(11)	C(14)	C(13)	108.0(9)	C(12)	C(14)	C(13)	108.1(9)
N(1)	C(15)	C(16)	123(1)	C(15)	C(16)	C(17)	118(1)
C(16)	C(17)	C(18)	119(1)	C(17)	C(18)	C(19)	120(1)
N(1)	C(19)	C(18)	121.4(10)	N(1)	C(19)	C(20)	112.8(9)
C(18)	C(19)	C(20)	125.7(10)	N(2)	C(20)	C(19)	113.6(9)
N(2)	C(20)	C(21)	120.3(9)	C(19)	C(20)	C(21)	126.1(9)
C(20)	C(21)	C(22)	117.6(10)	C(21)	C(22)	C(23)	122(1)
C(22)	C(23)	C(24)	118(1)	N(2)	C(24)	C(23)	119.3(10)
N(2)	C(24)	C(25)	112.0(9)	C(23)	C(24)	C(25)	128.7(9)
N(3)	C(25)	C(24)	115.5(8)	N(3)	C(25)	C(26)	120.2(10)
C(24)	C(25)	C(26)	124.3(10)	C(25)	C(26)	C(27)	119.6(10)
C(26)	C(27)	C(28)	120.6(10)	C(27)	C(28)	C(29)	118(1)

Table A12 (continued). Bond Distances and Bond Angles of $[Ru^{II}(trpy)(Bu_2SQ)(O^{\bullet -})]\cdot 3H_2O$ (**5**$\cdot 3H_2O$)

atom	atom	atom	angle	atom	atom	atom	angle
N(3)	C(29)	C(28)	121(1)				

Publication List

Katsuaki Kobayashi, Hideki Ohtsu, Tohru Wada, and Koji Tanaka, *Chem. Lett.* **2002**, 868.

"Ruthenium Oxyl Radical Complex Containing *o*-Quinone Ligand Detected by ESR Measurements of Spin Trapping Technique"

Acknowledgments

I would like to express to Professor Koji Tanaka of Institute for Molecular Science my deepest gratitude for his guidance through this work.

I would like to thank to Dr. Hideki Ohtsu of Institute for Molecular Science for his invaluable discussion and help.

I would like to thank to Dr. Tohru Wada of Institute for Molecular Science and Dr. Kiyoshi Tsuge of Hokkaido University for their appropriate advice.

I would like to thank to Professor Takeshi Yamamura for his guidance in my graduate life.

I wish thank to Mr. Takashi Tomon, Dr. Tetsuaki Fujiwara, Dr. Takeaki Koizumi, Dr. Kazushi Shiren, Dr. Rei Okamura, Mr. Tetsunori Mizukawa, Miss Takami Hino, and Miss Kanako Tsutsui in Prof. Tanaka's Laboratory and Dr. Toshi Nagata and Mr. Yoshihiro Kikusawa in Dr. Nagata's Laboratory for their advise and encouragements.

And thanks are also extended to all member of the Coordination Laboratories in Institute for Molecular Science.

Finally, I would like to express my thanks to my parents, my brother, my sister and friends for their encouragements.

Katsuaki Kobayashi

Katsuaki Kobayashi